NAVAL POSTGRADUATE SCHOOL

MONTEREY, CALIFORNIA

THESIS

OPTIMAL ARTIFICIAL BOUNDARY CONDITION CONFIGURATIONS FOR SENSITIVITY-BASED MODEL UPDATING AND DAMAGE DETECTION

by

Konstantinos Papagiannakis

September 2010

Thesis Advisor:	Joshua H. Gordis
Second Reader:	Young W. Kwon

Approved for public release; distribution is unlimited

THIS PAGE INTENTIONALLY LEFT BLANK

REPORT DOCUMENTATION PAGE			Form Approved OMB No. 0704-0188
Public reporting burden for this collection of information is estimated to average 1 hour per response, including the time for reviewing instruction, searching existing data sources, gathering and maintaining the data needed, and completing and reviewing the collection of information. Send comments regarding this burden estimate or any other aspect of this collection of information, including suggestions for reducing this burden, to Washington headquarters Services, Directorate for Information Operations and Reports, 1215 Jefferson Davis Highway, Suite 1204, Arlington, VA 22202-4302, and to the Office of Management and Budget, Paperwork Reduction Project (0704-0188) Washington DC 20503.			
1. AGENCY USE ONLY ***(Leave blank)***	**2. REPORT DATE** September 2010	**3. REPORT TYPE AND DATES COVERED** Master's Thesis	
4. TITLE AND SUBTITLE Optimal Artificial Boundary Condition Configurations for Sensitivity-Based Model Updating and Damage Detection		**5. FUNDING NUMBERS**	
6. AUTHOR(S) Konstantinos Papagiannakis			
7. PERFORMING ORGANIZATION NAME(S) AND ADDRESS(ES) Naval Postgraduate School Monterey, CA 93943-5000		**8. PERFORMING ORGANIZATION REPORT NUMBER**	
9. SPONSORING /MONITORING AGENCY NAME(S) AND ADDRESS(ES) N/A		**10. SPONSORING/MONITORING AGENCY REPORT NUMBER**	
11. SUPPLEMENTARY NOTES The views expressed in this thesis are those of the author and do not reflect the official policy or position of the Department of Defense or the U.S. government. IRB Protocol number _____.			
12a. DISTRIBUTION / AVAILABILITY STATEMENT Approved for public release; distribution is unlimited		**12b. DISTRIBUTION CODE** A	

13. ABSTRACT (maximum 200 words)

Frequently, in structural system identification (model updating or damage detection), the available set of data is incomplete, both spatially and in modal content. This incompleteness leads to the solution of underdetermined linear systems. In order to improve the identification, additional independent measured data must be found. In the past, it has been shown that such data can be easily obtained from the application of Artificial Boundary Conditions (ABC), imposed on both the baseline FE models and the measured frequency response data. This can be accomplished without any physical modifications to the experiment and, hence, no additional expense on different systems, or more than once, in order to get the modal data needed for the analysis. In this thesis, the procedure of sensitivity-based structural system identification, using ABCs, and enhanced by parameter grouping/clustering, is examined. It is shown that the optimal sensitivity matrix is a square and diagonal dominant one, which can be used with quite accurate results both for localization of parameter errors, and the determination of the magnitude of parameter error. The numerous ABC configurations available, even from a small measured data set, allow an optimal sensitivity matrix to be found for many parameters. These concepts are demonstrated using simulated measurements along with finite element models.

14. SUBJECT TERMS Artificial Boundary Conditions, Finite Element Model, Sensitivity Based FEM Updating, Damage Detection, Natural Frequencies, Diagonal Dominant			**15. NUMBER OF PAGES** 121
			16. PRICE CODE
17. SECURITY CLASSIFICATION OF REPORT Unclassified	**18. SECURITY CLASSIFICATION OF THIS PAGE** Unclassified	**19. SECURITY CLASSIFICATION OF ABSTRACT** Unclassified	**20. LIMITATION OF ABSTRACT** UU

NSN 7540-01-280-5500 Standard Form 298 (Rev. 2-89)
Prescribed by ANSI Std. 239-18

THIS PAGE INTENTIONALLY LEFT BLANK

Approved for public release; distribution is unlimited

OPTIMAL ARTIFICIAL BOUNDARY CONDITION CONFIGURATIONS FOR SENSITIVITY-BASED MODEL UPDATING AND DAMAGE DETECTION

Konstantinos Papagiannakis
Lieutenant, Hellenic Navy
B.S., Hellenic Naval Academy, 2000

Submitted in partial fulfillment of the
requirements for the degree of

MASTER OF SCIENCE IN MECHANICAL ENGINEERING

from the

NAVAL POSTGRADUATE SCHOOL
September 2010

Author: Konstantinos Papagiannakis

Approved by: Joshua H. Gordis
Thesis Advisor

Young W. Kwon
Second Reader

Knox T. Millsaps
Chairman, Department of Mechanical and Aerospace Engineering

THIS PAGE INTENTIONALLY LEFT BLANK

ABSTRACT

Frequently, in structural system identification (model updating or damage detection), the available set of data is incomplete, both spatially and in modal content. This incompleteness leads to the solution of underdetermined linear systems. In order to improve the identification, additional independent measured data must be found. In the past, it has been shown that such data can be easily obtained from the application of Artificial Boundary Conditions (ABC), imposed on both the baseline FE models and the measured frequency response data. This can be accomplished without any physical modifications to the experiment and, hence, no additional expense on different systems, or more than once, in order to get the modal data needed for the analysis. In this thesis, the procedure of sensitivity-based structural system identification, using ABCs, and enhanced by parameter grouping/clustering, is examined. It is shown that the optimal sensitivity matrix is a square and diagonal dominant one, which can be used with quite accurate results both for localization of parameter errors, and the determination of the magnitude of parameter error. The numerous ABC configurations available, even from a small measured data set, allow an optimal sensitivity matrix to be found for many parameters. These concepts are demonstrated using simulated measurements along with finite element models.

THIS PAGE INTENTIONALLY LEFT BLANK

TABLE OF CONTENTS

LIST OF FIGURES

LIST OF ACRONYMS AND ABBREVIATIONS

ABC	artificial boundary condition(s)
OCS	omitted coordinate system(s)
DOF	degree(s) of freedom
FE	finite element
FEM	finite element model
GA	genetic algorithm
ASET	analytical set
OSET	omitted set
FRF	frequency response function
FFT	fast fourier transform

THIS PAGE INTENTIONALLY LEFT BLANK

ACKNOWLEDGMENTS

I would like to express my gratitude to Professor Joshua H. Gordis for his unparalleled support and patience with my attempt to write this thesis. His assistance was critical both in the initial drafting of this work and in overcoming several issues encountered along the way, which would have been difficult to solve without his help.

I would also like to thank my parents, Yiannis and Eleftheria, for their love and great contribution to what I have achieved so far in my life. My deepest thanks go to my wife, Effie, for her unconditional love, patience and support throughout all the steps of our common life. Finally, I dedicate this work to the most beautiful flower ever to blossom in my life, my daughter, Konstantina.

THIS PAGE INTENTIONALLY LEFT BLANK

I. INTRODUCTION

A. MODEL UPDATING AND DAMAGE DETECTION

Finite element analysis (FE) is a computational tool that is widely used in cases where a closed-form solution to a partial differential equation is not available. In structural dynamics, FE models are used to predict the dynamic response of a system to external stimuli, such as dynamic excitations, or to assess the effect of parameter changes. The term “parameter” stands for all the individual physical and geometric data that define the structure, such as geometry, elastic moduli and element masses/densities.

The use of FE models aims at achieving higher accuracy in terms of response prediction; however, doing so may not always be possible for several reasons. Some of them are usually connected to uncertainties regarding the governing equation of the system, to assumptions made during the derivation, to inaccurate physical boundary conditions, to inexact characterization of joints and connections, etc. All these discrepancies are revealed and attempted to be overcome, when a necessary procedure for the validation of the FE model takes place. This procedure is called FEM updating. It involves measuring structure response, identifying modal data, comparing the modal parameters to those extracted from the FE model and finally, modifying appropriately the FE model to match the system’s design requirements. FEM updating is of vital importance as it verifies that the model can be used with acceptable reliability for a number of research fields in modal analysis, such as damage detection and error localization.

B. BACKGROUND

Over the last decades, a large volume of literature on structural identification, including both model updating and error localization has been produced. Friswell and Mottershead in their survey [1], extensively discuss methods that deal with various aspects of this field. Most of them are eigenvalue sensitivity-based and are thoroughly presented and analyzed in [2]. Each developed method has, as a main objective, to

overcome problems that arise during the procedure, which in general, converges to the solving of a linear system. The most common issue with the solution is the ill-conditioning of these systems. This ill-condition results from the lack of input data, which frequently leads to a severely underdetermined system of equations. The lack of input data is mainly caused either by the geometric limitation of measurement locations on a structure (spatial incompleteness) or by the bounds of the available bandwidth during modal testing (modal incompleteness). It is often observed that ill-conditioning may be a concern due to dependencies of the sensitivity matrix, or even due to the physical geometry of the structure, in cases where symmetry is present.

Dealing with this problem, Lallement and Piranda in [3] are the first to introduce the development of a rational procedure for parameter selection—which appears to be the main core in many updating methods—to facilitate the improvement of the conditioning of the equations. This has to do with an iterative procedure to find an appropriate subset of parameters that produce an optimal solution commonly known as forward selection. Then, the importance of vector subspaces and their wide application range in modal analysis is revealed [4], and in [5] the concept of selecting parameters groups using angles between subspaces is implemented, also incorporating side constraints to the equations to be solved. The methods of subset selection are outlined and extended to the selection of groups of parameters. Reference [6] is a representative example of the selection and updating of parameters in an actual application. Another approach to the same objective, parameter selection, is offered in [7] where an automated procedure to guide the parameter selection is suggested based on simple observations. The idea of grouping element sensitivities together, under the condition of selecting as few parameters as possible that comply with the above stated observations, is presented. These observations deal with the fact that the number of updating parameters can be reduced, but only by sacrificing the total sensitivity, which is a concept that will be covered and used in Chapter IV of this thesis. References [8], [9] and [10] address this concept in a different manner, using the principles of cluster analysis, along with optimal subset selection, and show how these methods can be successfully used in a number of applications.

Another path towards the improving the ill-conditioning aims at the enrichment of the available data, in order to decrease incompleteness, or be less underdetermined. Of course, care has to be exercised in preventing the addition of redundant data and in accordance with feasibility conditions. A first step of doing so without requiring any modifications to the physical structure is made by Gordis [11], where the concept of artificial constraints is initially introduced. The term artificial refers to the fact that a constraint is applied computationally to the measured data, as well as to the FE model. Another similar reference is made by Rade, Lallement and Silva in [12], stated here as Modified Configurations, describing related ways different artificial systems are used to enlarge the experimental data. In this work, the criterion established is the minimization of the condition number of the sensitivity matrix, or in other words, the maximization of the degree of linear independence between the columns and the rows of the sensitivity matrix. A theoretical investigation of this concept is made in [13], where the term ABC, standing for Artificial Boundary Condition, is first introduced. It proves that, with no additional testing, all the natural frequencies corresponding to ABC systems and the needed additional data can be obtained from any square FRF matrix measured in a modal test. In addition, it shows that structural sensitivities can be generated from both the baseline FE model and from the ABC systems, and combined in a global sensitivity matrix which can reduce or eliminate conditioning problems. A genetic algorithm (GA)-based methodology, to make effective use of the ABC frequencies for FE model updating, is presented in [14] by Lu and Tu, where a binary code, GA, is proposed for the selection of the desired artificial boundary conditions. The recent literature related to ABCs in general is completed with [15], where the practical aspects of the implementation of ABCs in an actual measurement environment is investigated and the feasibility of using only the lowest few ABC frequencies in conjunction with a variety of ABC configurations is examined.

C. REFERENCE TO PRESENT WORK

In this thesis, a sensitivity-based FE analysis is performed, with the goal of eliminating the discrepancies mentioned above. First of all, the properties of several

Matlab algorithms are examined in order to choose the one that best matches our requirements for linear system solution. These algorithms are invoked with the commands “pinv” and ‘\” and, eventually, involve SVD and QR decomposition with column pivoting, respectively. In addition, the correlation between the sensitivity matrix rows and modal strain energy is depicted. Then, the degree of the data incompleteness, which is related to the number of available modes, is connected to the qualitative result of the linear system solution. This leads further to the conclusion that there is a necessary but not sufficient condition for detecting potential damage everywhere in a structure, using only one sensitivity matrix for all the cases. The condition is that one must provide as many modes as the adjustable design parameters of the structure, i.e., building a square sensitivity matrix. Toward this end, several methods of data enrichment are taken into account, like eigenvector sensitivities and clustering/grouping parameters, with emphasis on the use of ABCs, since they are considered the most effective tool for all the aforementioned reasons. Keeping in mind that even with a potentially large number of ABC configurations available, a sufficient amount of additional data from the ABCs may not be sufficient, such as in very large and complex structures; in these cases, ABC configurations can be combined with grouped parameters into a global sensitivity matrix. Finally, it is shown that the optimal configurations result in a diagonal dominant global sensitivity matrix, which once built, will meet necessary and sufficient conditions for damage detection.

II. THEORY

Beginning from the governing equation that describes a dynamic system under an excitation, we have:

$$[M]\{\ddot{x}\}+[C]\{\dot{x}\}+[K]\{x\}=\{F(t)\} \tag{2.1}$$

where this system consists of mass, damping and stiffness parameters, expressed as the symmetric mass, damping and stiffness matrices shown above, of size n x n, where n is the number of degrees of freedom (DOF) in the model. The vector $\{F(t)\}$ represents the excitation force of size n x1.

If the damping $[C]$ is neglected, Equation (2.1) becomes:

$$[M]\{\ddot{x}\}+[K]\{x\}=\{F(t)\} \tag{2.2}$$

Expressing in a more explicit way each matrix shown in Equation (2.2), results in the following:

$$\begin{bmatrix} M_{11} & \cdots & M_{1n} \\ \vdots & \ddots & \vdots \\ M_{n1} & \cdots & M_{nn} \end{bmatrix} \begin{Bmatrix} \ddot{x}_1(t) \\ \\ \ddot{x}_n(t) \end{Bmatrix} + \begin{bmatrix} K_{11} & \cdots & K_{1n} \\ \vdots & \ddots & \vdots \\ K_{n1} & \cdots & K_{nn} \end{bmatrix} \begin{Bmatrix} x_1(t) \\ \\ x_n(t) \end{Bmatrix} = \begin{Bmatrix} f_1 \\ \vdots \\ f_n \end{Bmatrix} \tag{2.3}$$

Equation (2.3) describes a system of n degrees of freedom, which approximates a continuous system with an infinite number of degrees of freedom. An actual modal test involves the measurement of only a small percentage of a structure's DOFs. During this procedure, these measured coordinates are considered the analytical set or (ASET), and they are the locations where the measuring instruments (accelerometers) are positioned. The remaining unmeasured DOF are considered the omitted coordinate set or (OSET), and in theory, contain an infinite number of degrees of freedom.

A. ANALYTICAL AND OMITTED COORDINATE SETS

Going from the time domain to the frequency domain and getting the steady state response of the above described system, we get for the whole set of n DOF:

$$\left[\begin{bmatrix} K_{11} & \cdots & K_{1n} \\ \vdots & \ddots & \vdots \\ K_{n1} & \cdots & K_{nn} \end{bmatrix} - \Omega^2 \begin{bmatrix} M_{11} & \cdots & M_{1n} \\ \vdots & \ddots & \vdots \\ M_{n1} & \cdots & M_{nn} \end{bmatrix}\right] * \begin{Bmatrix} x_1(t) \\ \\ x_n(t) \end{Bmatrix} = \begin{Bmatrix} f_1 \\ \vdots \\ f_n \end{Bmatrix} \tag{2.4}$$

where Ω is the frequency of the harmonic excitation. Making use of the analytical (measured) and the omitted (unmeasured) set of coordinates, that is the ASET and OSET coordinates, Equation (2.4) takes the following form:

$$\left[\begin{bmatrix} K_{aa} & K_{ao} \\ K_{oa} & K_{oo} \end{bmatrix} - \Omega^2 \begin{bmatrix} M_{aa} & M_{ao} \\ M_{oa} & M_{oo} \end{bmatrix}\right] \begin{Bmatrix} x_a \\ x_o \end{Bmatrix} = \begin{Bmatrix} f_a \\ f_o \end{Bmatrix} \tag{2.5}$$

Without loss of any generality, we can assume that there is no excitation on the omitted coordinates, that is $\{f_o\} = \{0\}$, and get:

$$\left[\begin{bmatrix} K_{aa} & K_{ao} \\ K_{oa} & K_{oo} \end{bmatrix} - \Omega^2 \begin{bmatrix} M_{aa} & M_{ao} \\ M_{oa} & M_{oo} \end{bmatrix}\right] \begin{Bmatrix} x_a \\ x_o \end{Bmatrix} = \begin{Bmatrix} f_a \\ 0 \end{Bmatrix} \tag{2.6}$$

The above matrix form represents a system of two equations. From those equations, there is an obvious solution for the OSET coordinates in terms of ASET coordinates through:

$$[K_{oa}]\{x_a\} + [K_{oo}]\{x_o\} - \Omega^2 [[M_{oa}]\{x_a\} + [M_{oo}]\{x_o\}] = 0 \tag{2.7}$$

Rearranging and solving for $\{x_o\}$, Equation (2.7) becomes:

$$\{x_o\} = \left[I - \Omega^2 K_{oo}^{-1} M_{oo}\right]^{-1} \left[-K_{oo}^{-1} K_{oa} + \Omega^2 K_{oo}^{-1} M_{oa}\right] \{x_a\} \tag{2.8}$$

By definition, the term $\left[I - \Omega^2 K_{oo}^{-1} M_{oo}\right]^{-1}$ is equal to:

$$\left[I - \Omega^2 K_{oo}^{-1} M_{oo} \right]^{-1} = \frac{1}{Det\left[I - \Omega^2 K_{oo}^{-1} M_{oo} \right]} Adj\left[I - \Omega^2 K_{oo}^{-1} M_{oo} \right] \tag{2.9}$$

where the $\text{Det}\left[I - \Omega^2 K_{oo}{}^{-1} M_{oo} \right]$ indicates the determinant and $\text{Adj}\left[I - \Omega^2 K_{oo}{}^{-1} M_{oo} \right]$ indicates the adjoint matrix. From Equation (2.9), it is obvious that there are some frequency values for which the inverse does not exist, and these are the ones that satisfy:

$$Det\left[I - \Omega^2 K_{oo}^{-1} M_{oo} \right] = 0 \tag{2.10}$$

It is easily noticeable that the frequencies that satisfy the above equation are the eigenvalues of the system defined by the $\left[K_{oo} \right]$ and $\left[M_{oo} \right]$ matrices, hence, they correspond to the natural frequencies of the OSET system.

Realizing that the eigensolution of a dynamic system is defined by the unrestrained DOF of the corresponding system, the OSET coordinates are unrestrained and the ASET coordinates are considered constrained to the ground.

B. REDUCED ORDER MODEL

The fact that a finite number of transducers are used for a modal test, in contrast to the infinite number of DOF of the real system, defines a reduced order model. This model's impedance is nonlinearly dependent on the impedance of the full order model [13]. Considering this exact model, in terms of frequency response function (FRF) we have:

$$\left[H \right] = \begin{bmatrix} H_{aa} & H_{ao} \\ H_{oa} & H_{oo} \end{bmatrix} \tag{2.11}$$

The experimental set of data measured in a real test is carried in the partition $\left[H_{aa} \right]$ of the above full FRF. In other words, $\left[H_{aa} \right]$ represents a structural dynamic model, reduced via exact dynamic reduction [11]. Using the algebraic relation of FRF to its impedance, we have:

$$\begin{bmatrix} Z_{aa} & Z_{oa} \\ Z_{ao} & Z_{oo} \end{bmatrix} \begin{bmatrix} H_{aa} & H_{oa} \\ H_{ao} & H_{oo} \end{bmatrix} = \begin{bmatrix} 1 & 0 \\ 0 & 1 \end{bmatrix} \tag{2.12}$$

which, after decomposing the set of equations and solving for $[H_{aa}]$, leads to:

$$[H_{aa}] = [Z_{aa} - Z_{ao} Z_{oo}^{-1} Z_{oa}]^{-1} \tag{2.13}$$

Writing Equation (2.6) in terms of impedance, we get:

$$\begin{bmatrix} Z_{aa} & Z_{ao} \\ Z_{oa} & Z_{oo} \end{bmatrix} \begin{Bmatrix} x_a \\ x_o \end{Bmatrix} = \begin{Bmatrix} f_a \\ 0 \end{Bmatrix} \tag{2.14}$$

Rearranging (2.14), the exact dynamic relationship between the OSET coordinates and the ASET coordinates gives:

$$\begin{Bmatrix} x_a \\ x_o \end{Bmatrix} = \begin{bmatrix} I \\ -Z_{oo}^{-1} Z_{oa} \end{bmatrix} \{x_a\} \tag{2.15}$$

Combining Equation (2.14) and Equation (2.15), and solving the first equation of the matrix formula, the dynamic reduced model results:

$$\{f_a\} = [Z_{aa} - Z_{ao} Z_{oo}^{-1} Z_{oa}] \{x_a\} \tag{2.16}$$

Paralleling Equations (2.13) and (2.16), it is found that the FRF extracted from an actual modal test, i.e., the measured partition of an infinite-order FRF matrix, is equivalent to the inverse of a dynamically reduced impedance matrix. In addition, the term Z_{oo}^{-1} seems to be critical for the definition of $[H_{aa}]$, and since every element in the Z_{oo}^{-1} is singular at the natural frequencies of the OSET, Equation (2.13) shows that the elements of H_{aa}^{-1} will be singular at the OSET natural frequencies [13].

From what is proved above, it is obvious that the FE model can be manipulated in the same manner. This means that the FE model is used to calculate a full n x n FRF, and appropriate boundary conditions can be applied corresponding to the coordinates measured in a test.

C. FREQUENCY RESPONSE FUNCTION

The Frequency Response Function FRF is actually a ratio defined by the response of a system due to a harmonic excitation. It contains all the amplitude and phase information for the response of a specific DOF excited by an input force at a specific, and perhaps different, DOF. The FRF is constructed by measuring both the response and the excitation simultaneously. This data is transformed from the time domain to the frequency domain using FFT algorithm. Doing this for all the DOF that are set to be measured for certain external excitations, the FRF matrix $\left[H\left(\Omega\right)\right]$ can be built. As stated before, the inverse of this matrix is known as the impedance matrix $\left[Z\left(\Omega\right)\right]$:

$$\left[Z(\Omega)\right] = \left[H(\Omega)\right]^{-1} \tag{2.17}$$

where:

$$\left[Z(\Omega)\right] = \left[K - \Omega^2 M + j\Omega C\right] \tag{2.18}$$

In terms of an n DOF system and introducing impedance, Equation (2.4) can be written as:

$$\begin{bmatrix} Z_{11} & \cdots & Z_{1n} \\ \vdots & \ddots & \vdots \\ Z_{n1} & \cdots & Z_{nn} \end{bmatrix} \begin{Bmatrix} x_1(t) \\ \vdots \\ x_n(t) \end{Bmatrix} = \begin{Bmatrix} f_1 \\ \vdots \\ f_n \end{Bmatrix} \tag{2.19}$$

Letting $\{x\} = [\Phi]\{q\}$, where Φ is the mass normalized mode shapes of the system and q represents the generalized coordinate set, substituting in (2.19):

$$[Z][\Phi]\{q\} = \{f\} \tag{2.20}$$

Then premultiplying by $[\Phi]^T$ and combining Equations (2.18) and (2.20):

$$\left[[\Phi]^T[K][\Phi]-\Omega^2[\Phi]^T[M][\Phi]+j\Omega[\Phi]^T[C][\Phi]\right]\{q\}=[\Phi]^T\{F\} \tag{2.21}$$

Since Φ is mass normalized $[\Phi]^T[M][\Phi]=1$, and assuming proportional damping $[C]=\alpha*[K]+\beta*[M]$:

$$\left[\omega_i^2-\Omega^2+2j\zeta\Omega\omega_i\right]\{q\}=[\Phi]^T\{F\} \tag{2.22}$$

In Equation 2.22, ω_i is the i^{th} natural frequency, Ω is the forcing frequency and ζ is the systems damping ratio. The term $\left[\omega_i^2-\Omega^2+2j\zeta\Omega\omega_i\right]$ is known as the modal impedance matrix and is diagonal. Inverting the modal impedance matrix and moving back to physical coordinates by premultiplying by $[\Phi]$, the frequency response is:

$$\{x\}=[\Phi]\frac{1}{\left[\omega_i^2-\Omega^2+2j\zeta\Omega\omega_i\right]}[\Phi]^T\{F\} \tag{2.23}$$

From Equation (2.23), the FRF matrix $\left[H(\Omega)\right]$ can be defined as:

$$[H(\Omega)]=[\Phi]\frac{1}{\left[\omega_i^2-\Omega^2+2j\zeta\Omega\omega_i\right]}[\Phi]^T \tag{2.24}$$

The FRF matrix can be rewritten in summation form:

$$[H(\Omega)]=\sum_{k=1}^{modes}\frac{\{\Phi^k\}\{\Phi^k\}^T}{\omega_k^2-\Omega^2+2j\zeta\Omega\omega_k} \tag{2.25}$$

and descriptively for any element in terms of $\left[H_{ij}(\Omega)\right]$:

$$\left[H_{ij}(\Omega)\right] = \sum_{k=1}^{modes} \frac{\left\{\Phi_i^k\right\}\left\{\Phi_j^k\right\}^T}{\omega_k^2 - \Omega^2 + 2j\zeta\Omega\omega_k} \tag{2.26}$$

It is obvious from Equation (2.26) that the FRF contains all the modal data for the system.

1. Driving Point and Transfer Point Functions

The exact FRF matrix, as mentioned, contains all the modal data of the system and thus the resonance and anti-resonance frequencies, which are of particular interest in modal analysis. It should be noted here that, depending on the relationship, in terms of locality, of the i^{th} DOF where the response is measured with the j^{th} DOF where the force is applied, the FRF is referred to as the Driving Point Function for the case that these two DOF are identical and Transfer Function for all the other cases.

What follows is an example of FRF derivation, covering both Driving Point and Transfer Function, for a simple two DOF system with no damping [16].

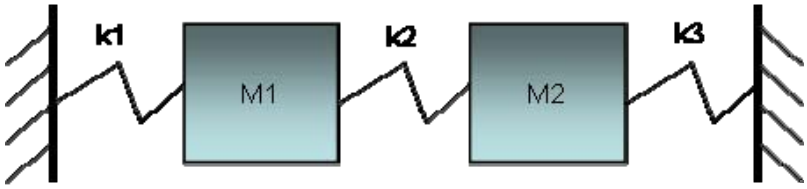

Figure 1. 2-DOF Example

The properties of this system are summarized in the stiffness and mass matrices above:

$$\left[K\right] = \begin{bmatrix} K_1 + K_2 & -K_2 \\ -K_2 & K_2 + K_3 \end{bmatrix} \quad \text{and} \quad \left[M\right] = \begin{bmatrix} M_1 & 0 \\ 0 & M_2 \end{bmatrix}$$

Let, for this example, $M_1 = M_2 = 1.0$ and $K_1 = K_3 = 0.4$ and $K_2 = 0.8$. This yields the following results:

Mode shapes: $\{\Phi^1\} = \begin{Bmatrix} -0.7071 \\ -0.7071 \end{Bmatrix}$ and $\{\Phi^2\} = \begin{Bmatrix} -0.7071 \\ 0.7071 \end{Bmatrix}$

Natural frequencies: $\{\omega(rad/\sec)\} = \begin{Bmatrix} 0.6325 \\ 1.0954 \end{Bmatrix}$

Using these values in Equation (2.26), $\left[H_{ij}(\Omega)\right] = \sum_{k=1}^{modes} \frac{\{\Phi_i^k\}\{\Phi_j^k\}^T}{\omega_k^2 - \Omega^2 + 2j\zeta\Omega\omega_k}$ results in:

$$\left[H_{11}(\Omega)\right] = \frac{\{\Phi_1^1\}\{\Phi_1^1\}^T}{\omega_1^2 - \Omega^2} + \frac{\{\Phi_1^2\}\{\Phi_1^2\}^T}{\omega_2^2 - \Omega^2} = \frac{\{-0.7071\}\{-0.7071\}^T}{0.4 - \Omega^2} + \frac{\{-0.7071\}\{-0.7071\}^T}{1.2 - \Omega^2} \qquad (2.27)$$

for the Driving Point function and for the Transfer function in:

$$\left[H_{12}(\Omega)\right] = \frac{\{\Phi_1^1\}\{\Phi_2^1\}^T}{\omega_1^2 - \Omega^2} + \frac{\{\Phi_1^2\}\{\Phi_2^2\}^T}{\omega_2^2 - \Omega^2} = \frac{\{-0.7071\}\{-0.7071\}^T}{0.4 - \Omega^2} + \frac{\{-0.7071\}\{0.7071\}^T}{1.2 - \Omega^2} \qquad (2.28)$$

What is evitable from Equation (2.27) for the driving point is that for frequencies below and above the natural frequencies of the system, the two terms will have the same sign, while between them, they will have the opposite sign. This means that in the first case, the two terms are additive, where in the second they are subtractive. Furthermore, this effect creates resonances at forcing frequencies equal to the natural frequencies and for the particular values between them, the two terms of the equation may result in zero value, thus points of anti-resonance are created. Therefore, anti-resonance follows every resonance, without exception, as seen in the top portion of Figure 2.

On the other hand, there is no reason to expect something similar for the Transfer Function, because obviously the two terms of Equation (2.28) will sometimes be additive and sometimes be subtractive, as the product of the two eigenvectors—called modal constant—will be sometimes positive and sometimes negative. Thus, we expect Transfer FRF measurements to show a mixture of anti-resonances and minima. It can be shown that, in general, the further apart the two points in question are, the more likely the two eigenvector elements are to alternate in sign as one progresses through the modes [17]. The above conclusions are shown in the lower portion of Figure 2.

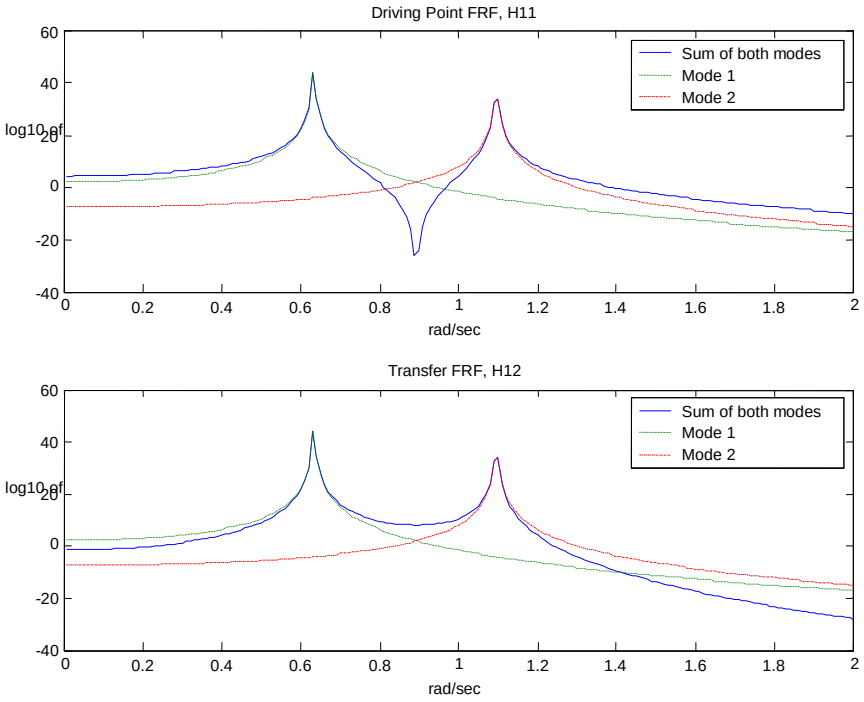

Figure 2. 2-DOF Frequency Response Function.

The principles demonstrated in the above example can be applied to any number of DOF. This concept of the existence of anti-resonance between any two modes of a driving point FRF is of great significance in the use of Artificial Boundary Conditions.

D. ARTIFICIAL BOUNDARY CONDITIONS

As discussed previously, the generation of additional data for a spatially incomplete FE model analysis can be pursued via Artificial Boundary Conditions, or ABC. This way, a number of ABC can be applied to an FE model, thus constructing several models differing only in boundary conditions. Hence, a new model configuration is provided, yet only one set of measured data is required. Applying the driving point function concept shows that the ABC frequencies of a certain ASET coordinate are defined by the corresponding driving point anti-resonances. In other words, these ABCs are the boundary conditions that define the OSET, from which it is shown that additional frequency information about the model is provided. The following examples describe

how anti-resonance frequencies are identical to the natural frequencies corresponding to the system with the associate driving point constrained to the ground [13].

1. ABC Frequencies for a 2-DOF System

Consider the system shown in Figure 3, excluding damping:

Figure 3. 2-DOF System

From Equation (2.26), the driving point FRF is

$$H_{ii}(\Omega) = \sum_{k=1}^{modes} \frac{(\Phi_i^k)^2}{\omega_k^2 - \Omega^2} \tag{2.29}$$

where Φ_i is the mass normalized mode shape element, ω_k is the ***k***th natural frequency, and Ω is the forcing frequency.

Solving for the frequency of the anti-resonance of $H_{11}(\Omega)$ yields:

$$\Omega_{anti-res}^2 = \frac{R_{11}^1 \omega_2^2 + R_{11}^2 \omega_1^2}{R_{11}^1 + R_{11}^2} \tag{2.30}$$

where the modal residue is given by $R_{ij}^k = \Phi_i^k \Phi_j^k$.

Let M1 = M2 = 1.0 and K1 = K2 = 1.0. Then the stiffness and mass matrices of the system are:

$$[K] = \begin{bmatrix} K_1 + K_2 & -K_2 \\ -K_2 & K_2 + K_3 \end{bmatrix} = \begin{bmatrix} 1 & -1 \\ -1 & 2 \end{bmatrix} \qquad \text{and} \qquad [M] = \begin{bmatrix} M_1 & 0 \\ 0 & M_2 \end{bmatrix} = \begin{bmatrix} 1 & 0 \\ 0 & 1 \end{bmatrix}$$

Solving the eigenproblem related to them yields to:

Mode shapes: $\{\Phi^1\} = \begin{Bmatrix} -0.85065 \\ -0.52573 \end{Bmatrix}$ $\{\Phi^2\} \begin{Bmatrix} -0.52573 \\ 0.85065 \end{Bmatrix}$

Natural frequencies: $\{\omega(rad/\sec)\} = \begin{Bmatrix} 0.618 \\ 1.618 \end{Bmatrix}$

and the single anti-resonance at $\Omega_{antires} = \sqrt{2}$ rad/sec, as shown in Figure 4.

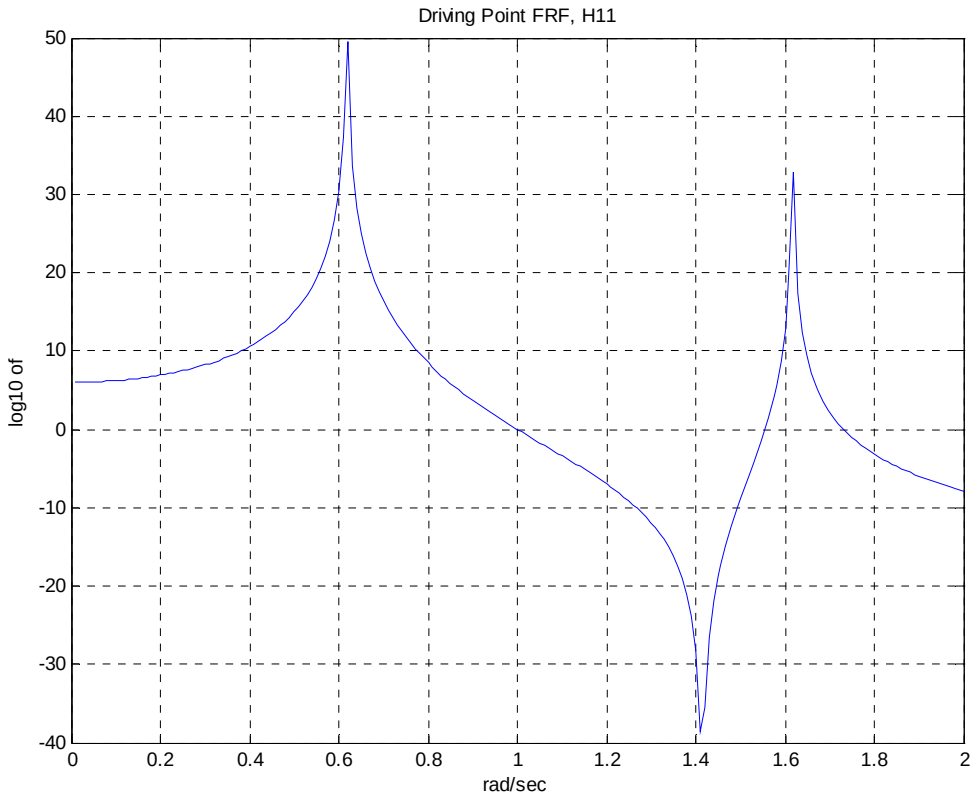

Figure 4. Driving Point FRF, H11

Now, consider the same system pinned at DOF 1, as shown in Figure 5:

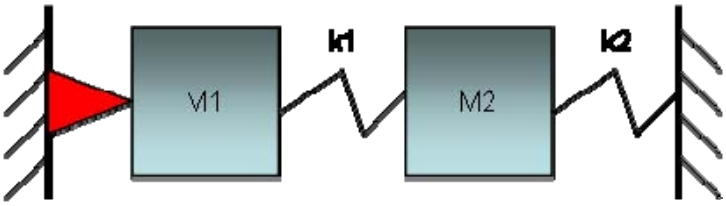

Figure 5. DOF #1 Constrained to Ground

This system's natural frequency is $\omega = \sqrt{2}$ rad/sec and identically equal to the anti-resonance of the unconstrained system of Figure 3. The same result for the constrained system can be found by making use of Equation (2.13), that is, by calculating the inverse of the ASET FRF partition that is constrained $H_{aa}^{-1}(\Omega)$, which in this case is the inverse of $H_{11}(\Omega)$. The correlation between the driving point anti-resonance and the natural frequency of the system with the driving point constrained to ground is shown in Figure 6 [13].

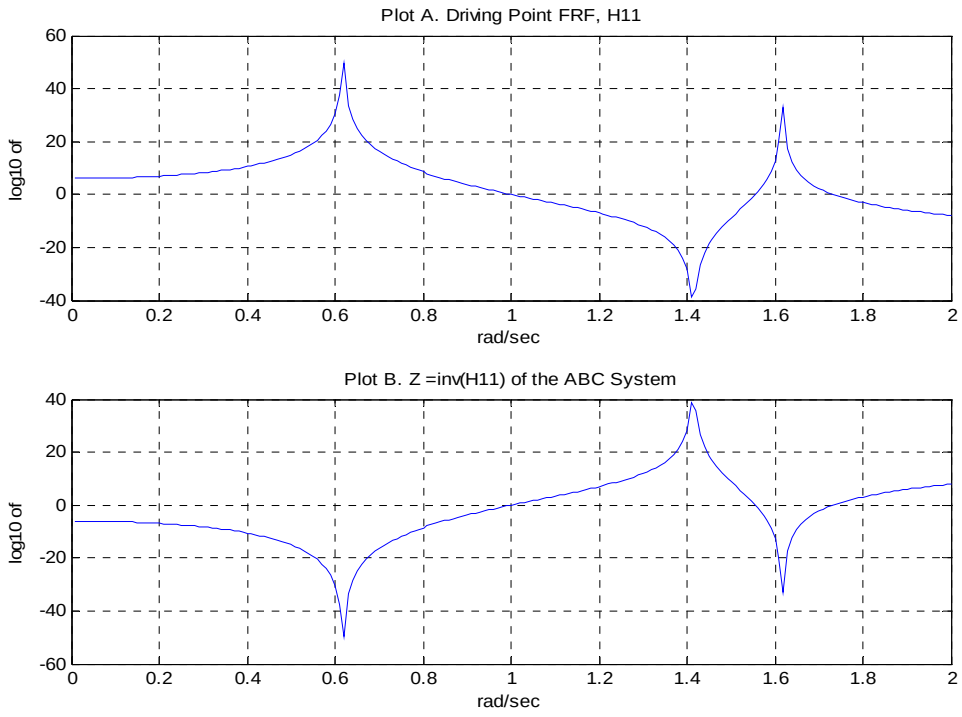

Figure 6. Plot A. Driving Point H11(Ω) of System 1, Plot B. [Haa(Ω)]-1 of System 2

2. ABC Frequencies for a Free-Free Beam

The model depicted in Figure 7 consists of ten beam elements and each element contains two nodes with two DOF each, the odd-numbered DOF being translational, and the even numbered DOF being rotational. Response transducers are set up at the translational DOF: 1, 5, 9, 13, 17, and 21 as follows:

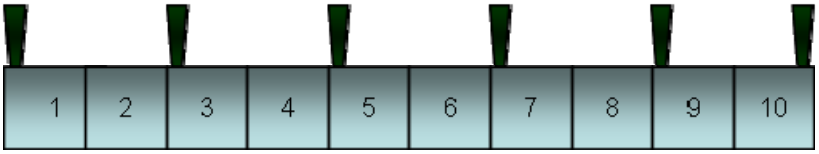

Figure 7. Transducers Located at DOF 1, 5, 9, 13, 17, and 21

The location of the response accelerators represent the ASET, defined as [1, 5, 9, 13, 17, 21]. If it is assumed that the excitation is applied at each of the ASET DOF, then a square (6 x 6) FRF matrix will result from the testing. Then the impedance matrix $H_{aa}^{-1}(\Omega)$ is calculated in the bandwidth 0-800 Hz. Figure 8 shows the driving point FRF of the system.

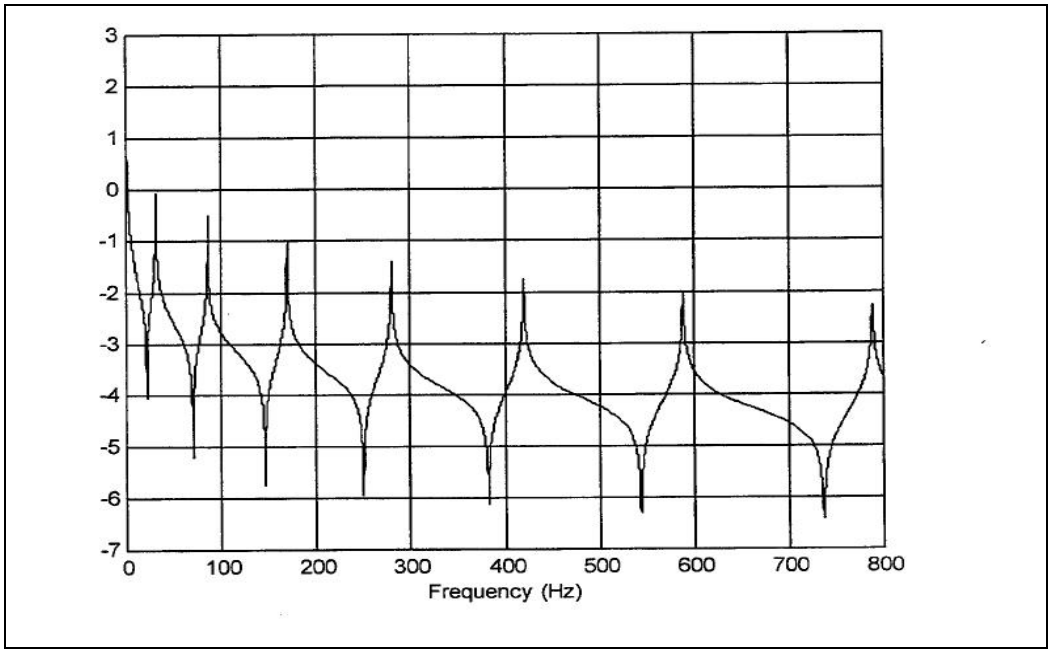

Figure 8. Driving Point FRF ASET DOF: 1 5 9 13 17 21. (From [13])

Now, consider the same system with all the ASET DOF constrained to the ground, as shown in Figure 9.

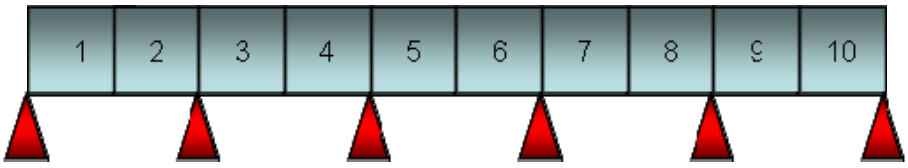

Figure 9. ABC Configuration ASET [1 5 9 13 17 21] (Measured Coordinates Restrained to Ground)

By calculating the impedance matrix $H_{aa}^{-1}(\Omega)$ and plotting the $H_{11}(\Omega)$ of the matrix in the same bandwidth of 0-800 Hz, Figure 10 is generated:

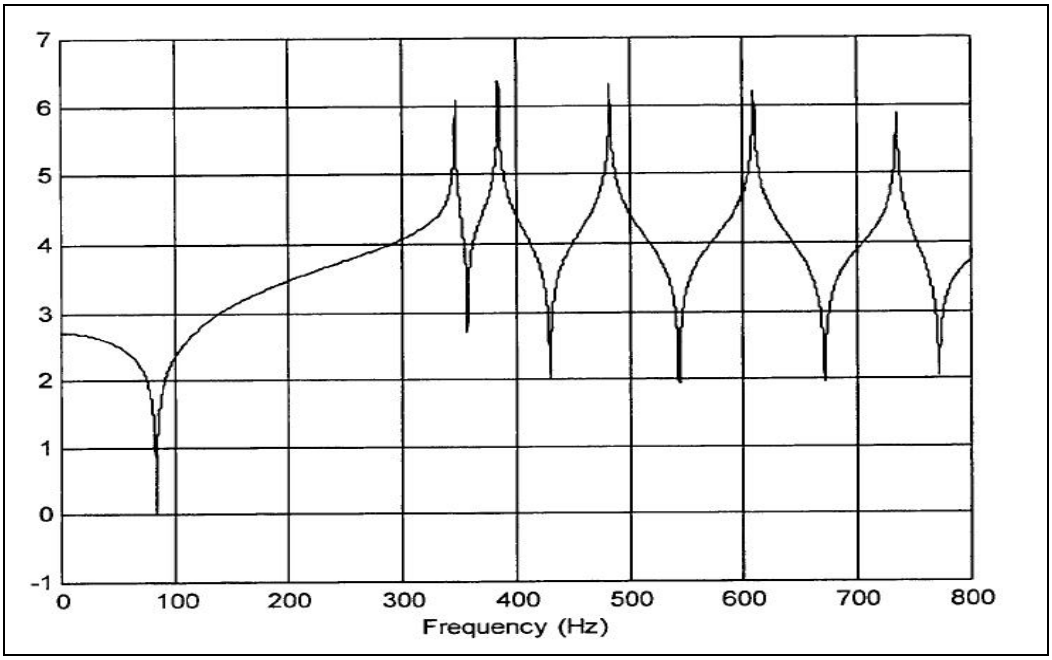

Figure 10. Impedance FRF for ASET DOF: 1 5 9 13 17 21 (From [13])

By deriving the ABC frequencies of the system in Figure 9, it is obvious that they correspond exactly to the resonances of the impedance FRF for ASET coordinates the DOF, which are constrained to the ground.

E. SENSITIVITY BASED FEM UPDATING

Sensitivity analysis in structural dynamics is a tool used for predicting the effect of small changes in design parameters on dynamic response characteristics. It involves finding how a system alters its dynamic response when some parameters that define its properties are subject to a change. From a mathematical point of view, it implies differentiation, which in the present analysis, is carried out through finite difference calculations. The parameters of the system to be changed, stated as design variables, are in this case, only stiffness parameters, whereas other parameters, like mass or density can be taken into consideration. The output of the system to be examined using sensitivities, due to an input parameter change, can be one or both of the following: natural frequencies, eigenvalue sensitivity and mode shapes, eigenvector sensitivity. Another aspect of modal data analysis via sensitivity is the Frequency Response Function Sensitivity Analysis, which is not covered in this thesis.

Recalling the ABC concept, it is shown that ABC configurations can be used along with the baseline system into a combined sensitivity matrix, for model updating [13]. The key part of this is that ABC frequencies can easily be found, as stated previously, and since the design variables are common for both the ABC and the baseline system, they can be used to reliably enlarge the modal data for the analysis.

The equation that describes what is mentioned above about sensitivity based updating is:

$$\left\{\Delta\omega^2\right\} = \left[T\right]\left\{\Delta DV\right\} \tag{2.31}$$

where $\left\{\Delta\omega^2\right\}$ is a vector containing the difference between the experimental and the analytical (FE baseline) natural frequencies $\left\{\omega_x^2 - \omega_\alpha^2\right\}$. The $\left\{\Delta DV\right\}$ term is the vector containing the design variables, and $\left[T\right]$ is the sensitivity matrix.

Each column of the sensitivity matrix represents an element of the model, whereas each row represents a mode of the model.

Each ABC system defines additional rows to Equation (2.31). It is obvious from this point that even with low modes, in terms of frequency spectrum, that is with the first few modes of baseline and ABC systems, a more determined sensitivity matrix can be built. Representing the baseline system quantities with the superscript "0" and the ABC systems with the superscripts from 1 to "k," where k represents the number of ABC used in the system, the following equation shows how this is compromised [13]:

$$\begin{Bmatrix} \Delta\omega_{BASE}^{2(0)} \\ \Delta\omega_{ABC1}^{2(1)} \\ \vdots \\ \Delta\omega_{ABCk}^{2(k)} \end{Bmatrix} = \begin{pmatrix} T^{(0)}{}_{BASE} \\ T^{(1)}{}_{ABC1} \\ \vdots \\ T^{(k)}{}_{ABCk} \end{pmatrix} \begin{Bmatrix} dV_1 \\ \vdots \\ dV_n \end{Bmatrix} \tag{2.32}$$

1. Eigenvalue Sensitivity Matrix Derivation.

The starting point of the derivation is the eigenvalue problem of an *n* DOF system:

$$\left[K - \lambda_i M\right]\left\{\Phi_i\right\} = \left\{0\right\} \tag{2.33}$$

Differentiating with respect to the design variable {DV}:

$$\left[\frac{\Delta K}{\Delta DV} - \lambda_i \frac{\Delta M}{\Delta DV} - \frac{\Delta \lambda_i}{\Delta DV}\right]\left\{\Phi_i\right\} + \left[K - \lambda_i M\right]\left\{\frac{\Delta \Phi_i}{\Delta DV}\right\} = \left\{0\right\} \tag{2.34}$$

Expanding Equation (2.34) and premultiplying by $\left\{\Phi\right\}^T$ leads to:

$$\left\{\Phi_i\right\}^T\left[\frac{\Delta K}{\Delta DV}\right]\left\{\Phi_i\right\} - \lambda_i\left\{\Phi_i\right\}^T\left[\frac{\Delta M}{\Delta DV}\right]\left\{\Phi_i\right\} - \left[\frac{\Delta \lambda_i}{\Delta DV}\right]\left\{\Phi_i\right\}^T\left[M\right]\left\{\Phi_i\right\} + \left\{\Phi_i\right\}^T\left[K - \lambda_i M\right]\left\{\frac{\Delta \Phi_i}{\Delta DV}\right\} = \left\{0\right\} \tag{2.35}$$

By invoking the matrix identity property $\left\{a\right\}^T\left[b\right]\left\{c\right\} = \left\{c\right\}^T\left[b\right]\left\{a\right\}$, the last term on the left hand side can be replaced by:

$$\left\{\frac{\Delta \Phi_i}{\Delta DV}\right\}^T\left[K - \lambda_i M\right]\left\{\Phi_i\right\} = 0 \tag{2.36}$$

Since $[K-\lambda_i M]\{\Phi_i\}=\{0\}$ and recalling the mass normalization of the mode shapes, where $[\Phi_i]^T[M][\Phi_i]=1$, the overall equation is reduced to:

$$\{\Phi_i\}^T\left[\frac{\Delta K}{\Delta DV}\right]\{\Phi_i\}-\lambda_i\{\Phi_i\}^T\left[\frac{\Delta M}{\Delta DV}\right]\{\Phi_i\}-\left[\frac{\Delta\lambda_i}{\Delta DV}\right]=\{0\} \tag{2.37}$$

Bringing the mass and stiffness portion to the right hand side

$$\left[\frac{\Delta\lambda_i}{\Delta DV}\right]=\{\Phi_i\}^T\left[\frac{\Delta K}{\Delta DV}-\lambda_i\frac{\Delta M}{\Delta DV}\right]\{\Phi_i\} \tag{2.38}$$

As stated previously, the present analysis only takes into account changes in the stiffness parameters. Therefore, the second term $\lambda_i\frac{\Delta M}{\Delta DV}$ in the square brackets of the right hand side can be neglected as $\Delta M=0$, yielding to:

$$\left[\frac{\Delta\lambda_i}{\Delta DV}\right]=\{\Phi_i\}^T\left[\frac{\Delta K}{\Delta DV}\right]\{\Phi_i\} \qquad \text{where} \quad [\Delta K]=[K_x-K_a] \tag{2.39}$$

and finally:

$$[T_{stiffness}]=\{\Phi_i\}^T\left[\frac{\Delta K}{\Delta DV}\right]\{\Phi_i\} \tag{2.40}$$

It has been shown [18] that when ABC are applied, the model tends to concentrate high stiffness sensitivity values around the particular DOF where the ABC is located. This concept, along with the fact that the baseline model is not likely to predict changes in natural frequencies in regions with low sensitivity values, is of great significance in the analysis of the following chapters.

2. Eigenvector Sensitivity Matrix Derivation

The calculation of the eigenvector sensitivity is a less straightforward problem than that of the eigenvalue sensitivity. The foundation for the calculation was laid primarily by Fox and Kapoor [19] and a simplified method, which is the basis of the

NASTRAN computation scheme, is provided later by Nelson [20]. A survey of several contributions to the literature regarding the eigenvector sensitivity calculation is available in [21].

The derivation that follows is based on Blelloch's report [22]. After having calculated the eigenvalue sensitivity from Equation (2.39), returning to Equation (2.34) and solving for the eigenvector derivative, again for no mass variation yields to:

$$\left[K-\lambda_i M\right]\left\{\frac{\Delta\phi_i}{\Delta DV}\right\}=-\left[\frac{\Delta K}{\Delta DV}-\frac{\Delta\lambda_i}{\Delta DV}M\right]\left\{\phi_i\right\} \tag{2.41}$$

Assume at this point that all the eigenvectors are available for the system under consideration. In this case, the eigenvector derivative can be expressed as a linear combination of all the eigenvectors:

$$\left\{\frac{\Delta\phi_i}{\Delta DV}\right\}=\left[\Phi\right]\left\{c\right\} \tag{2.42}$$

where $\left[\Phi\right]$ is the matrix containing all the eigenvectors and $\left\{c\right\}$ is the vector of the coefficients to be determined. Substituting to Equation (2.41) and premultiplying by $\left[\Phi\right]^T$ generates:

$$\left[\Phi\right]^{\mathrm{T}}\left[K-\lambda_i M\right]\left[\Phi\right]\left\{c\right\}=-\left[\Phi\right]^{\mathrm{T}}\left[\frac{\Delta K}{\Delta DV}-\frac{\Delta\lambda_i}{\Delta DV}M\right]\left\{\phi_i\right\} \tag{2.43}$$

The expression that premultiplies $\left\{c\right\}$ is of the form:

$$\left[\Phi\right]^{\mathrm{T}}\left[K-\lambda_i M\right]\left[\Phi\right]=\left[\Lambda-\lambda_i \mathrm{I}\right] \tag{2.44}$$

where Λ is the diagonal matrix of eigenvalues. The above implies that, for distinct eigenvalues, every element of the coefficient vector $\left\{c\right\}$ except for the *ith* element $\left(c_i\right)$ is uniquely determined as follows:

$$c_k = -\frac{\{\phi_k\}^{\mathrm{T}}\left[\frac{\Delta K}{\Delta DV} - \frac{\Delta \lambda_i}{\Delta DV} M\right]\{\phi_i\}}{\lambda_k - \lambda_i} \tag{2.45}$$

At this point, it should be noted that there is no reason to believe that the eigenvector derivative will predict the change in the eigenvector in models with closely spaced eigenvalues, since from what can be seen from Equation (2.45) numerical ill-conditioning will occur in these cases.

The eigenvector derivative can now be written as:

$$\left\{\frac{\Delta \phi_i}{\Delta DV}\right\} = \sum_{k \neq i} c_k \{\phi_k\} + c_i \{\phi_i\} = \{V_i\} + c_i \{\phi_i\} \tag{2.46}$$

In this expression, the vector $\{V_i\}$ is determined uniquely. The undetermined coefficient c_i will be found on the basis of differentiating the mass normalization formula for the eigenvectors:

$$\frac{\partial}{\partial DV}(\{\phi_i\}^T [M]\{\phi_i\} = 1)$$

to have:

$$2\{\phi_i\}^T [M]\left\{\frac{\partial \phi_i}{\partial DV}\right\} + \{\phi_i\}^T \left[\frac{\partial M}{\partial DV}\right]\{\phi_i\} = 0 \tag{2.47}$$

Again, for no mass variation and substituting Equation (2.46) into Equation (2.47):

$$c_i = -\{\phi_i\}^{\mathrm{T}} [M]\{V_i\} \tag{2.48}$$

The key to the whole method that Nelson [20] indicated is that there is no need to calculate the unique $\{V_i\}$. In fact, any vector that satisfies Equation (2.41) can be used and an available check, as stated in [22], is that the eigenvector derivative is orthogonal to the eigenvector. Following, in trying to find an arbitrary non- trivial solution for $\{V_i\}$, the any *kth* row and column are partitioned from the eigenproblem matrix as follows:

$$\begin{bmatrix} (K-\lambda_i M)_{11} & (K-\lambda_i M)_{1k} & (K-\lambda_i M)_{13} \\ (K-\lambda_i M)_{k1} & (K-\lambda_i M)_{2k} & (K-\lambda_i M)_{k1} \\ (K-\lambda_i M)_{31} & (K-\lambda_i M)_{3k} & (K-\lambda_i M)_{33} \end{bmatrix} \begin{Bmatrix} x_1 \\ x_k \\ x_3 \end{Bmatrix} = \begin{Bmatrix} 0 \\ 0 \\ 0 \end{Bmatrix} \tag{2.49}$$

Choosing *k* such that x_k is non-zero and solving for x_1 and x_3 in terms of x_k:

$$\begin{bmatrix} (K-\lambda_i M)_{11} & (K-\lambda_i M)_{13} \\ (K-\lambda_i M)_{k1} & (K-\lambda_i M)_{k3} \\ (K-\lambda_i M)_{31} & (K-\lambda_i M)_{33} \end{bmatrix} \begin{Bmatrix} x_1 \\ x_3 \end{Bmatrix} = -x_k \begin{Bmatrix} (K-\lambda_i M)_{1k} \\ (K-\lambda_i M)_{kk} \\ (K-\lambda_i M)_{3k} \end{Bmatrix} \tag{2.50}$$

Since the *kth* row (equal to the *kth* column due to symmetric matrices) is linearly dependent on the (*n-1*) remaining rows, the *kth* row can be eliminated and a system of (*n-1*) equations of rank (*n-1*) is guaranteed as follows:

$$\begin{bmatrix} (K-\lambda_i M)_{11} & (K-\lambda_i M)_{13} \\ (K-\lambda_i M)_{31} & (K-\lambda_i M)_{33} \end{bmatrix} \begin{Bmatrix} x_1 \\ x_3 \end{Bmatrix} = -x_k \begin{Bmatrix} (K-\lambda_i M)_{1k} \\ (K-\lambda_i M)_{3k} \end{Bmatrix} \tag{2.51}$$

Evoking that $\{V_i\}$ is arbitrary; its *kth* element can be set to zero and using Equation (2.51) to solve for $\{V_i\}$ results:

$$\begin{bmatrix} (K-\lambda_i M)_{11} & (K-\lambda_i M)_{13} \\ (K-\lambda_i M)_{31} & (K-\lambda_i M)_{33} \end{bmatrix} \begin{Bmatrix} V_1 \\ V_3 \end{Bmatrix} = -\begin{Bmatrix} \left(\left[\frac{\Delta K}{\Delta DV} - \frac{\Delta \lambda_i}{\Delta DV} M \right] \{\phi_i\} \right)_1 \\ \left(\left[\frac{\Delta K}{\Delta DV} - \frac{\Delta \lambda_i}{\Delta DV} M \right] \{\phi_i\} \right)_3 \end{Bmatrix} \tag{2.52}$$

The unique solution for the eigenvector derivative will then be:

$$\left\{ \frac{\partial \phi_i}{\partial DV} \right\} = \begin{Bmatrix} V_1 \\ 0 \\ V_3 \end{Bmatrix} + c_i \phi_i \tag{2.53}$$

where $\{V_1\}$ and $\{V_3\}$ are calculated from Equation (2.52) and c_i from Equation (2.48). An algorithm for calculating the eigenvector derivative (sensitivity), assuming eigenvalue sensitivity has already been calculated, is given below [22]:

- Loop over all eigenvalues
  - Calculate the left hand side matrix $[D_i] = [K - \lambda_i M]$
  - Select *k* based on the largest element of $\{\phi_i\}$
  - Partition out *kth* row and column from $[D_i]$
  - Decompose the matrix $[D_i]$
  - Loop overall design variables
    - Calculate the RHS vector $\{F_i\} = -\left[\frac{\Delta K}{\Delta DV} - \frac{\Delta \lambda_i}{\Delta DV} M\right]\{\phi_i\}$
    - Forward Backwards Substitution to calculate $\{V_i\}$
    - Merge $\{V_i\}$ to an *n*-vector by adding zero *kth* element
    - Calculate $c_i = -\{\phi_i\}^{\mathrm{T}}[M]\{V_i\}$
    - Eigenvector derivative is given by $\{V_i\} + c_i\{\phi_i\}$
  - End of design variable loop
- End of eigenvalue loop

F. CORRELATION OF STRAIN ENERGY TO SENSITIVITY MATRIX

At this point, it would be useful to make a brief analysis of the strain energy of a dynamic system and to examine how it is correlated to the sensitivity matrix. A relevant analysis has been performed in [18], where the shape functions of an Euler- Bernoulli beam were used for the derivation of the strain energy of the system. In this work, after having set the FE model for the structure, which requires the calculation of the system's mode shapes and of each element stiffness matrix, a simpler approach was made using the trivial equation:

$$U = \frac{1}{2} kx^2 \tag{2.54}$$

which for each element of the model using modal data is translated into:

$$U^e = \frac{1}{2} \left[\Phi^e \right]^{\mathrm{T}} \left[K^e \right] \left[\Phi^e \right] \tag{2.55}$$

where $\left[K^e \right]$ stands for the element stiffness matrix and $\left[\Phi^e \right]$ stands for the partition of the mode shape matrix that contains the eigenvectors related to the DOF associated with the particular element. It is of vital importance to be noted here, that this mode shape matrix is not the original eigenvector matrix of the baseline system, in the way that it has been modified in order to take into account the physical boundary conditions of the system which may occur in some of the elements' boundaries. For example, consider a cantilever beam with its left end clamped is examined and the $\left[\Phi^e \right]$ corresponding to the first element of the FE model. The entries of the matrix associated with the right two DOF of the element will be covered by the entries of the baseline system eigenvector matrix associated with the first two (unconstrained as trivially defined) DOF of the cantilever beam, while the entries associated with the left two DOF of the element must be fulfilled with zeros corresponding to the constraint imposed to both the translational and the rotational DOF.

That said, and having derived the stiffness sensitivity matrix for the same system, a very remarkable conclusion is reached. As shown in the following Figures 11 and 12, where all the modes of a 10 element cantilever beam are depicted, there is an exact and direct correlation between the stiffness sensitivity matrix and the flexural properties of the structure. An appropriate scaling with normalization to the maximum value of its mode has been made to both of them in order to make the correlation more legible. In these figures, the x-axis has the number of elements; the y-axis has the normalized value of both the sensitivity matrix and the strain energy, which are referred to each mode of the system, respectively.

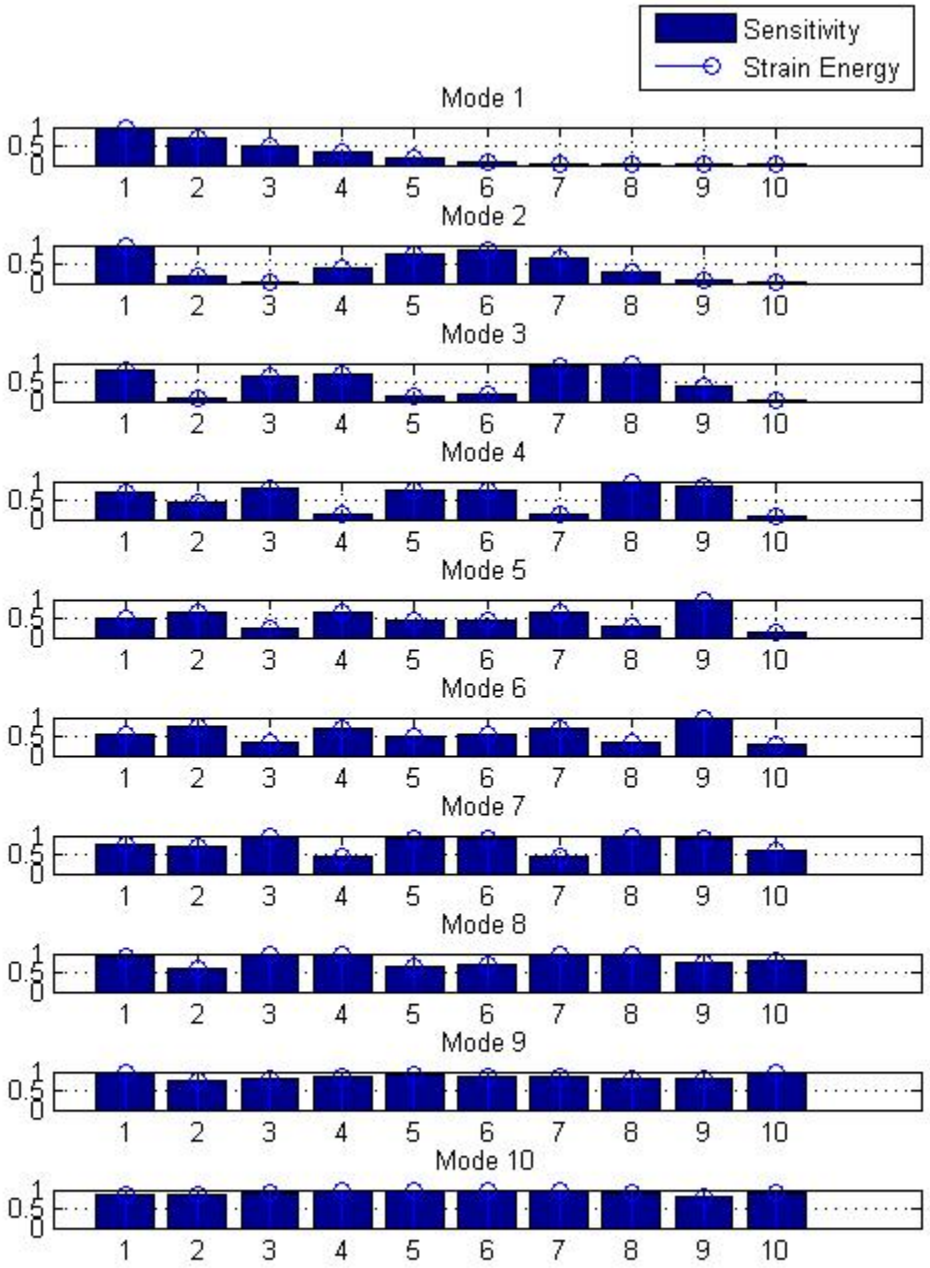

Figure 11. Correlation of Sensitivity Matrix to Strain Energy for Modes 1 Through 10

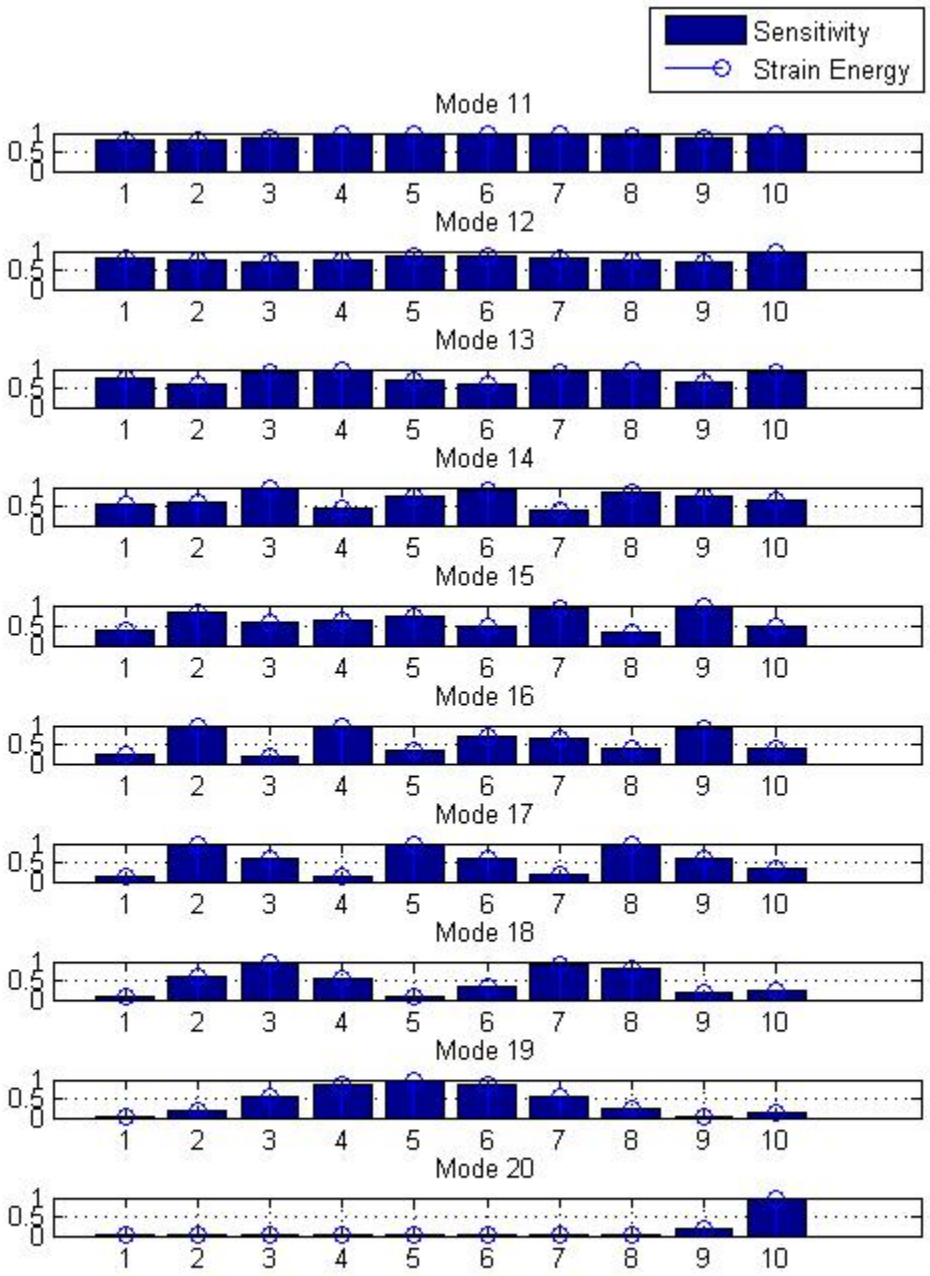

Figure 12. Correlation of Sensitivity Matrix to Strain Energy for Modes 11 Through 20

III. LINEAR SYSTEM SOLUTIONS IN SENSITIVITY BASED FEM UPDATING

As demonstrated in the previous chapters, the procedure of sensitivity-based FEM updating involved the solution of a linear system, which was almost always underdetermined. This linear system is governed by the Equation (2.31):

$$\left\{\Delta\omega^2\right\} = [T]\{\Delta DV\}$$

In FEM updating, the vector $\{\Delta DV\}$ contains corrections to the model parameters, while in damage detection, the vector $\{\Delta DV\}$ contains flags to both the location and severity of structural damage, relative to the undamaged FEM. In both cases, Equation (2.31) has to be solved for the design variables $\{\Delta DV\}$. This process constitutes an inverse type of mathematical problem, which requires the inversion of the sensitivity matrix $[T]$. Of course, this is feasible only if the matrix is square and full rank, which is rarely the case. For all cases where the sensitivity matrix is underdetermined, there are several algebraic methods of linear systems for solving the problem, which are covered in the literature [2].

A. USING BACKSLASH "\" AND "PINV" IN MATLAB

In this work, Matlab is used to carry out this procedure. In dealing with these kinds of systems, there are two available commands/operators that can provide the required pseudo-inverse of the sensitivity matrix; these are "\" or "mldivide," and "pinv." Respectively, they use orthogonal-triangular (QR) decomposition, and singular value decomposition (SVD). Eventually, they both give a least-squares (square and full rank overdetermined cases) or a least-norm (underdetermined and rank deficient cases) solution to Equation (2.31), which is pursued by minimizing the norm of the residual, i.e., $\min\left\|[T]\{\Delta DV\} - \left\{\Delta\omega^2\right\}\right\|_2$, except that they do it in different ways. From what has

already been discussed, it is obvious that for rank deficient problems, the solution obtained from each one is not exact. Some brief descriptions of how each of them is used [23] are given below.

1. Using "\" or "mldivide

The mldivide(A,B) and the equivalent A\B, perform matrix left division (back slash). A and B must be matrices that have the same number of rows, unless A is a scalar, in which case A\B performs element-wise division. If A is a square matrix, A\B is the same as inv(A)*B, where inv(A) stands for the inverse of A, except it is computed in a different way. If A is an n-by-n matrix and B is a column vector with n elements, or a matrix with several such columns, then X = A\B is the solution to the Equation AX = B computed by Gaussian elimination with partial pivoting. A warning message is displayed if A is badly scaled or nearly singular. If A is an m-by-n matrix and B is a column vector with m components, or a matrix with several such columns, then X = A\B is the solution in the least squares sense to the overdetermined system of Equations AX = B, only if the rank k is equal to n (number of columns). In other words, X minimizes norm(A*X - B), the length of the vector AX - B. The rank k of A is determined from the QR decomposition with column pivoting. If k < n or the system is underdetermined, this is not the same solution as x = pinv(A)*B, which returns a least-norm solution, but in this case X=A\B returns a solution that is called "basic" solution and has at most k non-zero elements per column.

2. Using "pinv"

The syntax B = pinv(A) returns the Moore-Penrose pseudoinverse of A. The Moore-Penrose pseudoinverse is a matrix B of the same dimensions as A' (transpose of A) satisfying the four following conditions: A*B*A = A, B*A*B = B, A*B and B*A are Hermitian. The computation is based on singular value decomposition of A. If A is square and not singular, then pinv(A) is an expensive way to compute inv(A). If A is not square, or is square and singular, then inv(A) does not exist. In these cases, pinv(A) has some, but not all of the properties of inv(A). If A has more rows than columns and is not

of full rank, then the overdetermined least squares problem of minimizing norm(A*x-b) does not have a unique solution. Two of the infinitely many solutions are x = pinv(A)*b and y = A\b. These two are distinguished by the facts that norm(x) is smaller than the norm of any other solution and that y has the fewest possible non-zero components as described for the use of "\".

3. Example Demonstrating the Difference Between the Two Commands

The following example is totally representative of the properties of the two Matlab operators for this kind of linear systems solving [23].

Assume the matrix generated by A = magic(8); A = A(:,1:6). This is an 8-by-6 matrix that happens to have rank(A) = 3:

$$A = \begin{bmatrix} 64 & 2 & 3 & 61 & 60 & 6 \\ 9 & 55 & 54 & 12 & 13 & 51 \\ 17 & 47 & 46 & 20 & 21 & 43 \\ 40 & 26 & 27 & 37 & 36 & 30 \\ 32 & 34 & 35 & 29 & 28 & 38 \\ 41 & 23 & 22 & 44 & 45 & 19 \\ 49 & 15 & 14 & 52 & 53 & 11 \\ 8 & 58 & 59 & 5 & 4 & 62 \end{bmatrix}$$, and the RHS is b = 260*ones(8,1), that is: $b = \begin{Bmatrix} 260 \\ 260 \\ 260 \\ 260 \\ 260 \\ 260 \\ 260 \\ 260 \end{Bmatrix}$

The scale factor 260 is the 8-by-8 magic sum. With all eight columns, one solution to A*x = b would be a vector of all 1s. With only six columns, the equations are still consistent, so a solution exists, but it is not all 1s. Since the matrix is rank deficient, there are an infinite number of solutions. Two of them are x = pinv(A)*b, which is:

$x = \begin{Bmatrix} 1.1538 \\ 1.4615 \\ 1.3846 \\ 1.3846 \\ 1.4615 \\ 1.1538 \end{Bmatrix}$, and y = A\b which produces the result: $y = \begin{Bmatrix} 4 \\ 5 \\ 0 \\ 0 \\ 0 \\ -1 \end{Bmatrix}$ with the following

warning: Rank deficient, rank= 3, tol= 1.8829e-013.

Both of these are exact solutions in the sense that norm(A*x-b) and norm(A*y-b) are on the order of round-off error. The solution x is special because norm(x) = 3.2817 is smaller than the norm of any other solution, including norm(y) = 6.4807. On the other hand, the solution y is special because it has only three non-zero components.

From the statement above, it is clear that in terms of damage detection and error localization, the most preferable operator for solving for the linear system corresponding to the structure's model is the "\", as it returns the minimum number of non-zero components. Using only one mode that is one sensitivity matrix row, it will return only one non-zero element, which for the right choice of mode, will be the element with the true error (as will be shown later, the right mode is the one whose highest value happens to be at the element where the true error occurs); whereas "pinv" will return a vector scaled by the mode used. Using more than one mode will provide the user with a more transparent result in terms of localization until a square matrix is reached where there is no difference between the two commands, provided the matrix is not rank deficient. This may prove to be of vital importance during the pursuing of optimal configurations, especially because it makes clear that modes of systems/configurations with locally concentrated sensitivity values will reveal errors at the corresponding elements where these values are laid.

B. SPATIALLY INCOMPLETE UNDERDETERMINED SYSTEMS

Realizing from what is demonstrated above, the least square and/or the least norm sense in which Matlab approaches that inverse mathematical problem, it is essential that a thorough understanding of how this linear system solution is depicted to the dynamic system in terms of damage detection, is possessed. For this purpose, an FE model of a cantilever beam consisting of ten beam elements is used. First, the baseline model is set and the modal data of the system, i.e., natural frequencies and mode shapes, are calculated, along with the stiffness sensitivity matrix through a perturbation of one percent reduction to the rigidity of each beam element, recursively. Then, another FE model is built, identical to the baseline with the only difference being the presence of damage somewhere in the structure. This damage is represented by a 10 percent rigidity

reduction and this model is used to provide simulated modal data from a structure that has localized damage. We will refer to the damage as the "error," recognizing that these concepts apply equally to identification of model error, or structural damage. The main objective is, after having the data for both the baseline and the damaged model and using the stiffness sensitivity matrix, to examine how the model can predict the true element in error, which is the design variable that is subject to the 10 percent rigidity reduction. It is noted here that the procedure is repeated iteratively for all the beam elements, in order to assess possible errors anywhere in the model.

1. Using Individual Modes

The starting point of this analysis is the use of only one mode of the available data. For demonstration purposes, only the first five out of the total twenty modes will be taken into consideration. The rows of the stiffness sensitivity matrix $[T]$ of the cantilever beam, which correspond to the modes of the system, are shown in the Figures 11 and 12 of the previous chapter. The first five rows are reproduced in Figure 13. Again the values are normalized to the maximum value of each row:

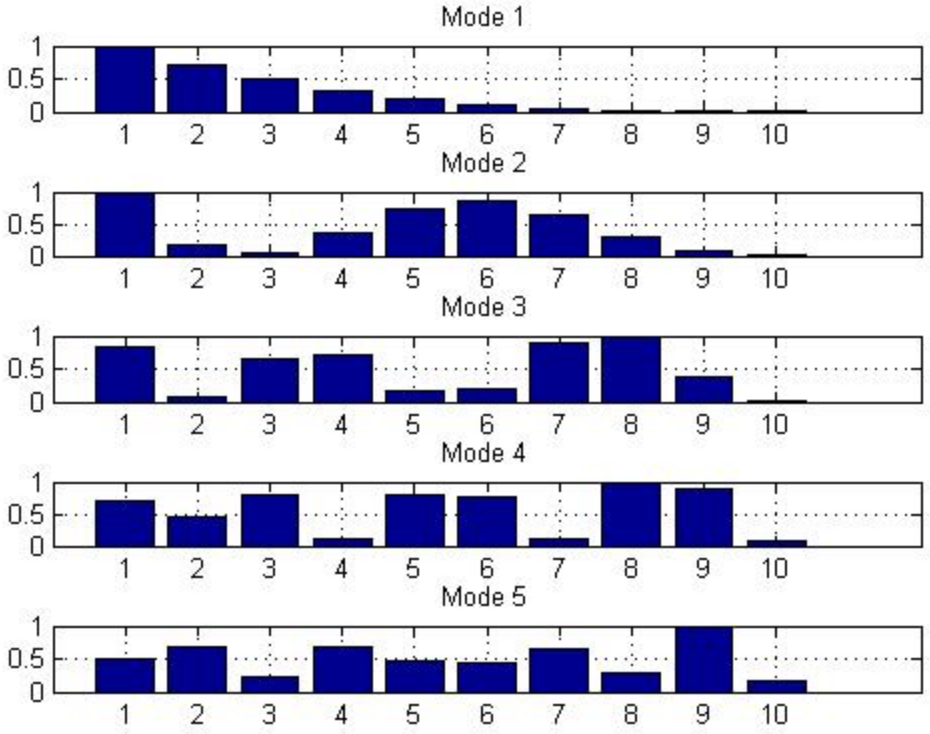

Figure 13. First 5 Rows of Stiffness Sensitivity Matrix

The numerical representation of these first five modes is given below:

$$[T_{1:5}] = \begin{bmatrix} 0.0006 & 0.0004 & 0.0003 & 0.0002 & 0.0001 & 0.0001 & 0.0000 & 0.0000 & 0.0000 & 0.0000 \\ 0.0163 & 0.0028 & 0.0008 & 0.0061 & 0.0121 & 0.0138 & 0.0103 & 0.0048 & 0.0011 & 0.0000 \\ 0.0904 & 0.0094 & 0.0691 & 0.0778 & 0.0170 & 0.0221 & 0.0977 & 0.1083 & 0.0407 & 0.0025 \\ 0.2518 & 0.1633 & 0.2888 & 0.0390 & 0.2834 & 0.2793 & 0.0435 & 0.3602 & 0.3188 & 0.0291 \\ 0.5564 & 0.7459 & 0.2616 & 0.7508 & 0.5051 & 0.4994 & 0.7337 & 0.3113 & 1.1042 & 0.1708 \end{bmatrix}$$

Now, the first five natural frequencies of the baseline system and of the perturbed (damaged) system, and the first five entries of vector $\{\Delta\omega^2\}$ formed by their difference are provided from the FE models.

This is all the information needed for solving Equation (2.31) for the change in the design variables $\{\Delta DV\}$. The following figures show the results for using a single

mode, i.e., individual modes 1 through 5, respectively, with the error being at each element, recursively. In all the figures, the y-axis represents the percentage error and the x-axis the number of the element:

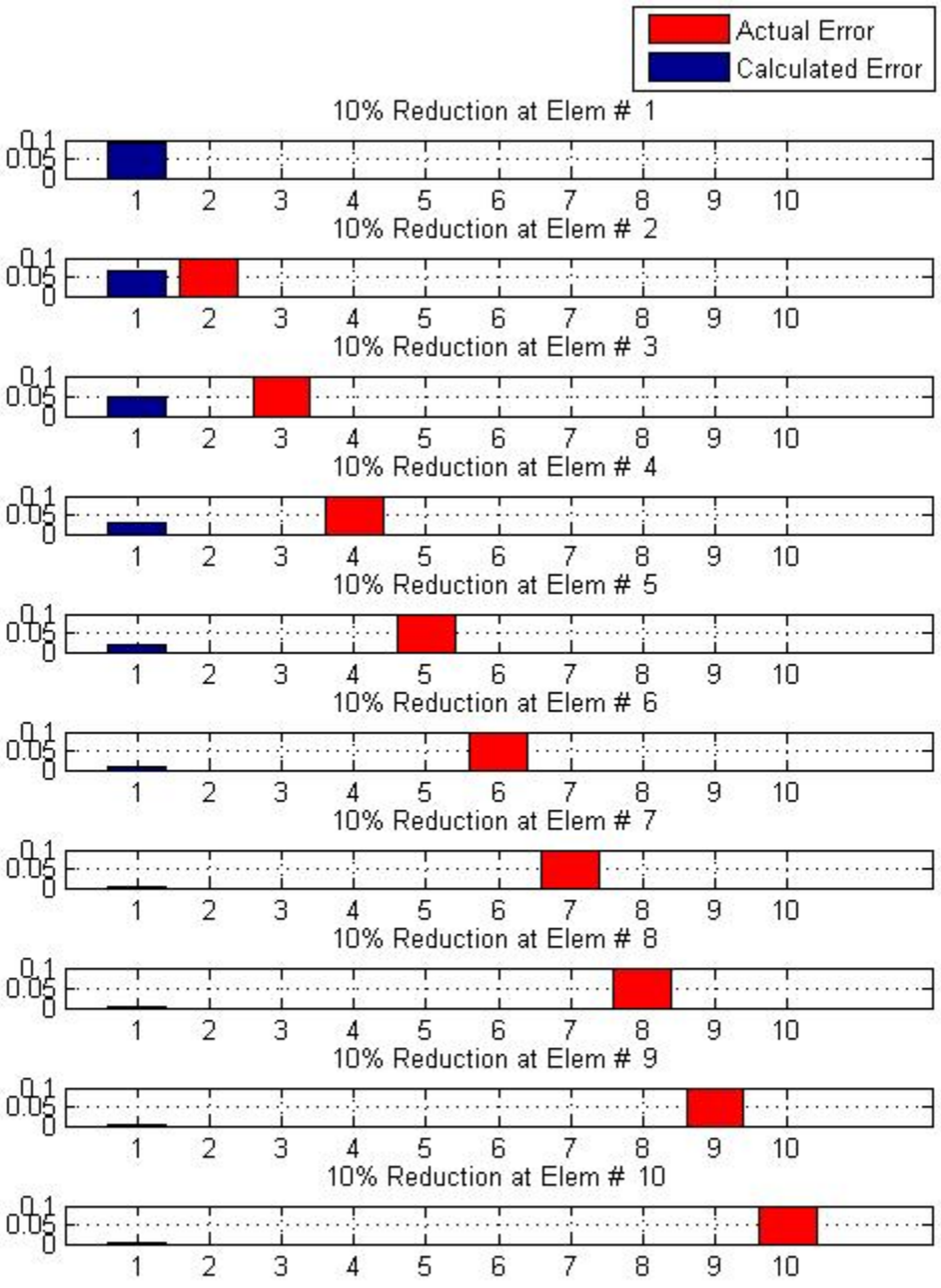

Figure 14. Solution Using the First Mode Only

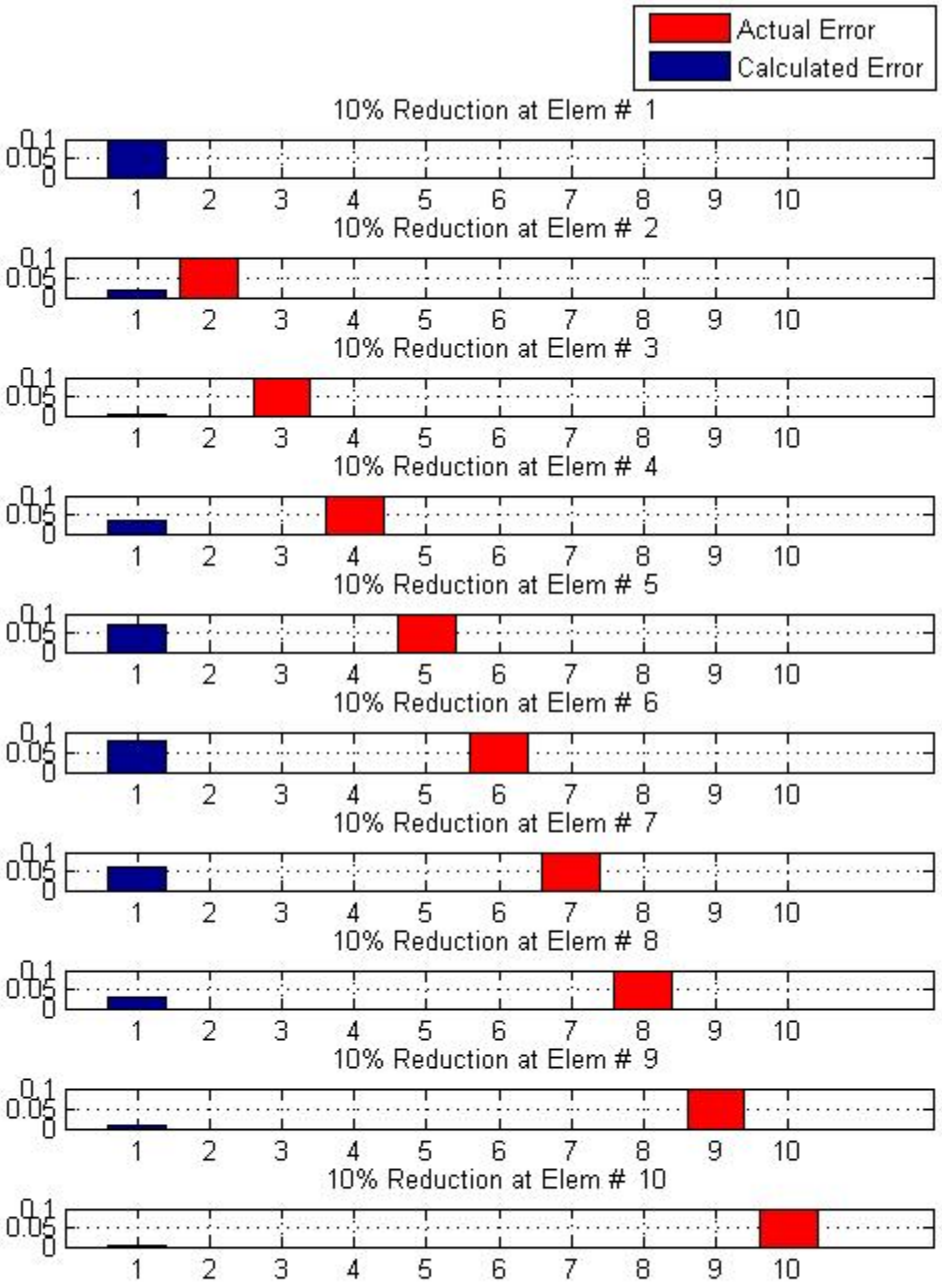

Figure 15. Solution Using the Second Mode Only

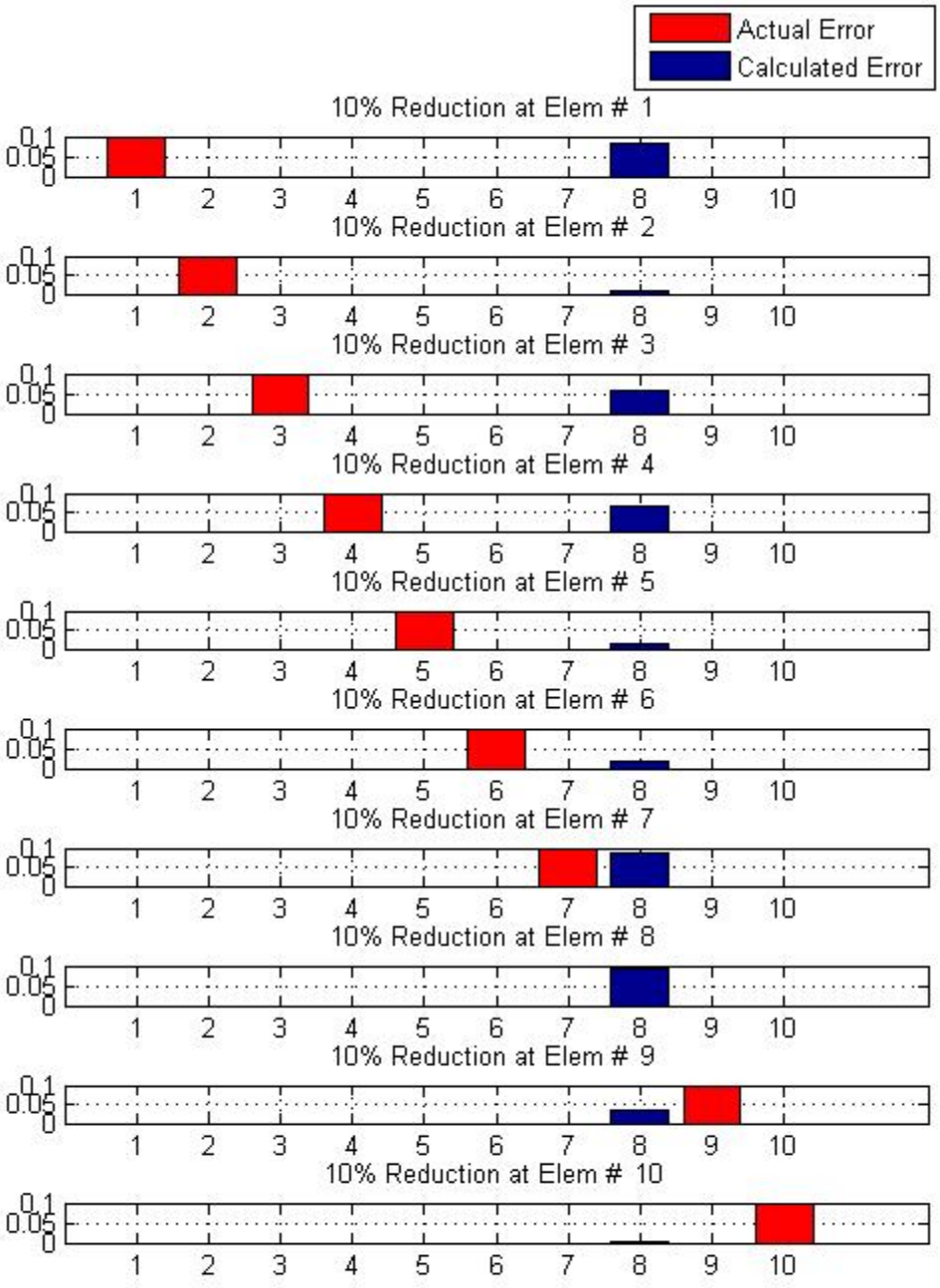

Figure 16. Solution Using the Third Mode Only

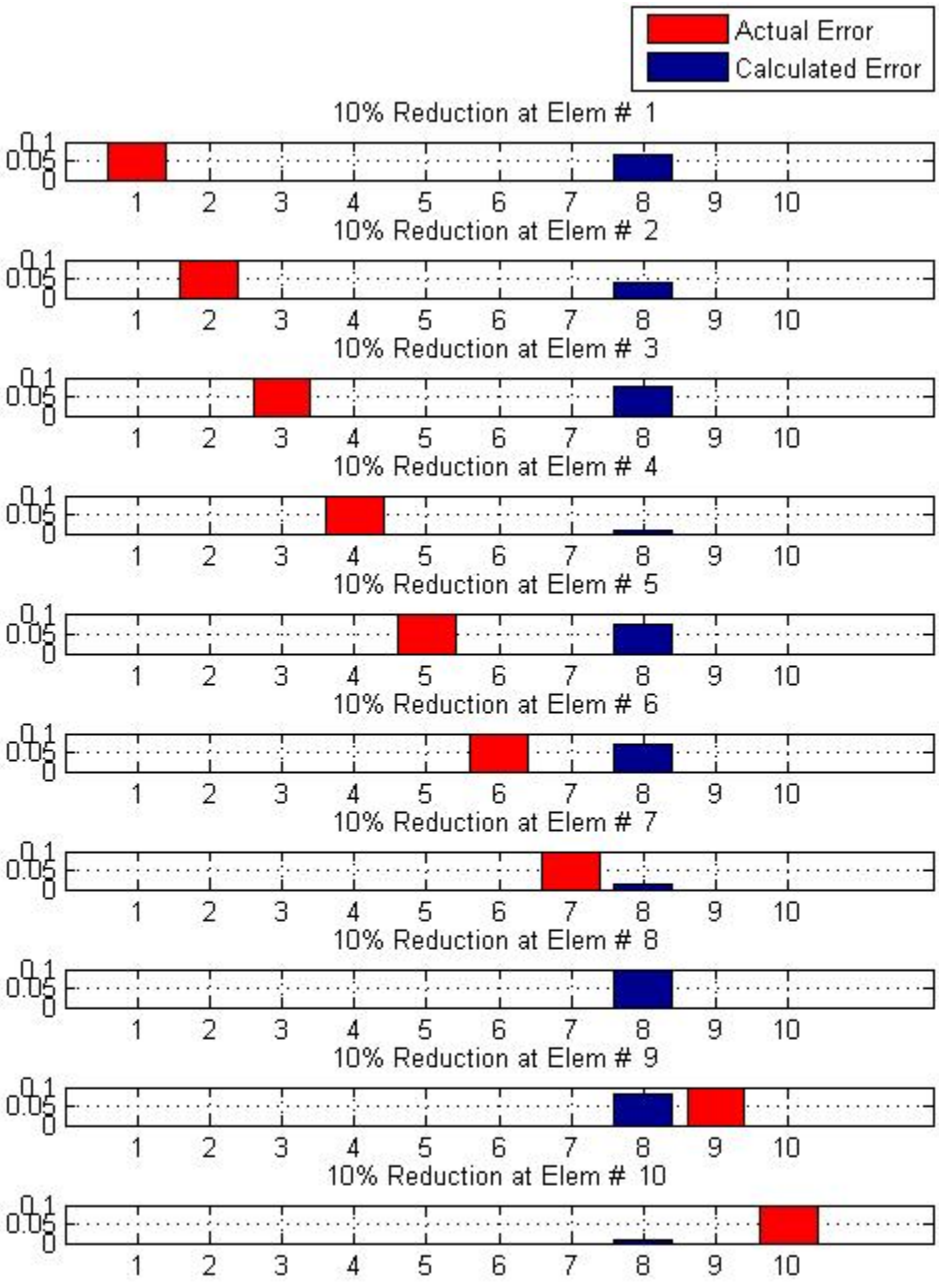

Figure 17. Solution Using the Fourth Mode Only

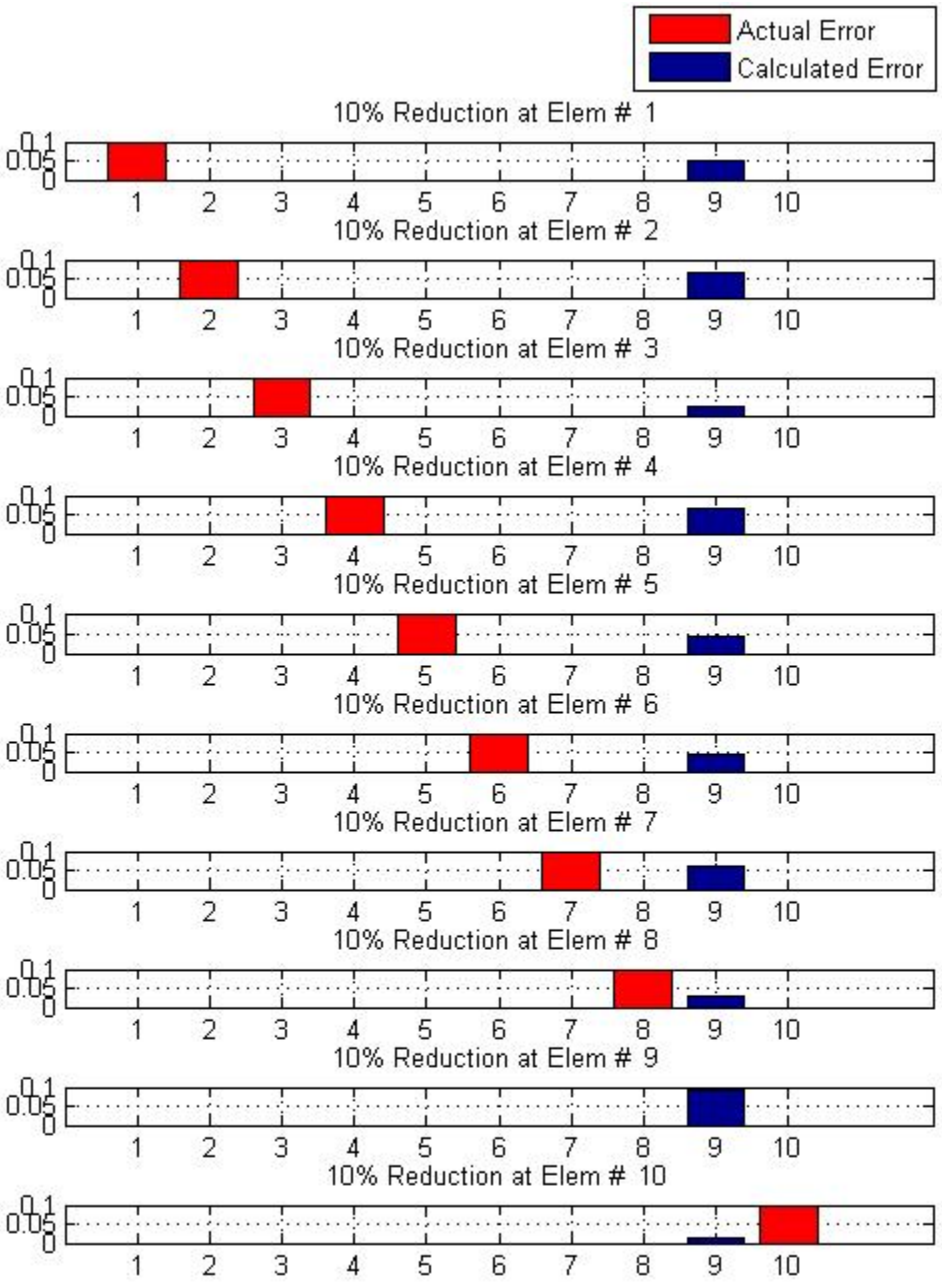

Figure 18. Solution Using the Fifth Mode Only

Keeping in mind from Figure 13 that the maximum sensitivity values occur at elements 1, 1, 8, 8, 9 for modes 1, 2, 3, 4, 5, respectively, a very important conclusion is reached for the FE model solution using only individual modes, as this is clearly derived

from the study of Figures 14 through 18. The conclusion here is that no matter where the actual error is, the calculated result depends on and is exclusively led by the highest sensitivity value of the individual mode used for the solution. This covers the localization aspect of the error prediction. Moreover, it is observed that when the highest sensitivity value corresponds to the element being actually in error, then not only will the location of the damage be detected, but also, the true magnitude of the error will be revealed. This is the reason that there is an exact correlation of the calculated error to the actual error in cases like: first element in error using first or second mode, eighth element in error using third or fourth mode and ninth element in error using fifth mode. It can be predicted at this point that if, for example, only the nineteenth mode is used, which has the fifth element with the highest sensitivity value, only when the fifth element actually is in error will there be a positive result, which can be verified in Figure 19.

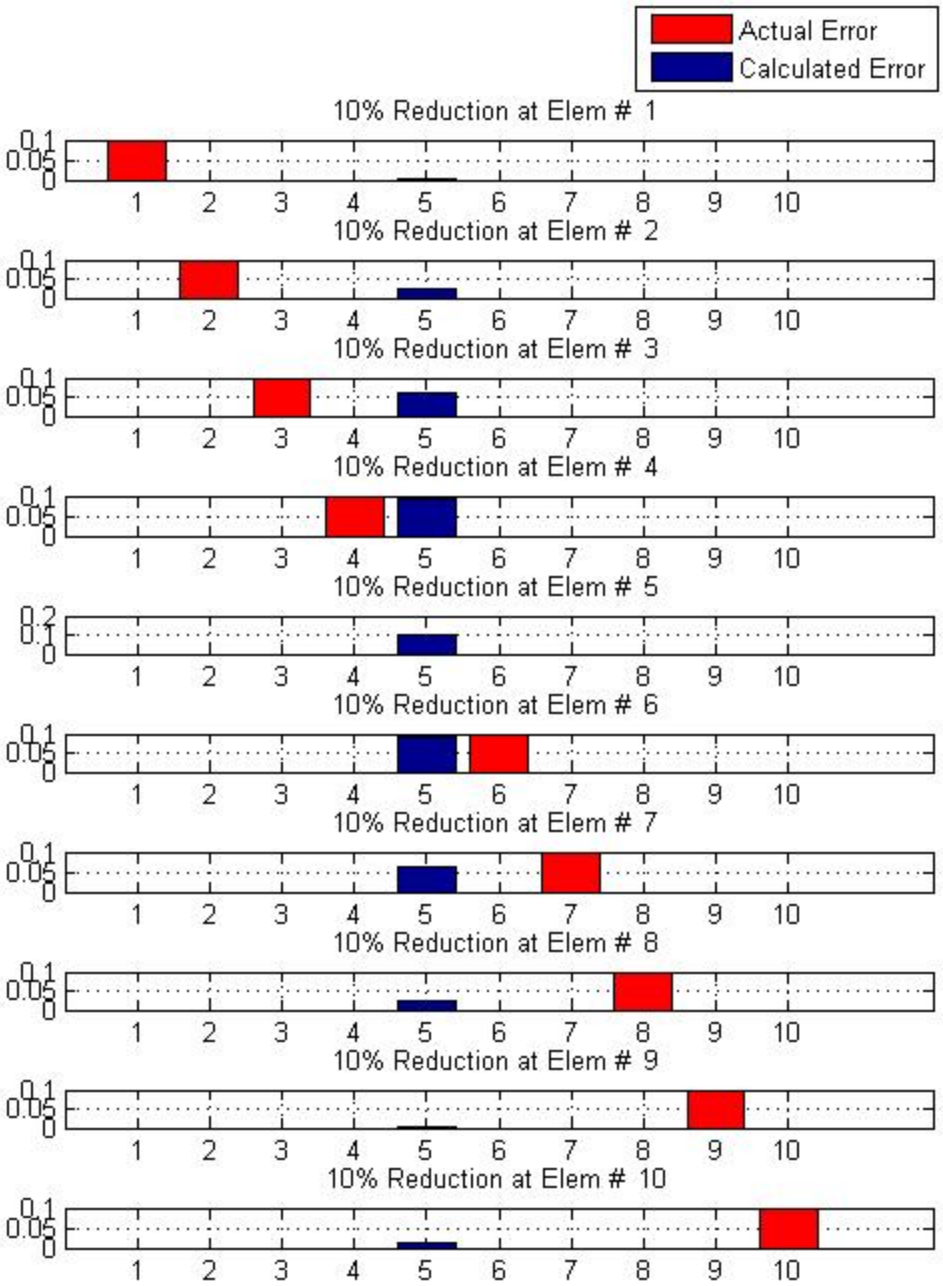

Figure 19. Solution Using the Nineteenth Mode Only

2. Using More Than One Mode

The next step of the current analysis will be the examination of the use of more than one mode, starting with the use of pairs of modes. Consider the first two modes and the corresponding stiffness sensitivity matrix rows from the two top plots of Figure 13. The numerical representation of them, denoted by $\left[T_{1,2}\right]$ and using four significant digits is:

$$\left[T_{1,2}\right]=\begin{bmatrix} 0.0006 & 0.0004 & 0.0003 & 0.0002 & 0.0001 & 0.0001 & 0.0000 & 0.0000 & 0.0000 & 0.0000 \\ 0.0163 & 0.0028 & 0.0008 & 0.0061 & 0.0121 & 0.0138 & 0.0103 & 0.0048 & 0.0011 & 0.0000 \end{bmatrix}$$

while the natural frequencies of the baseline and the damaged system and their difference will again be calculated from the FE models.

Now, solving for the design variables using the first two modes, we get the following figure, again looping over all the elements being in actual error recursively:

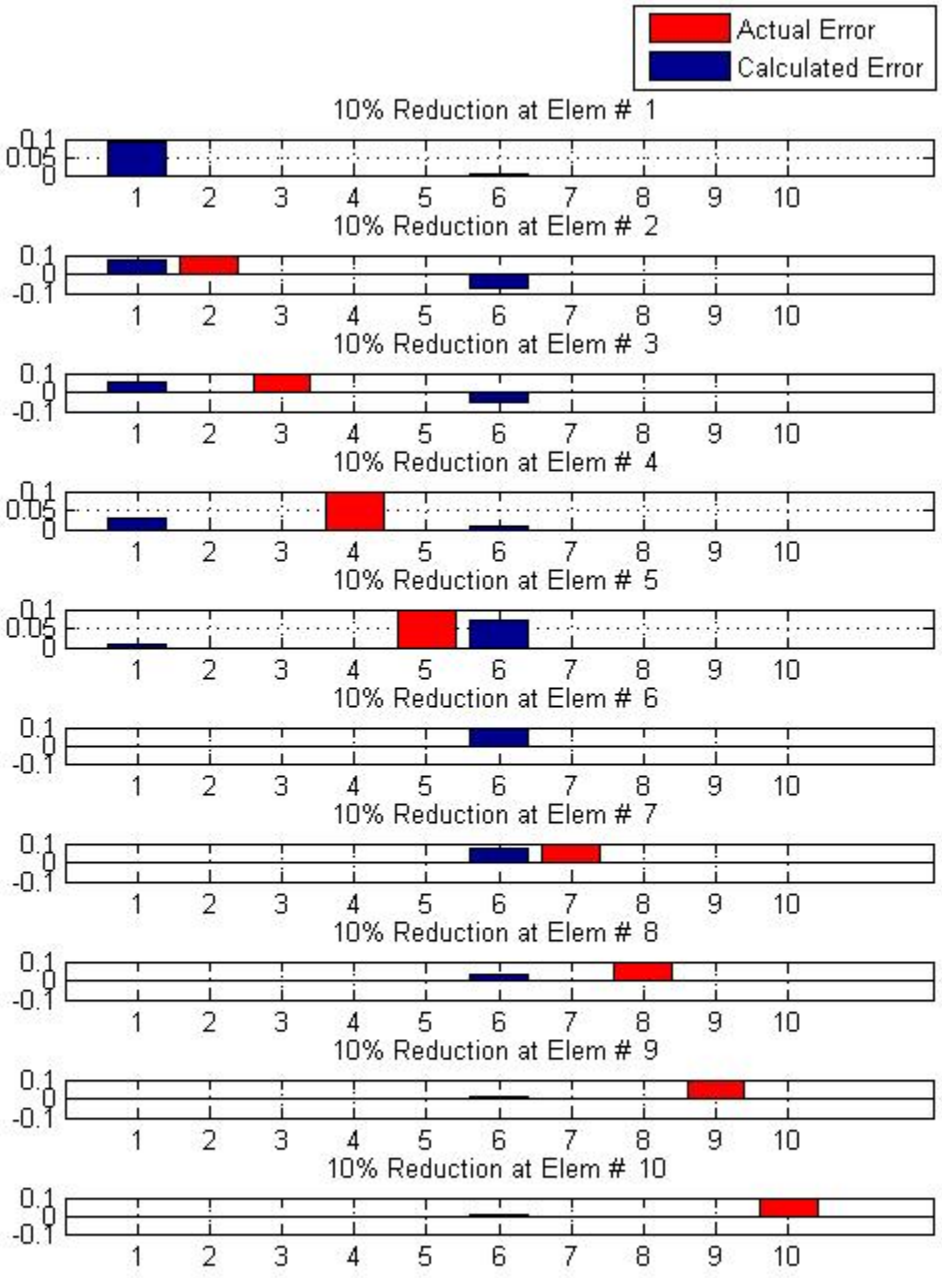

Figure 20. Solution Using Modes 1 and 2

As shown in Figure 20, the solution always returns a vector with only two non-zero values (even with the last four elements being in error, there is a value at element 1, but it is relatively minor compared to that of the sixth element), since the rank of the

sensitivity matrix used, consisting of the first two rows of the full sensitivity matrix, is 2. Furthermore, these non-zero values always occur at elements 1 and 6 of the beam. As explained above, it is no surprise that a positive result is obtained only when the actual error occurs at element 1 or element 6 or both, as will be shown later. In order to investigate the reason for this trend, the procedure for the solution will be examined in successive steps as follows:

Consider again the stiffness sensitivity matrix of the first two modes shown above:

$$[T_{1,2}] = \begin{bmatrix} 0.0006 & 0.0004 & 0.0003 & 0.0002 & 0.0001 & 0.0001 & 0.0000 & 0.0000 & 0.0000 & 0.0000 \\ 0.0163 & 0.0028 & 0.0008 & 0.0061 & 0.0121 & 0.0138 & 0.0103 & 0.0048 & 0.0011 & 0.0000 \end{bmatrix}$$

This is a case of an underdetermined problem, which as discussed previously in this chapter, Matlab solves using QR decomposition with column pivoting. Column pivoting means that the columns' norm is the factor taken into consideration for the pivoting and a permutation matrix is effectively applied to the columns of T. It is of vital importance to note here that higher modes have higher sensitivities and. Therefore, the higher modes tend to govern the norm of the sensitivity matrix columns. Keeping this in mind and for purposes of demonstration it can be considered, without any loss of generality, that a partial pivoting is adequate to explain how Matlab reaches this solution for this linear system.

Moving on with this procedure, the largest entry that is considered the first pivot is entry 1 of the 2nd row.

$$[T_{1,2}] = \begin{bmatrix} 0.0006 & 0.0004 & 0.0003 & 0.0002 & 0.0001 & 0.0001 & 0.0000 & 0.0000 & 0.0000 & 0.0000 \\ 0.0163 & 0.0028 & 0.0008 & 0.0061 & 0.0121 & 0.0138 & 0.0103 & 0.0048 & 0.0011 & 0.0000 \end{bmatrix}$$

Performing a Gaussian elimination the matrix becomes:

$$[T_{1,2}] = \begin{bmatrix} 0 & 0.0003 & 0.0003 & -0.0000 & -0.0003 & -0.0005 & -0.0004 & -0.0002 & -0.0000 & -0.0000 \\ 0.0163 & 0.0028 & 0.0008 & 0.0061 & 0.0121 & 0.0138 & 0.0103 & 0.0048 & 0.0011 & 0.0000 \end{bmatrix}$$

The next pivot will be chosen from the first row, and it will be the entry with the highest absolute value, and it turns out to be entry 6:

$$\left[T_{1,2}\right]=\begin{bmatrix} 0 & 0.0003 & 0.0003 & -0.0000 & -0.0003 & -0.0005 & -0.0004 & -0.0002 & -0.0000 & -0.0000 \\ 0.0163 & 0.0028 & 0.0008 & 0.0061 & 0.0121 & 0.0138 & 0.0103 & 0.0048 & 0.0011 & 0.0000 \end{bmatrix}$$

Performing the next elimination, the matrix becomes:

$$\left[T_{1,2}\right]=\begin{bmatrix} 0 & 0.0003 & 0.0003 & -0.0000 & -0.0003 & -0.0005 & -0.0004 & -0.0002 & -0.0000 & -0.0000 \\ 0.0163 & 0.0130 & 0.0091 & 0.0051 & 0.0019 & 0 & -0.0006 & -0.0004 & -0.0001 & -0.0000 \end{bmatrix}$$

At this point, it can arbitrarily be said that the solution is governed qualitatively by the highest values of the final stage of the elimination of the rank-deficient matrix, as shown above. Comparing Figure 20 to this final stage, in terms of location, the solution for the design variables will always give non-zero values at the pivots, which also happen to have the highest values in each row. Again, remember that this is not absolutely the way Matlab manipulates its solution to this linear problem, but it serves to demonstrate the main ideas of this result and to illustrate how several model updating methods can be properly used.

In order to validate what is stated above, modes 2 and 5 will be used together and an attempt to predict the result will be made. The distribution of these particular sensitivity rows over the beam is shown in Figure 13, while their arithmetic representation in a common matrix is given below:

$$\left[T_{2,5}\right]=\begin{bmatrix} 0.0163 & 0.0028 & 0.0008 & 0.0061 & 0.0121 & 0.0138 & 0.0103 & 0.0048 & 0.0011 & 0.0000 \\ 0.5564 & 0.7459 & 0.2616 & 0.7508 & 0.5051 & 0.4994 & 0.7337 & 0.3113 & 1.1042 & 0.1708 \end{bmatrix}$$

The first pivot will be entry 9 from the 2nd row:

$$\left[T_{2,5}\right]=\begin{bmatrix} 0.0163 & 0.0028 & 0.0008 & 0.0061 & 0.0121 & 0.0138 & 0.0103 & 0.0048 & 0.0011 & 0.0000 \\ 0.5564 & 0.7459 & 0.2616 & 0.7508 & 0.5051 & 0.4994 & 0.7337 & 0.3113 & 1.1042 & 0.1708 \end{bmatrix}$$

From this point already, the first non-zero solution for the outcome should be expected at element 9. The elimination based on that pivot gives:

$$\left[T_{2,5}\right]=\begin{bmatrix} 0.0158 & 0.0021 & 0.0006 & 0.0053 & 0.0116 & 0.0133 & 0.0096 & 0.0045 & 0 & -0.0001 \\ 0.5564 & 0.7459 & 0.2616 & 0.7508 & 0.5051 & 0.4994 & 0.7337 & 0.3113 & 1.1042 & 0.1708 \end{bmatrix}$$

The next pivot, that is the 1st row of the above matrix, will be entry 1:

$$\left[T_{2,5}\right]=\begin{bmatrix} 0.0158 & 0.0021 & 0.0006 & 0.0053 & 0.0116 & 0.0133 & 0.0096 & 0.0045 & 0 & -0.0001 \\ 0.5564 & 0.7459 & 0.2616 & 0.7508 & 0.5051 & 0.4994 & 0.7337 & 0.3113 & 1.1042 & 0.1708 \end{bmatrix}$$

Even at this point, the second non-zero value of the outcome should be expected at the 1st element, but for consistency reasons, the next elimination is presented:

$$\left[T_{2,5}\right]=\begin{bmatrix} 0.0158 & 0.0021 & 0.0006 & 0.0053 & 0.0116 & 0.0133 & 0.0096 & 0.0045 & 0 & -0.0001 \\ 0 & 0.6727 & 0.2422 & 0.5635 & 0.0965 & 0.0308 & 0.3955 & 0.1516 & 1.1042 & 0.1751 \end{bmatrix}$$

So, the prediction for this configuration is that no matter where the actual error is, Matlab will return a result with non-zero values at elements 1 and 9, which will be positive only when these elements are actually in error, either one or both. By the term positive result, the correct damage detection is meant in a qualitative aspect (error location), which might sometimes be consistent quantitatively (error magnitude). Yet the quantitative aspect cannot be proved, although in the cases analyzed in this subchapter, it is revealed.

Solving now the fundamental Equation (2.31) for the design variables and looping again over all the elements that are in error recursively, we get:

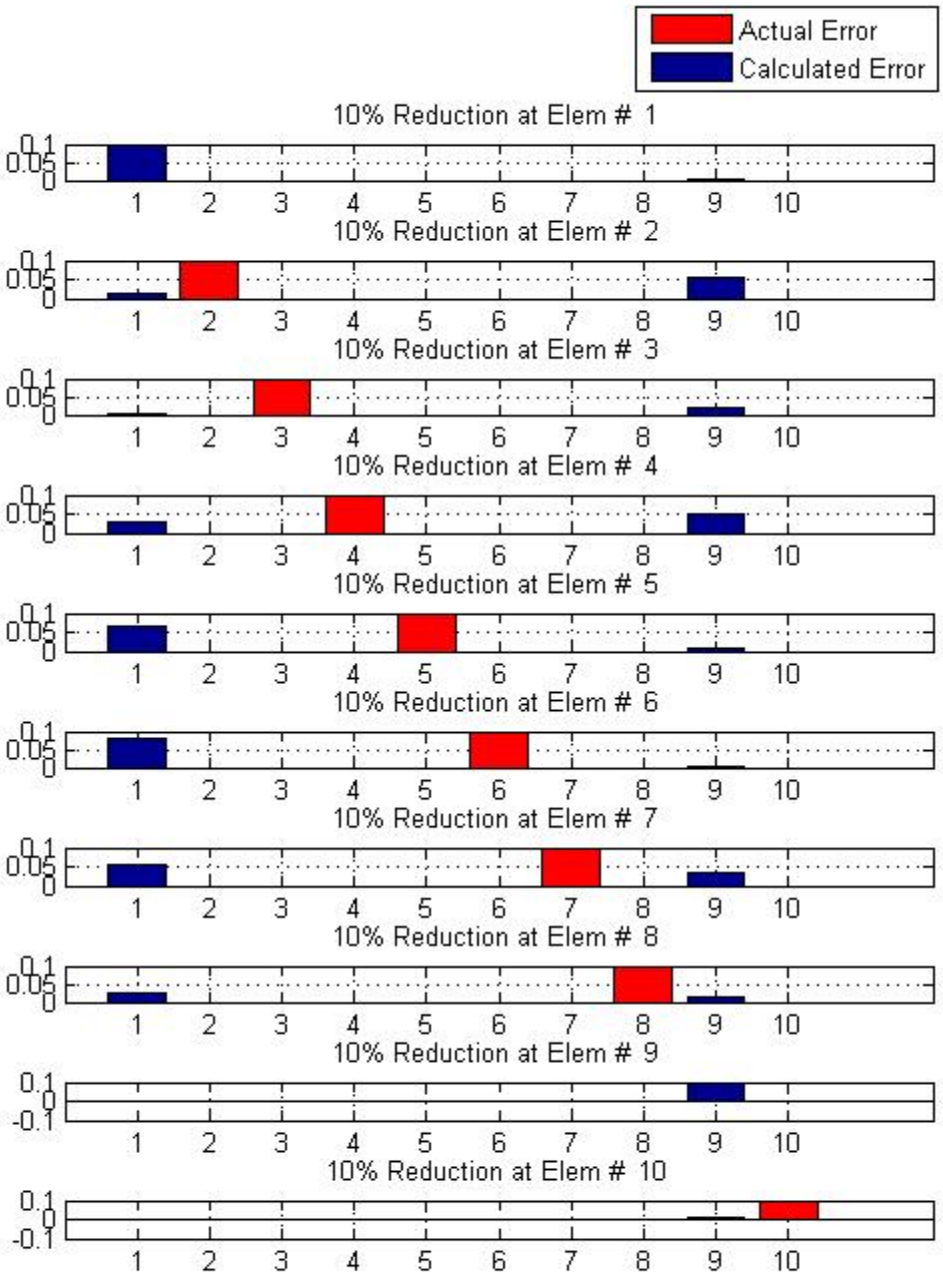

Figure 21. Solution Using Modes 2 and 5

It is easily shown in Figure 21 that what is stated above is validated exactly.

In order to validate the presented procedure in a more generic manner, the first five modes will be used and again the result will be predicted without actually solving

Equation (2.31). A priori, the solution expected should have only 5 non-zero values, since the rank of the used sensitivity matrix, shown in Figure 13 is 5. In this case, all five plots of Figure 13 are used with the following arithmetic representation:

$$[T_{1:5}] = \begin{bmatrix} 0.0006 & 0.0004 & 0.0003 & 0.0002 & 0.0001 & 0.0001 & 0.0000 & 0.0000 & 0.0000 & 0.0000 \\ 0.0163 & 0.0028 & 0.0008 & 0.0061 & 0.0121 & 0.0138 & 0.0103 & 0.0048 & 0.0011 & 0.0000 \\ 0.0904 & 0.0094 & 0.0691 & 0.0778 & 0.0170 & 0.0221 & 0.0977 & 0.1083 & 0.0407 & 0.0025 \\ 0.2518 & 0.1633 & 0.2888 & 0.0390 & 0.2834 & 0.2793 & 0.0435 & 0.3602 & 0.3188 & 0.0291 \\ 0.5564 & 0.7459 & 0.2616 & 0.7508 & 0.5051 & 0.4994 & 0.7337 & 0.3113 & 1.1042 & 0.1708 \end{bmatrix}$$

The first pivot in this case is entry 9 of the 5th row:

$$[T_{1:5}] = \begin{bmatrix} 0.0006 & 0.0004 & 0.0003 & 0.0002 & 0.0001 & 0.0001 & 0.0000 & 0.0000 & 0.0000 & 0.0000 \\ 0.0163 & 0.0028 & 0.0008 & 0.0061 & 0.0121 & 0.0138 & 0.0103 & 0.0048 & 0.0011 & 0.0000 \\ 0.0904 & 0.0094 & 0.0691 & 0.0778 & 0.0170 & 0.0221 & 0.0977 & 0.1083 & 0.0407 & 0.0025 \\ 0.2518 & 0.1633 & 0.2888 & 0.0390 & 0.2834 & 0.2793 & 0.0435 & 0.3602 & 0.3188 & 0.0291 \\ 0.5564 & 0.7459 & 0.2616 & 0.7508 & 0.5051 & 0.4994 & 0.7337 & 0.3113 & 1.1042 & 0.1708 \end{bmatrix}$$

so one non-zero value should be expected at element 9. After the elimination based on the first pivot, the matrix becomes:

$$[T_{1:5}] = \begin{bmatrix} 0.0006 & 0.0004 & 0.0003 & 0.0002 & 0.0001 & 0.0001 & 0.0000 & 0.0000 & 0 & -0.0000 \\ 0.0158 & 0.0021 & 0.0006 & 0.0053 & 0.0116 & 0.0133 & 0.0096 & 0.0045 & 0 & -0.0001 \\ 0.0699 & -0.0181 & 0.0594 & 0.0501 & -0.0017 & 0.0037 & 0.0707 & 0.0968 & 0 & -0.0038 \\ 0.0912 & -0.0521 & 0.2133 & -0.1777 & 0.1376 & 0.1351 & -0.1683 & 0.2704 & 0 & -0.0203 \\ 0.5564 & 0.7459 & 0.2616 & 0.7508 & 0.5051 & 0.4994 & 0.7337 & 0.3113 & 1.1042 & 0.1708 \end{bmatrix}$$

The second pivot will now be entry 8 of the 4th row:

$$[T_{1:5}] = \begin{bmatrix} 0.0006 & 0.0004 & 0.0003 & 0.0002 & 0.0001 & 0.0001 & 0.0000 & 0.0000 & 0 & -0.0000 \\ 0.0158 & 0.0021 & 0.0006 & 0.0053 & 0.0116 & 0.0133 & 0.0096 & 0.0045 & 0 & -0.0001 \\ 0.0699 & -0.0181 & 0.0594 & 0.0501 & -0.0017 & 0.0037 & 0.0707 & 0.0968 & 0 & -0.0038 \\ 0.0912 & -0.0521 & 0.2133 & -0.1777 & 0.1376 & 0.1351 & -0.1683 & 0.2704 & 0 & -0.0203 \\ 0.5564 & 0.7459 & 0.2616 & 0.7508 & 0.5051 & 0.4994 & 0.7337 & 0.3113 & 1.1042 & 0.1708 \end{bmatrix}$$

so another non-zero value should be expected at element 8. After the elimination based on the second pivot, the matrix becomes:

$$[T_{1:5}] = \begin{bmatrix} 0.0006 & 0.0004 & 0.0003 & 0.0002 & 0.0001 & 0.0001 & 0.0000 & 0 & 0 & 0.0000 \\ 0.0142 & 0.0029 & -0.0030 & 0.0083 & 0.0093 & 0.0110 & 0.0124 & 0 & 0 & 0.0002 \\ 0.0373 & 0.0005 & -0.0169 & 0.1137 & -0.0509 & -0.0447 & 0.1309 & 0 & 0 & 0.0034 \\ 0.0912 & -0.0521 & 0.2133 & -0.1777 & 0.1376 & 0.1351 & -0.1683 & 0.2704 & 0 & -0.0203 \\ 0.5564 & 0.7459 & 0.2616 & 0.7508 & 0.5051 & 0.4994 & 0.7337 & 0.3113 & 1.1042 & 0.1708 \end{bmatrix}$$

It must be said here that, in fact, there is no need to eliminate entries both above and below the pivots. The only elimination needed for the purpose of this demonstration is of the remaining rows not yet containing any pivot, which, as can easily be shown, yields to the form of an upper or lower triangular matrix after the appropriate column shifting.

The third pivot will be entry 7 of the third row:

$$[T_{1:5}] = \begin{bmatrix} 0.0006 & 0.0004 & 0.0003 & 0.0002 & 0.0001 & 0.0001 & 0.0000 & 0 & 0 & 0.0000 \\ 0.0142 & 0.0029 & -0.0030 & 0.0083 & 0.0093 & 0.0110 & 0.0124 & 0 & 0 & 0.0002 \\ 0.0373 & 0.0005 & -0.0169 & 0.1137 & -0.0509 & -0.0447 & 0.1309 & 0 & 0 & 0.0034 \\ 0.0912 & -0.0521 & 0.2133 & -0.1777 & 0.1376 & 0.1351 & -0.1683 & 0.2704 & 0 & -0.0203 \\ 0.5564 & 0.7459 & 0.2616 & 0.7508 & 0.5051 & 0.4994 & 0.7337 & 0.3113 & 1.1042 & 0.1708 \end{bmatrix}$$

making element 7 likely to have a non-zero value at the result.

Again, after the elimination of the remaining rows without pivot, the matrix becomes:

$$[T_{1:5}] = \begin{bmatrix} 0.0006 & 0.0004 & 0.0003 & 0.0002 & 0.0001 & 0.0001 & 0 & 0 & 0 & -0.0000 \\ 0.0107 & 0.0029 & -0.0014 & -0.0025 & 0.0141 & 0.0153 & 0 & 0 & 0 & -0.0001 \\ 0.0373 & 0.0005 & -0.0169 & 0.1137 & -0.0509 & -0.0447 & 0.1309 & 0 & 0 & 0.0034 \\ 0.0912 & -0.0521 & 0.2133 & -0.1777 & 0.1376 & 0.1351 & -0.1683 & 0.2704 & 0 & -0.0203 \\ 0.5564 & 0.7459 & 0.2616 & 0.7508 & 0.5051 & 0.4994 & 0.7337 & 0.3113 & 1.1042 & 0.1708 \end{bmatrix}$$

and now the next pivot is entry 6 of the second row, which makes element 6 one of those with a non-zero corresponding value:

$$[T_{1:5}] = \begin{bmatrix} 0.0006 & 0.0004 & 0.0003 & 0.0002 & 0.0001 & 0.0001 & 0 & 0 & 0 & -0.0000 \\ 0.0107 & 0.0029 & -0.0014 & -0.0025 & 0.0141 & 0.0153 & 0 & 0 & 0 & -0.0001 \\ 0.0373 & 0.0005 & -0.0169 & 0.1137 & -0.0509 & -0.0447 & 0.1309 & 0 & 0 & 0.0034 \\ 0.0912 & -0.0521 & 0.2133 & -0.1777 & 0.1376 & 0.1351 & -0.1683 & 0.2704 & 0 & -0.0203 \\ 0.5564 & 0.7459 & 0.2616 & 0.7508 & 0.5051 & 0.4994 & 0.7337 & 0.3113 & 1.1042 & 0.1708 \end{bmatrix}$$

After the last elimination, that of the first row, the matrix becomes:

$$[T_{1:5}] = \begin{bmatrix} 0.0005 & 0.0004 & 0.0003 & 0.0002 & 0.0001 & 0 & 0 & 0 & 0 & 0.0000 \\ 0.0107 & 0.0029 & -0.0014 & -0.0025 & 0.0141 & 0.0153 & 0 & 0 & 0 & -0.0001 \\ 0.0373 & 0.0005 & -0.0169 & 0.1137 & -0.0509 & -0.0447 & 0.1309 & 0 & 0 & 0.0034 \\ 0.0912 & -0.0521 & 0.2133 & -0.1777 & 0.1376 & 0.1351 & -0.1683 & 0.2704 & 0 & -0.0203 \\ 0.5564 & 0.7459 & 0.2616 & 0.7508 & 0.5051 & 0.4994 & 0.7337 & 0.3113 & 1.1042 & 0.1708 \end{bmatrix}$$

In this last matrix, the highest value of the first row occurs at entry 1:

$$[T_{1:5}] = \begin{bmatrix} 0.0005 & 0.0004 & 0.0003 & 0.0002 & 0.0001 & 0 & 0 & 0 & 0 & 0.0000 \\ 0.0107 & 0.0029 & -0.0014 & -0.0025 & 0.0141 & 0.0153 & 0 & 0 & 0 & -0.0001 \\ 0.0373 & 0.0005 & -0.0169 & 0.1137 & -0.0509 & -0.0447 & 0.1309 & 0 & 0 & 0.0034 \\ 0.0912 & -0.0521 & 0.2133 & -0.1777 & 0.1376 & 0.1351 & -0.1683 & 0.2704 & 0 & -0.0203 \\ 0.5564 & 0.7459 & 0.2616 & 0.7508 & 0.5051 & 0.4994 & 0.7337 & 0.3113 & 1.1042 & 0.1708 \end{bmatrix}$$

Having reached the final stage of this procedure using the first five modes, the predicted solution is expected to have non-zero values at elements 1, 6, 7, 8, 9 and these values will constitute a positive result when the actual error occurs in each, or any combination of these elements.

As far as the calculated solution from the solution of Equation (2.31) is concerned, the following figure is generated, which again validates what is stated above (again where the existence of non-zero values at elements 1, 6, 7, 8, 9 is not obvious due to the very low value relative to the other values):

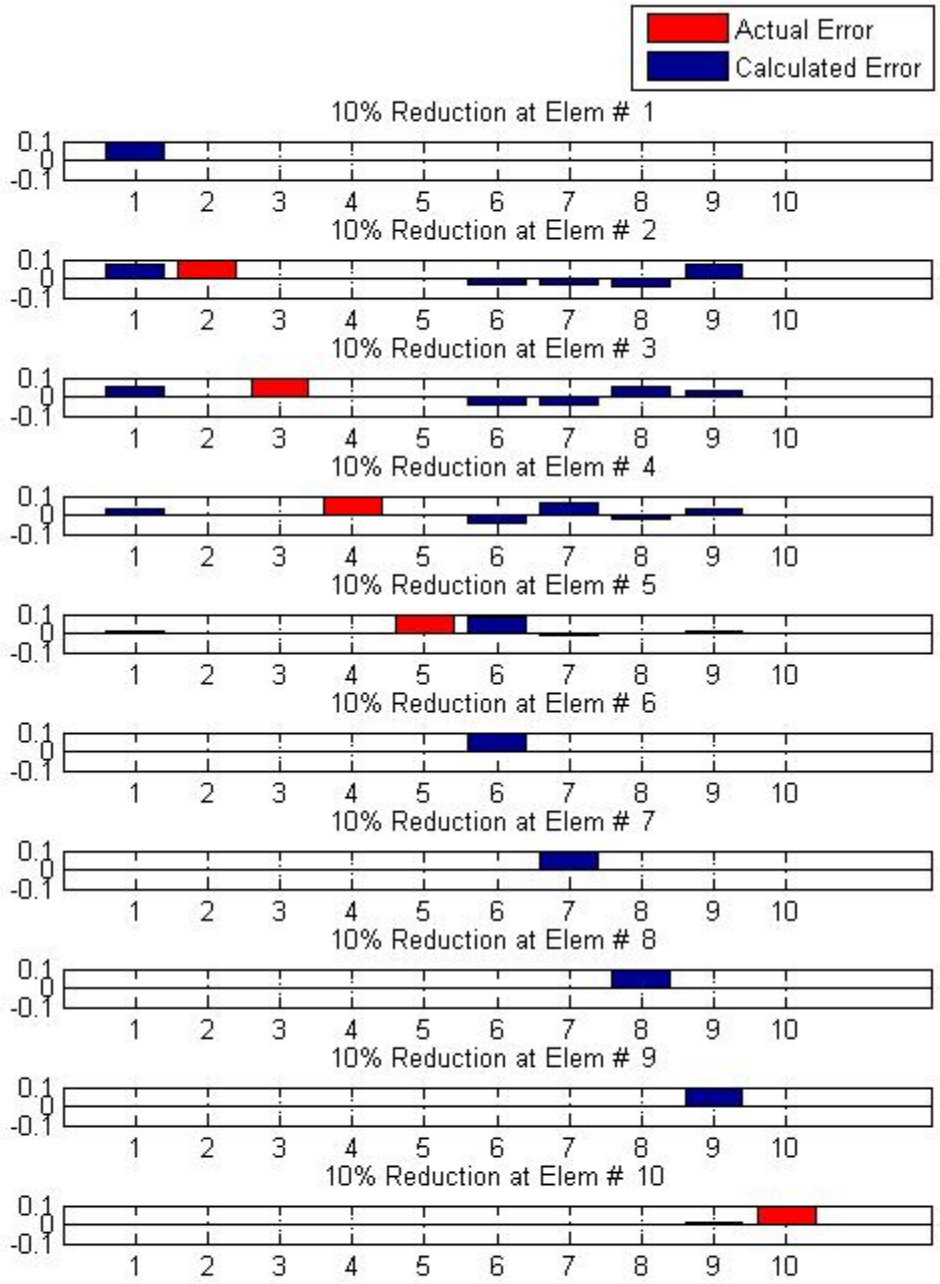

Figure 22. Solution Using Modes 1 through 5

It has to be recalled at this point that, although the quantitative aspect of damage detection (error magnitude) is present in the cases examined above, it is not proved in a

generic way for all situations. It will later be shown that there may be some discrepancies which distract the result from being positive as far as the error magnitude or the exclusivity of the location are concerned. These discrepancies will be dealt with in a later chapter.

3. What if a Fully Determined Square Matrix is Available?

From what is stated so far, a very important conclusion is reached. For a structure consisting of n elements, and considering one design variable for each element, if m modes are used for the sensitivity-based analysis, with $m<n$, then the maximum number of elements that can be positively identified to be in error is k, where k is the rank of the sensitivity matrix, which at most, is equal to m. In other words, if it is assumed that there is no linear dependency between the rows of the sensitivity matrix, then the maximum number of positive damage-detected elements is equal to the number of the modes used for the analysis.

Therefore, it can be concluded that if damage detection throughout the structure is desired using one and only one sensitivity matrix, then this matrix must not only be square, but also full rank. This is the condition that the present work has been based on. It has to be said that even if a matrix is full rank, there may be some near-dependencies that are crucially negative for the desired result. This is why the enlargement of the data used must first be pursued and then the optimal configurations contained in this data must be found and used for globally positive structure identification.

The following figures show that with a square matrix, comprised of either the first 10 modes, or of the second 10 modes of the structure examined previously (cantilever beam), potentially good results are obtained (Figure 24) because all the elements may have a non-zero value in the solution vector. Apparently, this is only necessary, and yet not sufficient condition for positive damage detection (Figure 23), since different configurations give different results even though both are square and full rank.

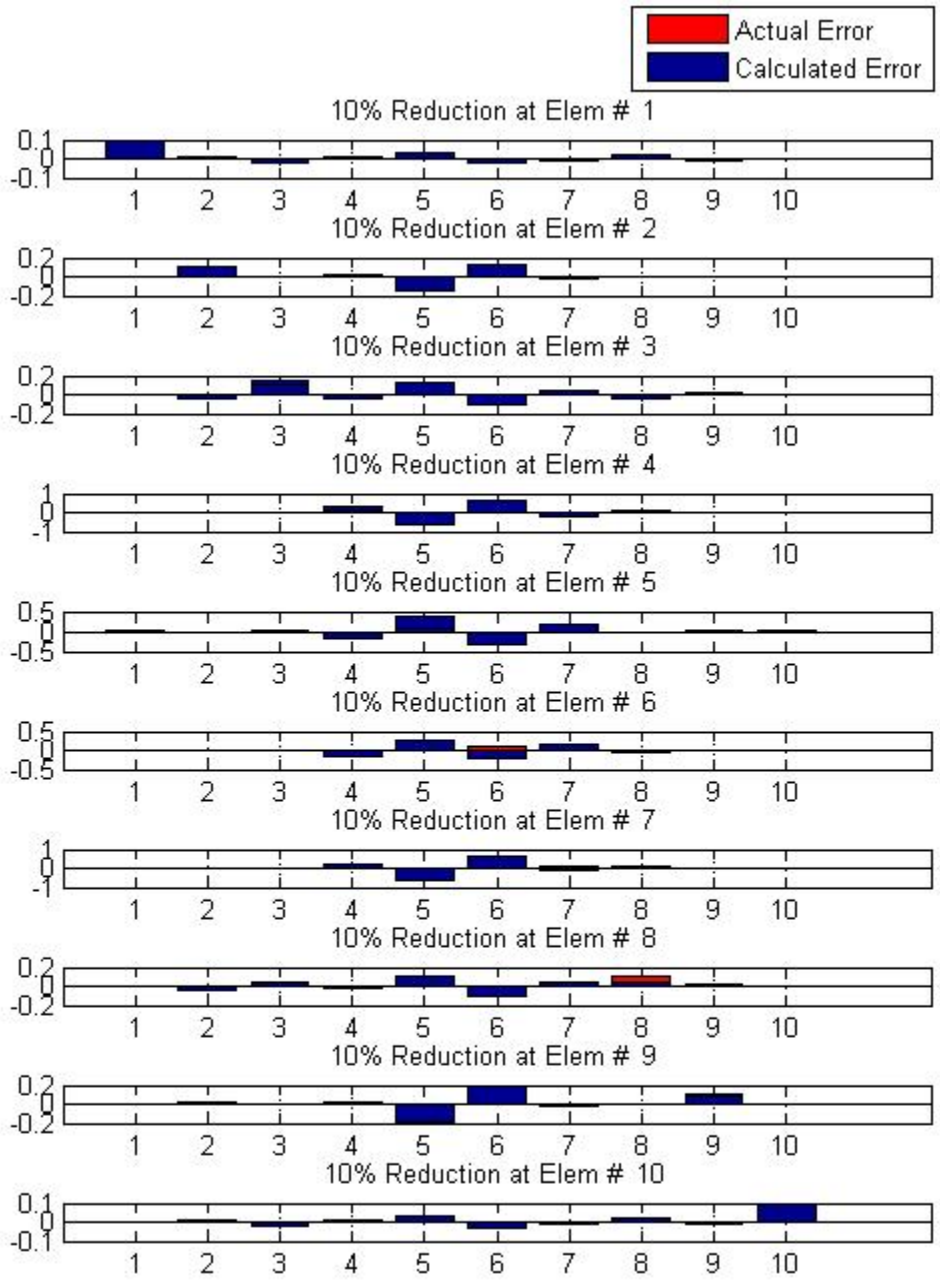

Figure 23. Solution Using Modes 1 Through 10

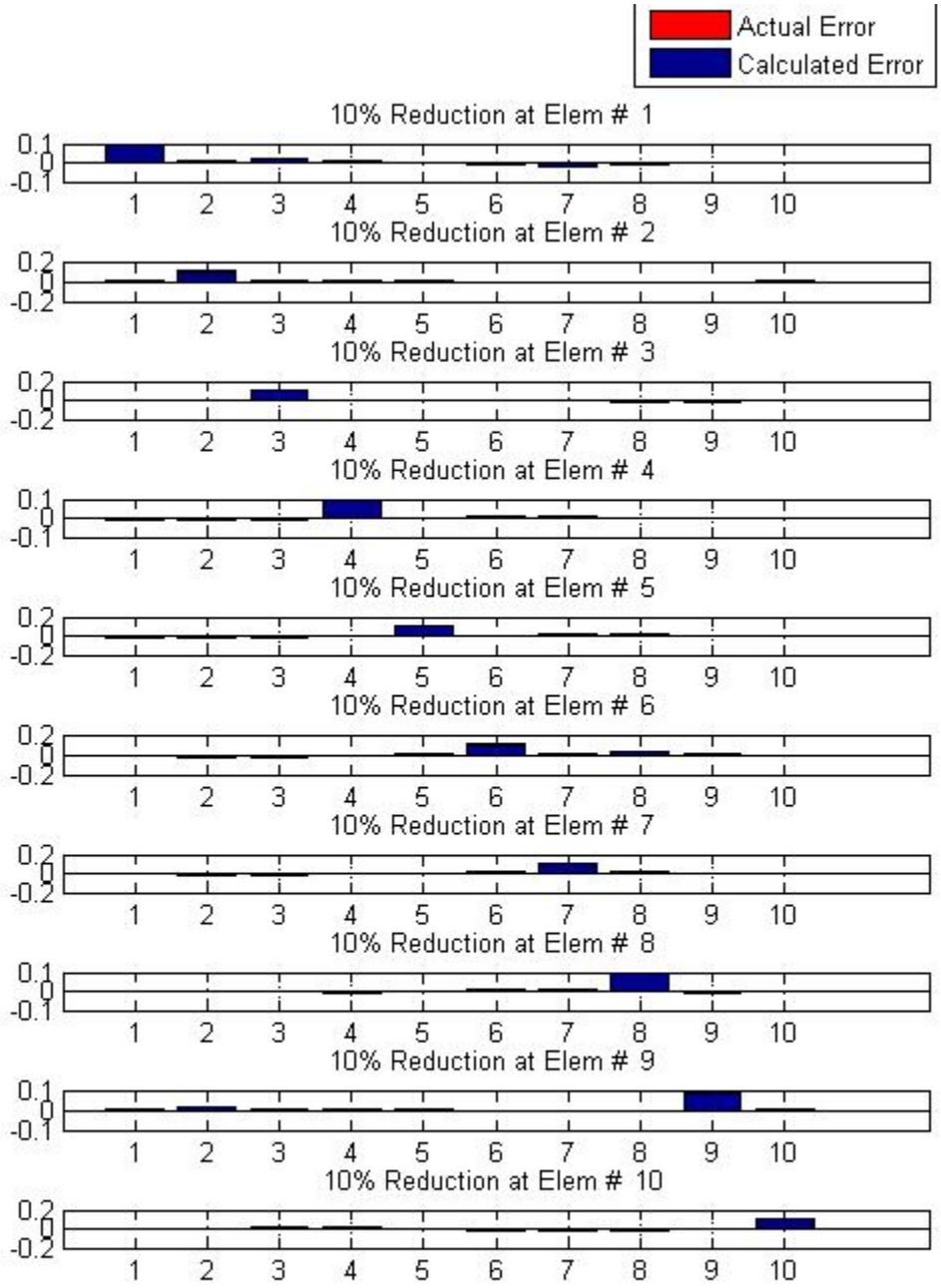

Figure 24. Solution Using Modes 11 Through 20

IV. ENLARGEMENT OF TEST DATA- ENHANCEMENT OF SENSITIVITY MATRIX DETERMINABILITY/ CONDITIONING

In the previous chapter, the need for the construction of a fully determined sensitivity matrix for the detection of potential damage throughout the structure was justified. In this chapter, several methods will be pursued in this direction until the point that optimal ABC configurations are reached and prove more essential than other methods.

A. USING EIGENVECTOR SENSITIVITY DATA

In the theory chapter, a method was presented for the calculation of the eigenvector sensitivity matrix. This algorithm is applied to the same model that was analyzed in terms of eigenvalue sensitivity and the results are provided below.

It should be mentioned at this point that even if data from eigenvector are used, resulting in an improved FEM updating, two major drawbacks as far as this analysis is concerned cannot be ignored. The first is the accuracy of the test measurements needed to accurately identify the mode shapes of a structure since typical measurement errors can be caused by noise, nonlinearities, etc. The second is that for large and complex structures, the mode shape sensitivity analysis produces a large quantity of data, resulting in a more expensive problem in terms of calculation time and memory storage. Nevertheless, a possible combination of the two aforementioned discrepancies may cause the whole process to converge less rapidly or possibly converge into incorrect results as described in [24].

For this analysis, the same 10 element cantilever beam is considered. Using the algorithm described in Chapter II, a full eigenvector sensitivity matrix is generated. The size of this matrix is 400x10. The number of columns is equal to the number of the design parameters, which again, are the rigidities corresponding to each one of the 10 beam elements. The number of rows corresponds to 20 entries related to each DOF of each beam element, respectively, which entries are generated for each one of the 20 modes of the system. Obviously, the same FE model that was used for the derivation of the

eigenvalue sensitivity matrix is used again. The distribution of the eigenvector sensitivity matrix for Mode #1, over all the elements, and for each DOF is displayed in Figures 25 and 26, while the first mode of the eigenvalue sensitivity matrix is available in the first plot of Figure 13. Each plot is normalized to the maximum value of each row for displaying reasons. It should be mentioned that in absolute values, the magnitude of the eigenvector sensitivities is much less than that of the eigenvalue sensitivities, as shown in the arithmetic representation with four significant digits of the first mode of each one below, and this may play a significant role in the procedure of linear system solving:

$$T_{eigval,Mode1} = 10^{-3} * \begin{bmatrix} 0.6034 & 0.4388 & 0.3017 & 0.1928 & 0.1117 & 0.0565 & 0.0234 & 0.0070 & 0.0011 & 0.0000 \end{bmatrix}$$

$$T_{eigvec,Mode1} = 10^{-6} * \begin{bmatrix} -0.2217 & 0.0842 & 0.0588 & 0.0381 & 0.0224 & 0.0115 & 0.0048 & 0.0015 & 0.0002 & 0.0000 \\ -0.0721 & 0.0274 & 0.0191 & 0.0124 & 0.0073 & 0.0037 & 0.0016 & 0.0005 & 0.0001 & 0.0000 \\ -0.5550 & 0.0334 & 0.2235 & 0.1447 & 0.0850 & 0.0436 & 0.0183 & 0.0055 & 0.0009 & 0.0000 \\ -0.0399 & -0.0423 & 0.0353 & 0.0228 & 0.0134 & 0.0068 & 0.0029 & 0.0009 & 0.0001 & 0.0000 \\ -0.7109 & -0.1599 & 0.2373 & 0.3081 & 0.1806 & 0.0925 & 0.0387 & 0.0117 & 0.0019 & 0.0001 \\ -0.0129 & -0.0228 & -0.0285 & 0.0313 & 0.0183 & 0.0093 & 0.0039 & 0.0012 & 0.0002 & 0.0000 \\ -0.7201 & -0.2476 & 0.0992 & 0.3243 & 0.3024 & 0.1545 & 0.0646 & 0.0195 & 0.0032 & 0.0001 \\ 0.0090 & -0.0071 & -0.0179 & -0.0237 & 0.0221 & 0.0112 & 0.0047 & 0.0014 & 0.0002 & 0.0000 \\ -0.6131 & -0.2520 & 0.0172 & 0.1980 & 0.2960 & 0.2263 & 0.0944 & 0.0285 & 0.0046 & 0.0002 \\ 0.0259 & 0.0050 & -0.0098 & -0.0187 & -0.0220 & 0.0126 & 0.0052 & 0.0016 & 0.0003 & 0.0000 \\ -0.4191 & -0.1946 & -0.0235 & 0.0971 & 0.1702 & 0.1985 & 0.1269 & 0.0382 & 0.0062 & 0.0002 \\ 0.0380 & 0.0136 & -0.0041 & -0.0152 & -0.0201 & -0.0198 & 0.0056 & 0.0017 & 0.0003 & 0.0000 \\ -0.1653 & -0.0948 & -0.0362 & 0.0132 & 0.0536 & 0.0816 & 0.0915 & 0.0483 & 0.0078 & 0.0003 \\ 0.0459 & 0.0192 & -0.0004 & -0.0130 & -0.0189 & -0.0192 & -0.0156 & 0.0017 & 0.0003 & 0.0000 \\ 0.1247 & 0.0306 & -0.0320 & -0.0605 & -0.0577 & -0.0330 & -0.0016 & 0.0198 & 0.0095 & 0.0003 \\ 0.0502 & 0.0222 & 0.0016 & -0.0118 & -0.0183 & -0.0190 & -0.0155 & -0.0098 & 0.0003 & 0.0000 \\ 0.4322 & 0.1682 & -0.0198 & -0.1295 & -0.1665 & -0.1465 & -0.0943 & -0.0391 & -0.0050 & 0.0004 \\ 0.0519 & 0.0234 & 0.0023 & -0.0113 & -0.0180 & -0.0189 & -0.0154 & -0.0098 & -0.0042 & 0.0000 \\ 0.7449 & 0.3094 & -0.0052 & -0.1971 & -0.2746 & -0.2597 & -0.1870 & -0.0979 & -0.0302 & -0.0025 \\ 0.0522 & 0.0236 & 0.0025 & -0.0112 & -0.0180 & -0.0189 & -0.0154 & -0.0098 & -0.0042 & -0.0007 \end{bmatrix}$$

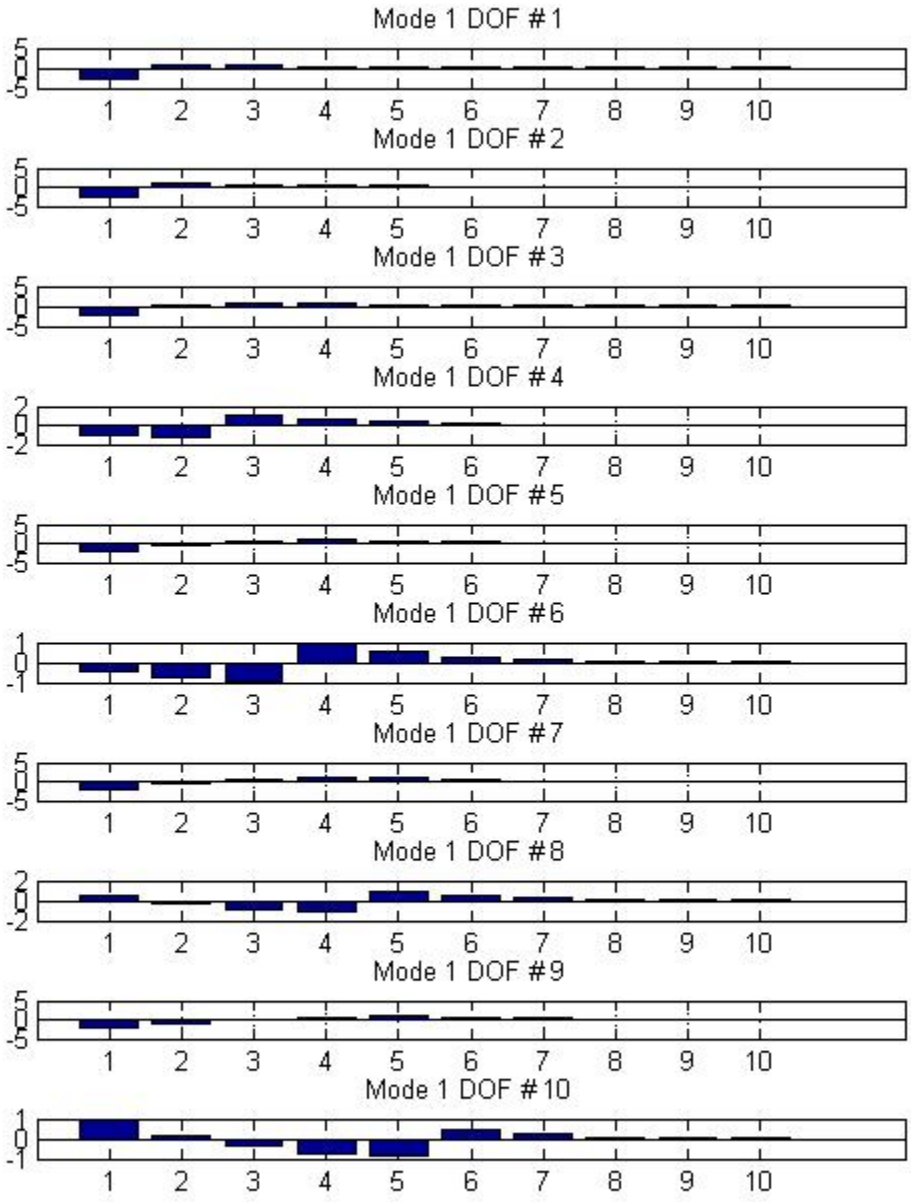

Figure 25. Mode 1 of Eigenvector Sensitivity Matrix for DOF 1 Through 10

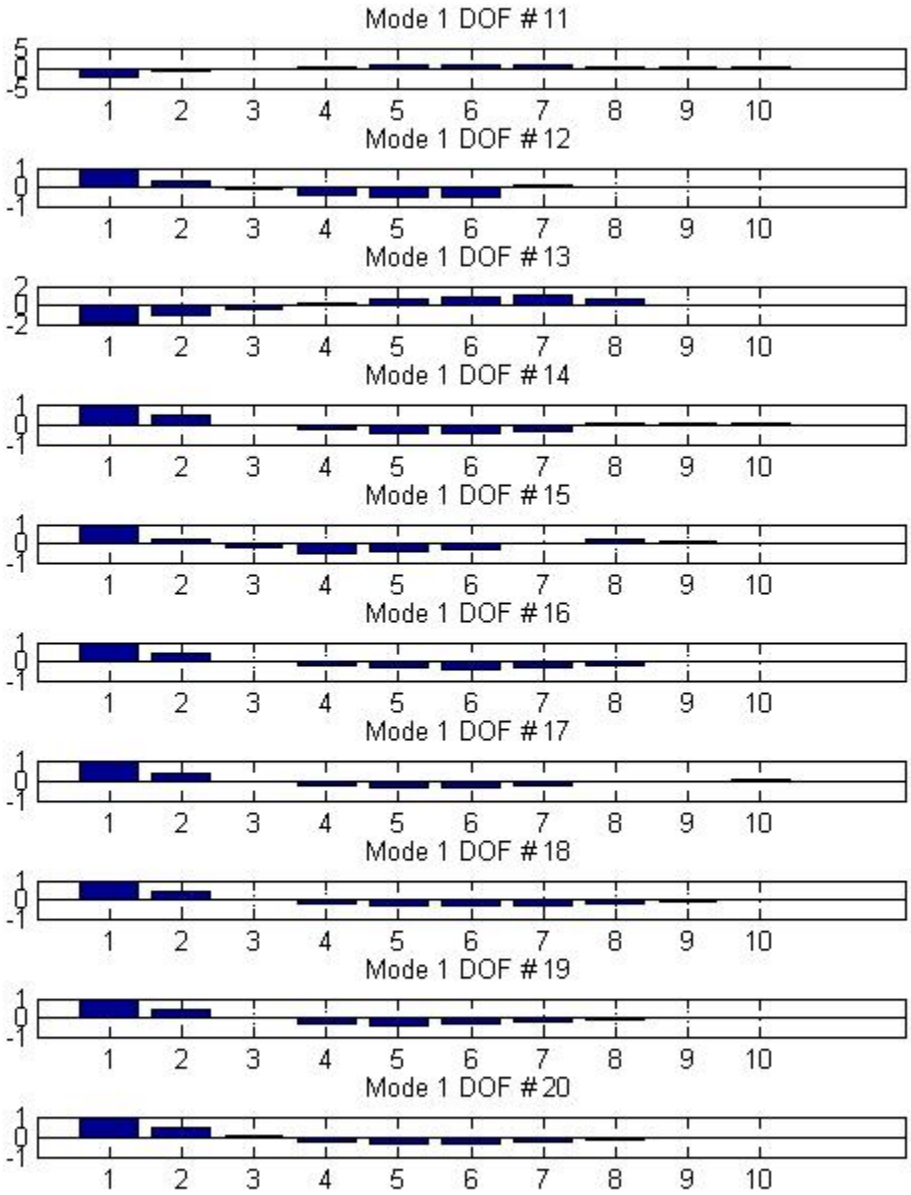

Figure 26. Mode 1 of Eigenvector Sensitivity Matrix for DOF 11 Through 20

The natural frequency and the eigenvector differences corresponding to the first mode can be derived from the baseline and the damaged model as before. In this case, the $\Delta\Phi_{Mode1}$ vector will have a dimension of 20x1.

Two approaches will now be made to the identification of the effectiveness of the use of eigenvector sensitivity. The first one will use only mode shape data for the analysis, while the second will combine the same modes from both eigenvalue and eigenvector data. It is quite sufficient to use only the first mode for displaying the result for both cases as there are not many qualitative variations using other modes as well.

Solving the fundamental Equation (2.31) for the design variables using only the eigenvector sensitivity data and looping over all the elements being in error recursively yields the following figure:

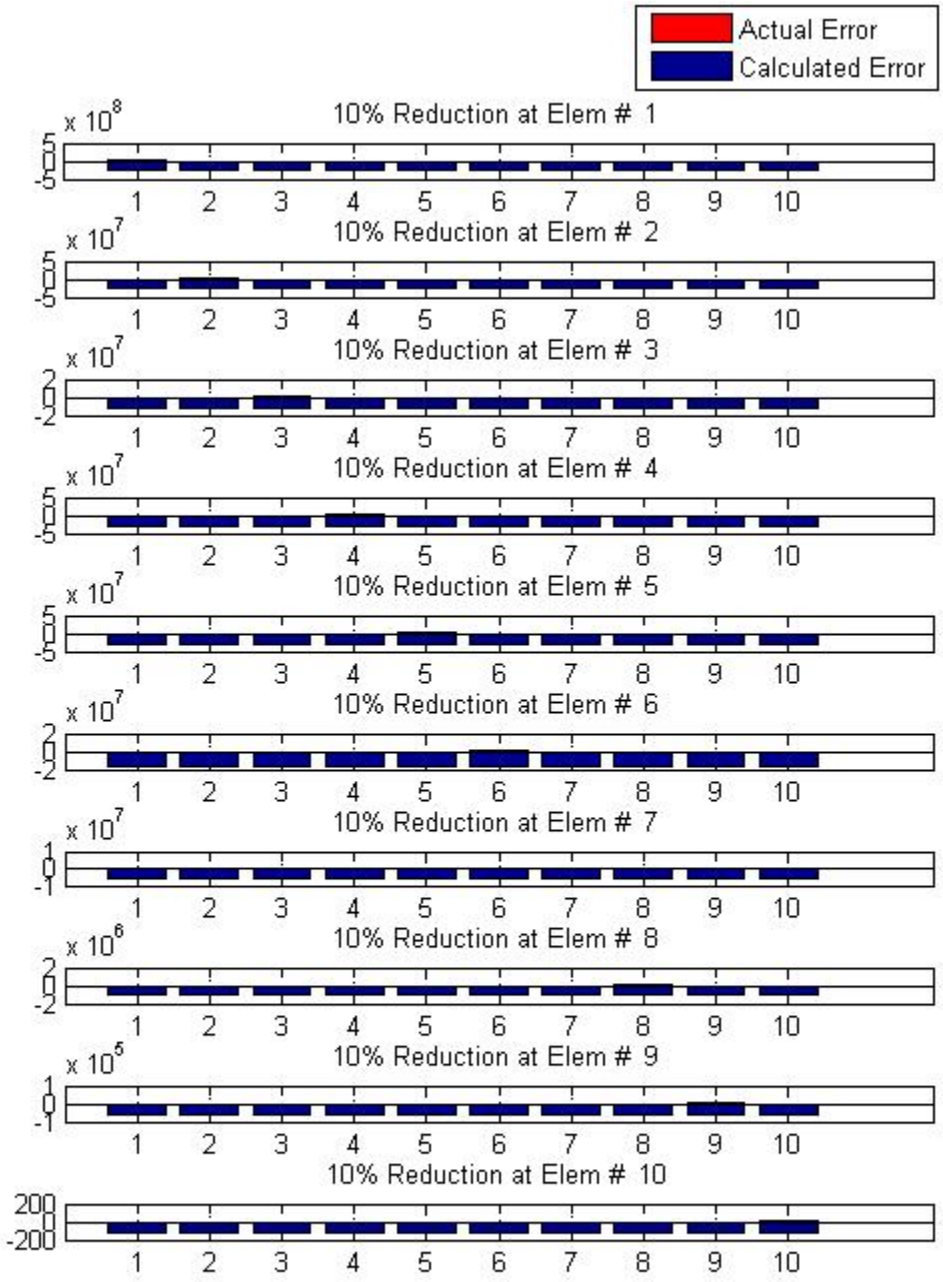

Figure 27. Solution Using Mode 1 of Full Eigenvector Sensitivity Matrix Only

It is pretty obvious that no positive result can be extracted from this approach, even though more than a square matrix, an over-determined matrix, is used for the analysis.

However, if eigenvalue sensitivity data is used along with mode shape data, a totally different outcome is produced. Using only the first mode, as seen in Figure 28, this configuration is capable of predicting damage anywhere in the structure:

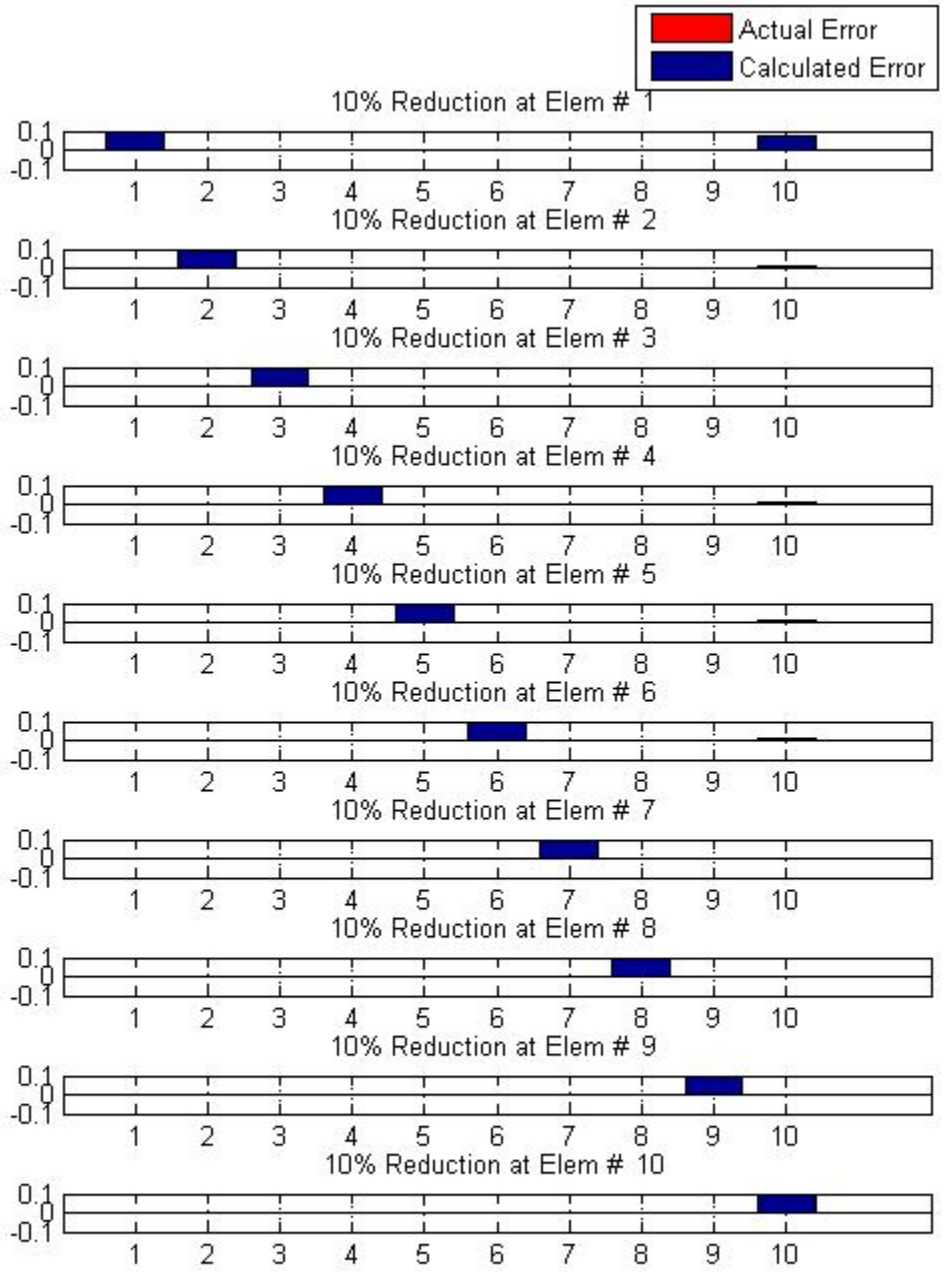

Figure 28. Solution Using Mode 1 of Eigenvalue and Full Eigenvector Sensitivity Matrix

The same positive results yield if only the translational DOFs are considered to be measured and, thus, be considered in the mode shape data, as is shown in Figure 29.

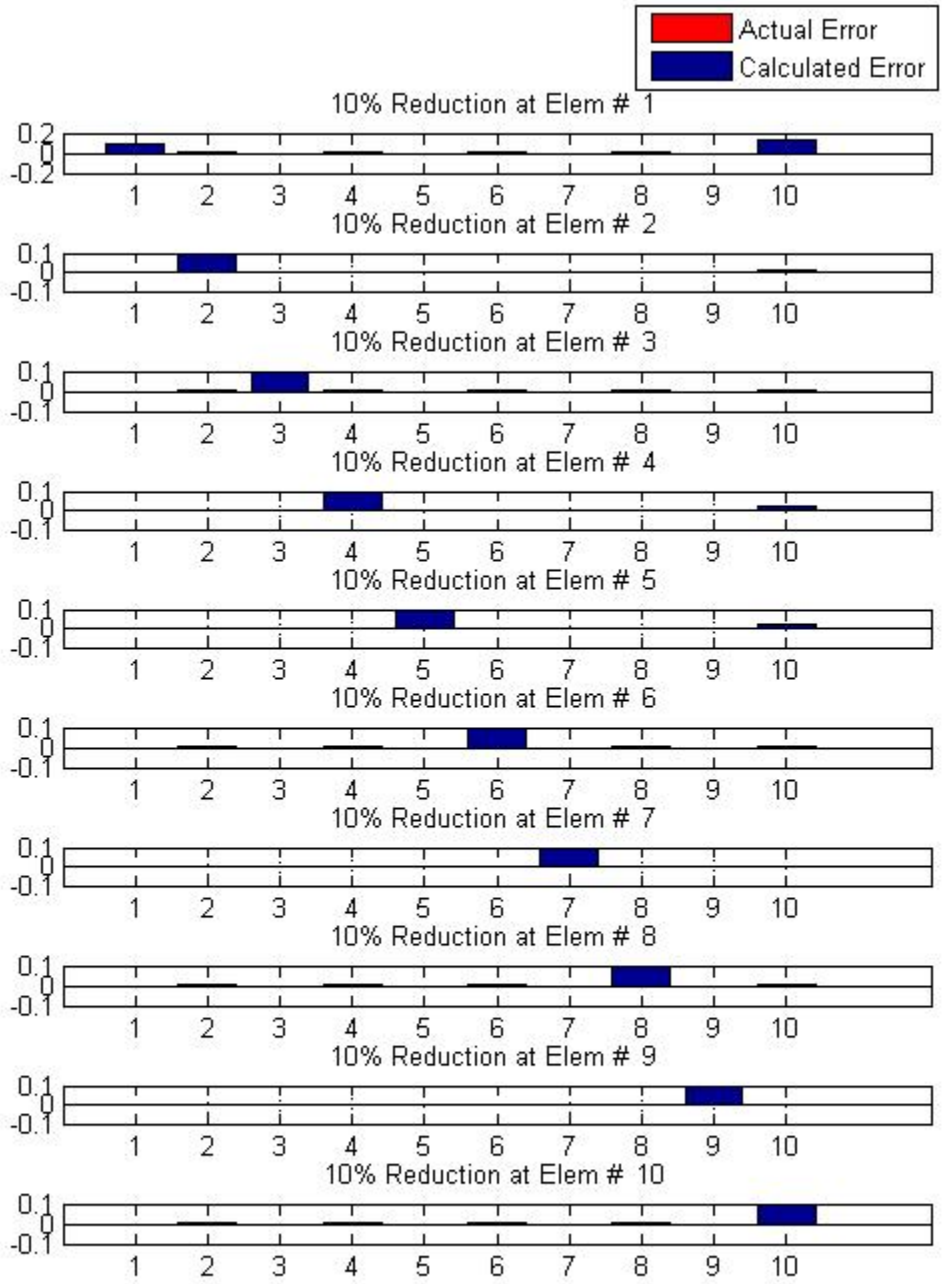

Figure 29. Solution Using Mode 1 of Eigenvalue And All Translational DOF of Eigenvector Sensitivity Matrix

In spite of the positive results shown in Figures 28 and 29, it is realistically impossible for all DOF, or even all the translational DOF to be measured. Therefore, spatially incomplete mode shape data are examined in the following two ways. The first considers DOFs 3, 7, 11, 15, 19 of the cantilever beam to be measured and provides accurate mode shape data. The second one considers DOFs 3, 5, 7, 9, 11, 13, 15, 17, and 19 to be measured. Then, the first mode of this data is used in each case for system identification through a combined eigenvalue and eigenvector sensitivity matrix, which are, respectively, a 6x10 underdetermined and a 10x10 square matrix. The solutions corresponding to these cases are demonstrated in Figures 30 and 31. The figures show that these are not configurations that give positive results no matter where the true error is. Actually, the first case positively identifies the error in six out of ten locations (which in terms of efficiency is the best it could do, since the sensitivity matrix is 6x10, as was described in Chapter III), and it will never predict the error in the remaining four locations, since the output vector has only six fixed non-zero components. On the other hand, although in the second case a square matrix is used, it is not able to predict the correct element being in error in all the locations. This is another example of why a square matrix is a necessary (first case, Figure 30) but not sufficient (second case, Figure 31) condition for damage detection through a unique sensitivity matrix.

Conclusively, it can be said that mode shape design sensitivity data may be used for the augmentation of the modal frequency data used for the sensitivity based FEM updating, while by themselves they do not constitute a reliable way to identify errors in the structure. Of course, considerable thought relative to the right choice of DOF to be measured should not be neglected, because different configurations have quite different effects on the output result as shown in the cases examined above. Beyond that, the drawbacks referred to in the beginning of this chapter must be taken into account in terms of the availability of measurement locations and of the accuracy associated with those measurements.

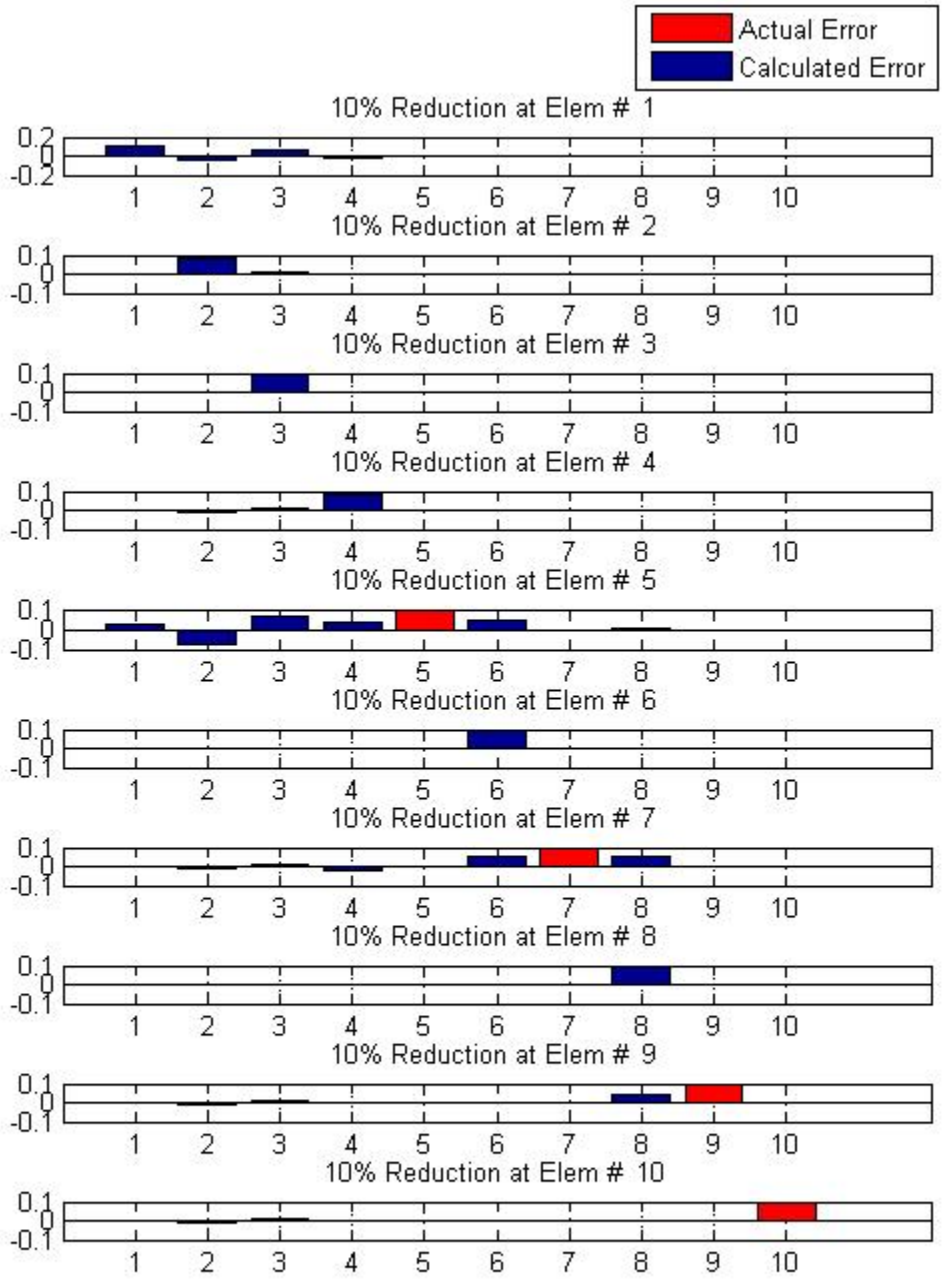

Figure 30. Solution Using Mode 1 of Eigenvalue and Translational DOFs [3, 7, 11, 15, 19] of Eigenvector Sensitivity Matrix (Underdetermined)

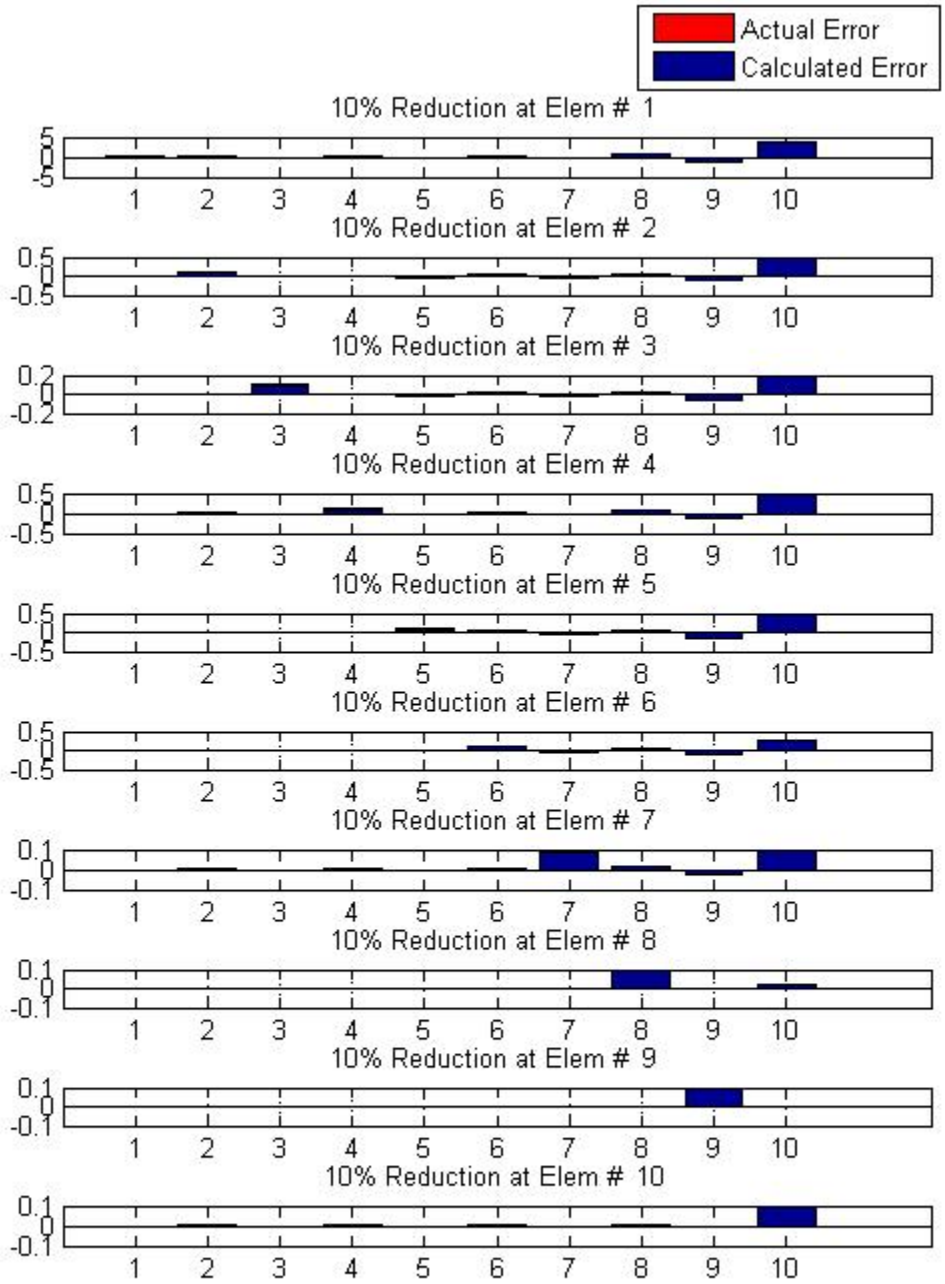

Figure 31. Solution Using Mode 1 of Eigenvalue and Translational DOFs [3, 5, 7, 9, 11, 13, 15, 17, 19] of Eigenvector Sensitivity Matrix (Square)

B. PARAMETER SELECTION

As outlined in Chapter I under the background section, the first attempts to override discrepancies that are generated during the updating procedure were focused on what is called parameter selection. This method can be viewed in different variations, since several analyses have been made through the years and are provided in the literature. Some of them will briefly be described in the following paragraphs.

1. Subset Selection

The parameter subset selection method chooses a subset of the design variables that minimizes a penalty function based on the norm of the residual of Equation (2.31) as it is summarized in [5]. In that sense, it is assumed that only a subset of the parameters has corresponding independent columns of the sensitivity matrix and the optimum subset is chosen through an iterative procedure to produce a sub-optimal solution, commonly known as forward selection [3].

The first step is to find a single column among the columns of the sensitivity matrix that best represents the frequency differences vector $\Delta\omega^2$. Next, the combination of two columns that constitute the best sub-basis for the spanning of $\Delta\omega^2$ is determined, while the first parameter selected is retained. Then a Gram-Schmidt orthogonalization is performed and both the sensitivity columns and the $\Delta\omega^2$ are replaced by the corresponding vectors. The procedure is now repeated on this reduced problem for the next parameter that gives the smallest residual. An iterative process is then produced in order to combine the best parameters chosen with each one of those remaining to pursue the best data representation. It should be noted that the criterion of the smallest residual is equivalent to the smallest angle or distance of the vectors or the vector subspaces existing or created respectively.

The subset selection problem may also be solved by using an exhaustive search of all possible subsets that minimize the penalty function and eventually choose the best subset that constitutes the global minimum of all the cases. However, taking into account

that the number of parameters and also the size of the subsets may be large for reasonable realistic problems, the computation required for an exhaustive search is prohibitive [5].

2. Clustering of Design Variables

Another approach, similar to the subset selection method, is that dealing with clustering analysis. In this approach, the columns of the sensitivity matrix are considered as vectors in multi-dimensional space. For example, if they are identical, they appear as co-linear vectors, meaning that the corresponding parameters affect the same way the modes of the structure. The eigenvalue sensitivity matrix for a large FE model will contain many quasi-dependent columns; these can be identified via the clustering approach and may be combined so that the conditioning of the problem is improved. The most similar columns are added together, and in this way, the information available from the measurements is used to converge the model by the smallest adjustment to the updating parameters [9]. Again, in the general application of the clustering method, a distance criterion is needed to assess the similarity of different objects as is described in [10] and then as is also described, a method of linking the similar objects within the cluster is necessary. Clustering methods have been successfully demonstrated in [8], [9], [10], however, it has to be said that if during the updating, the sensitivities columns change, different clusters might be formed. Nevertheless, in the case of large and complex systems, clustering analysis is able to carry out the task of efficiently comparing many possible sensitivity columns. Together with sensitivity analysis and subset selection, it provides a method for including the effects of changes to less sensitive substructures by combining those columns of the sensitivity matrix that are close over the bandwidth of the modal testing.

3. Grouped Elements Sensitivities

A different manner in which selecting parameter is considered is presented in [7]. The concept of total sensitivity is introduced as the absolute sum of the sensitivities. The simple observation that this analysis is based on is the following. Suppose n design variables are considered and they are about to be merged into one that groups in a way

the effectiveness of the selected parameters into one sensitivity value. Then, if T_{tot} represents this value and T_i represents the sensitivity value corresponding to each design variable, for $i = 1:n$, it is easy to see that:

$$T_{tot} = T_1 + T_2 + \cdots + T_n = \sum_{i=1}^{n} T_i \tag{4.1}$$

The total sensitivity, as defined above, will be:

$$\left|T_{tot}\right| = \left|T_1 + T_2 + \cdots + T_n\right| \le \sum_{i=1}^{n} \left|T_i\right| \tag{4.2}$$

The equality holds only when the signs of the individual sensitivity values of the design variables have the same sign. This leads to the conclusion that by grouping design variables into larger parameters, the number of parameters can be reduced, but the total sensitivity decreases, in general. From this basic observation, the parameter selection procedure, sets of parameters can be constructed with the objective that their effect on the residual of Equation (2.31) is maximized, meaning that the residual to be minimized is more sensitive to those selected parameters.

This procedure is accomplished by a sequence of two different selection phases [7]. The first phase involves merging two neighboring elements into one parameter, as long as the signs of their sensitivity values are the same. Then, Equation (4.2) turns out to be equality and identical to Equation (4.1), so that the total sensitivity is just the sum of the merged parameters' sensitivities. This phase ends when no neighboring parameters have the same sensitivity sign.

If the number of the reduced parameters is not acceptable, then the second phase begins, but in this case, the sacrifice of total sensitivity is unavoidable. Obviously, none of the neighboring parameters have the same sign of sensitivities and by merging two neighboring design variables, the total sensitivity is changed:

$$\sum_{\substack{k=1 \\ k \ne i,\, j}}^{n} \left|T_k\right| + \left|T_i\right| + \left|T_j\right| \rightarrow \sum_{\substack{k=1 \\ k \ne i,\, j}}^{n} \left|T_k\right| + \left|T_i + T_j\right| \tag{4.3}$$

so that the decrement of the total sensitivity is expressed as:

$$|T_i| + |T_j| - |T_i + T_j| \tag{4.4}$$

In other words, the sacrifice for reducing one parameter in terms of sensitivity, in this phase, is equal to Equation (4.4). This phase ends when some criteria that have been imposed, such as the number of design variables or the maximum allowed sacrifice, or both, are met.

In this work, the concept of grouping neighboring elements is used to enlarge the available data. Since a cantilever beam is examined, and as seen in Figures 11 and 12, the sensitivity values are positive for all the design variables and for all the modes, no total sensitivity sacrifice is required. In other words, the first phase described above is sufficient for the analysis. So, the grouping of the *10* elements of the cantilever beam into *5* pairs of neighboring elements results in the sensitivity matrix of dimension *20x5* whose distribution of all the rows is presented in Figures 32 and 33. Note, that in the following figures, the first bar corresponds to elements 1 and 2, the second bar corresponds to 3 and 4 and so on until the fifth bar, which corresponds to elements 9 and 10. This means that, for example, the highest value of the first row of the grouped sensitivity can be taken to occur at either the first or the second element of a *10* element cantilever beam. This will prove of crucial importance later on when the concept of grouped sensitivity will be used to enhance the use of ABC for this analysis.

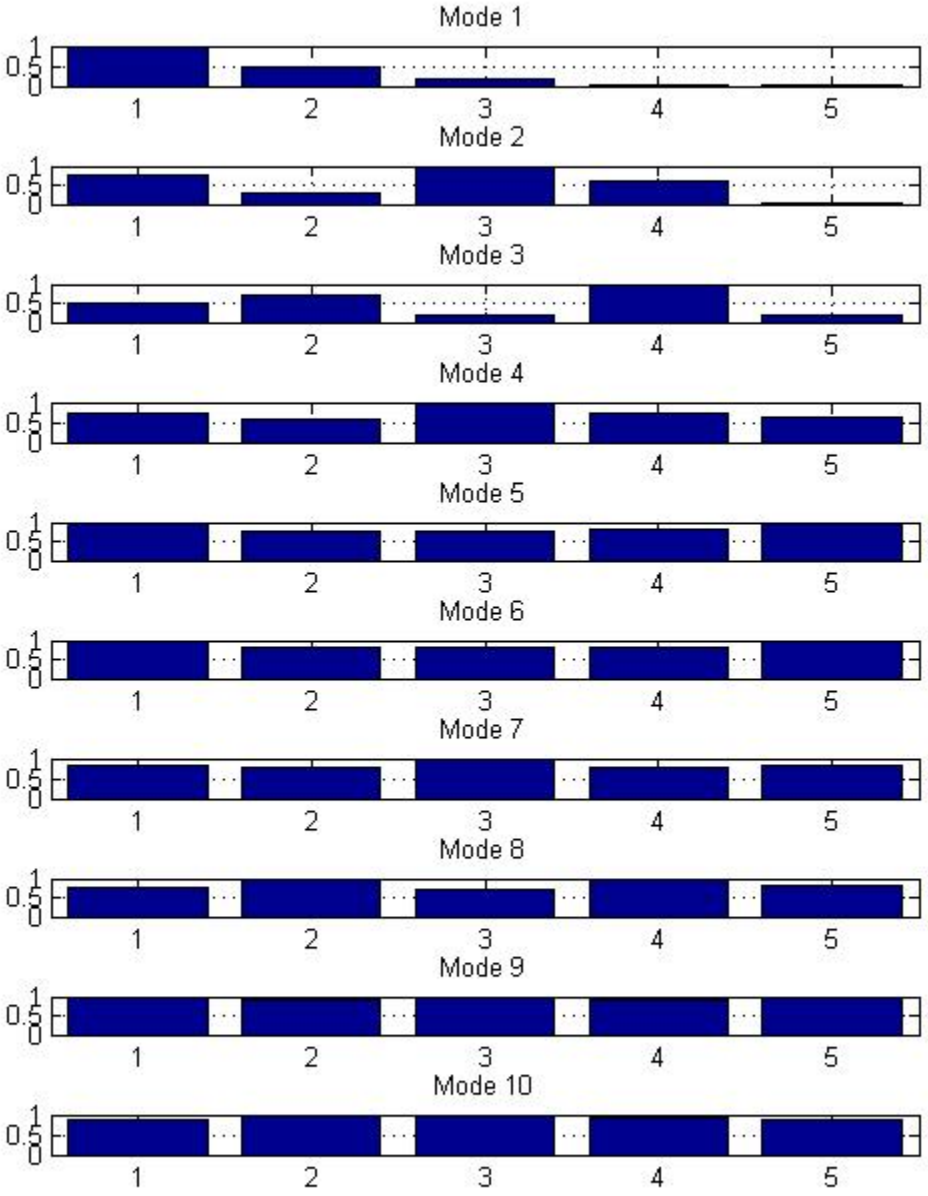

Figure 32. Grouped Sensitivity Modes 1 Through 10

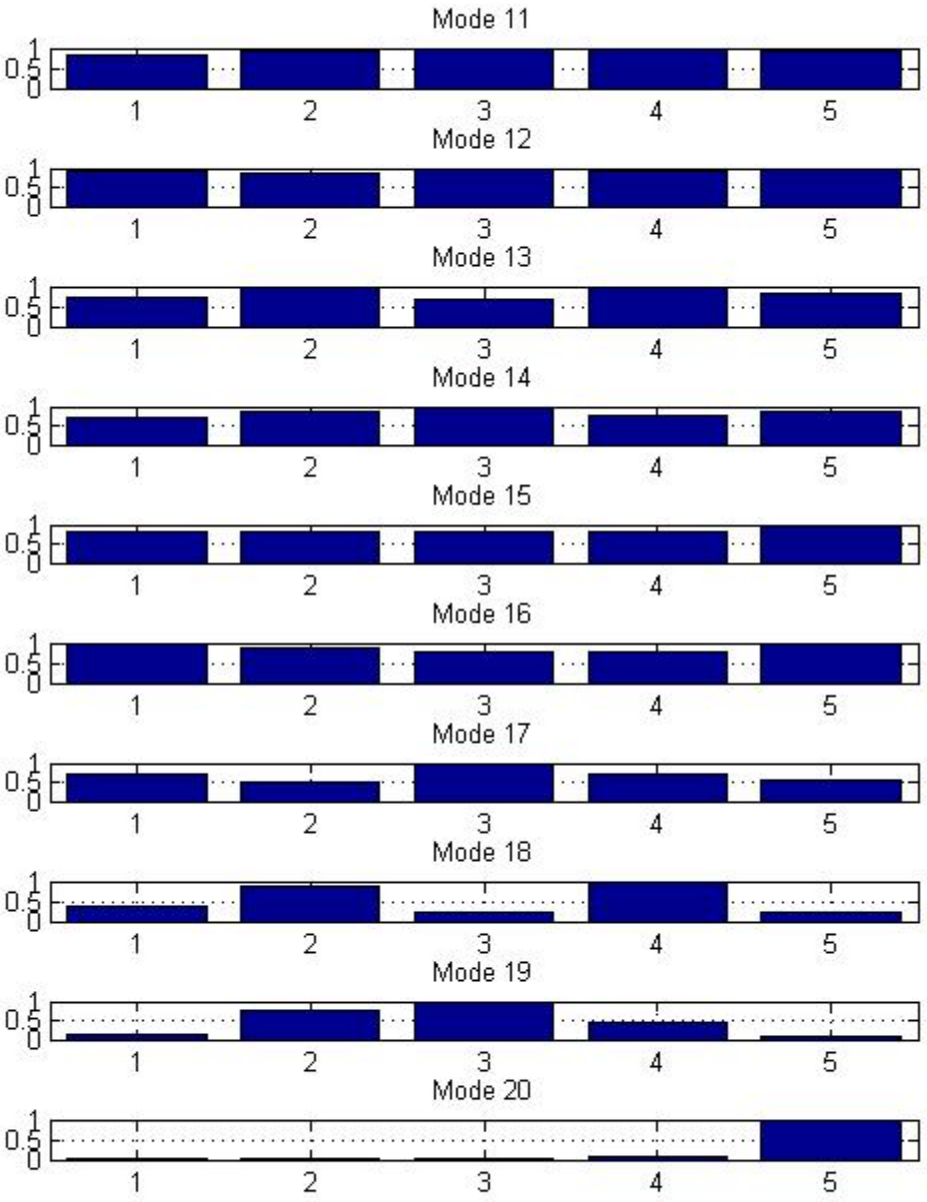

Figure 33. Grouped Sensitivity Modes 11 Through 20

C. THE USE OF ABC

Before getting into the details of using ABC as an efficient way of enhancing the sensitivity matrix determinability, it is useful to mention several things about the natural frequencies of the ABC systems and their connection to the baseline system natural frequencies, with a short reference to Cauchy's Interlace Theorem.

1. Cauchy's Interlace Theorem

Interlace theorem, in general, deals with the eigenvalues of a principal submatrix related to those of the main matrix. According to the analysis made in [25], assume a matrix A of dimension *nxn* and the submatrix H of dimension *mxm*:

$A=\begin{bmatrix} H & B^{*} \\ B & H \end{bmatrix}$ with A's eigenvalues: $a_1 \le a_2 \le a_3 \cdots \le a_n$ and H's: $\theta_1 \le \theta_2 \le \theta_3 \cdots \le \theta_m$

The theorem states that for $j=1,\ldots,m$ it is:

$a_j \le \theta_j \le a_{j+n-m}$ and equivalently, $a_{-(j+n-m)} \le \theta_{-j} \le a_{-j}$.

Alternatively, for $k=1,2,\ldots,n$ it is:

$\theta_{k-n+m} \le a_k \le \theta_k$ and $\theta_{-k} \le a_{-k} \le \theta_{-(k-n+m)}$.

In other words, $\theta_{\pm j}$ is an inner bound on $a_{\pm j}$ relative to A's spectrum. For example, consider the following example, where $H=\begin{bmatrix} 0 & \varepsilon \\ \varepsilon & 0 \end{bmatrix}$ and $A=\begin{bmatrix} 0 & \varepsilon & 0 \\ \varepsilon & 0 & 1 \\ 0 & 1 & 0 \end{bmatrix}$ Figure 34, below, contains a schematic representation that demonstrates the theorem using the values of the above example.

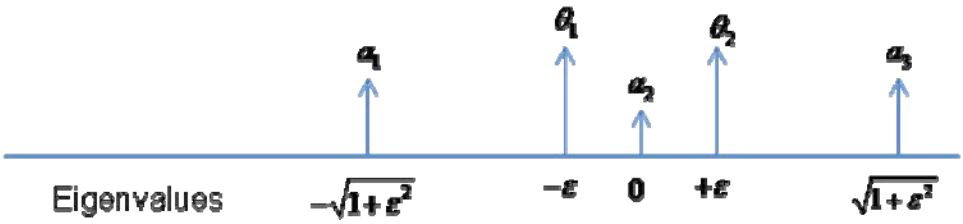

Figure 34. Schematic Representation of Cauchy's Interlacing Theorem

The actual application of this theorem to the ABC natural frequencies is that these frequencies will always interlace the natural frequencies of the system of higher order. This means that if a baseline system is considered, like the cantilever beam of the previous analyses, and one ABC is imposed on this system, then the eigenvalues of the ABC system will interlace the eigenvalues of the unconstrained cantilever beam. So, the first eigenvalue of the ABC system will be between the first and the second eigenvalue of the baseline system and so on. If a second ABC is imposed on the system, then the ABC system, with the two artificial constraints, will have natural frequencies that will interlace those of the ABC system with the one constraint. Therefore, in terms of bandwidth limitations, it is even better to use the *ith* mode of an ABC system than the *ith+1* mode of the baseline system, if no other obvious reason for the use of each is present. Figure 35 may be useful for the demonstration of this interlacing:

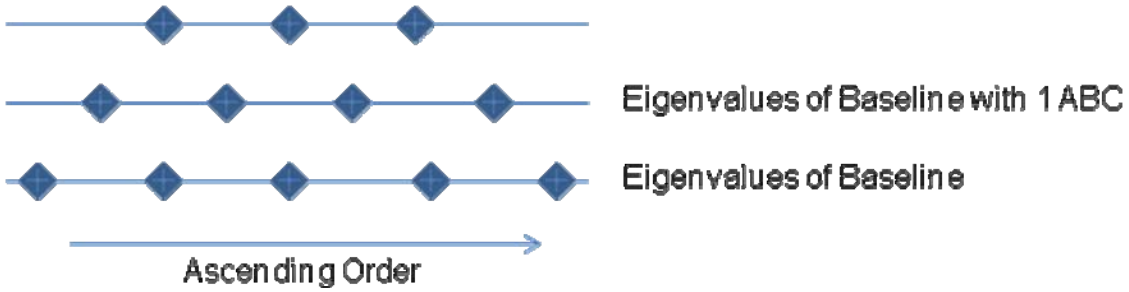

Figure 35. Schematic Representation of Interlacing Between ABC and Baseline Natural Frequencies

2. Using ABC

Having said how ABC information can be obtained and where this information is relative to the spectrum of the baseline system, several ABC systems are used to facilitate the error prediction in the cantilever beam that is examined in this work. All these configurations are used in the concept of building an at least square sensitivity matrix that will be able to manipulate data from the FE model, and from the modal testing of the structure, and provide a positive outcome via the Matlab linear system solution.

The manner in which ABC are selected is based on the principle that sensitivity is increased in areas near the artificially imposed constraint, as shown in [18]. This observation can help since the sensitivity distribution throughout the structure is likely predictable, at least for the fundamental mode, of each ABC configuration. Therefore, the first step is to create 10 different ABC systems, which will consist of the baseline cantilever beam and a pin imposed on each one of the 10 unconstrained translational DOF, respectively. All the data needed for these systems, like natural frequencies, mode shapes and sensitivities, are obtained the same exact way as for the baseline system. The first mode of the corresponding sensitivities, along with that of the baseline system, is showed in Figure 36, where the red triangle depicts the DOF where the constraint is imposed and all the values are normalized to the maximum value of the first mode of each system. It is easily noticeable how the constraints increase the sensitivity near the DOF that they are imposed on, as long as these DOF are not near the free end of the cantilever. As one can see,, the three last configurations tend to simulate the second mode of the baseline system, which is not strange considering the values of their natural frequencies (close to the second baseline eigenvalue) and their mode shapes (qualitatively close to the second baseline mode shape).

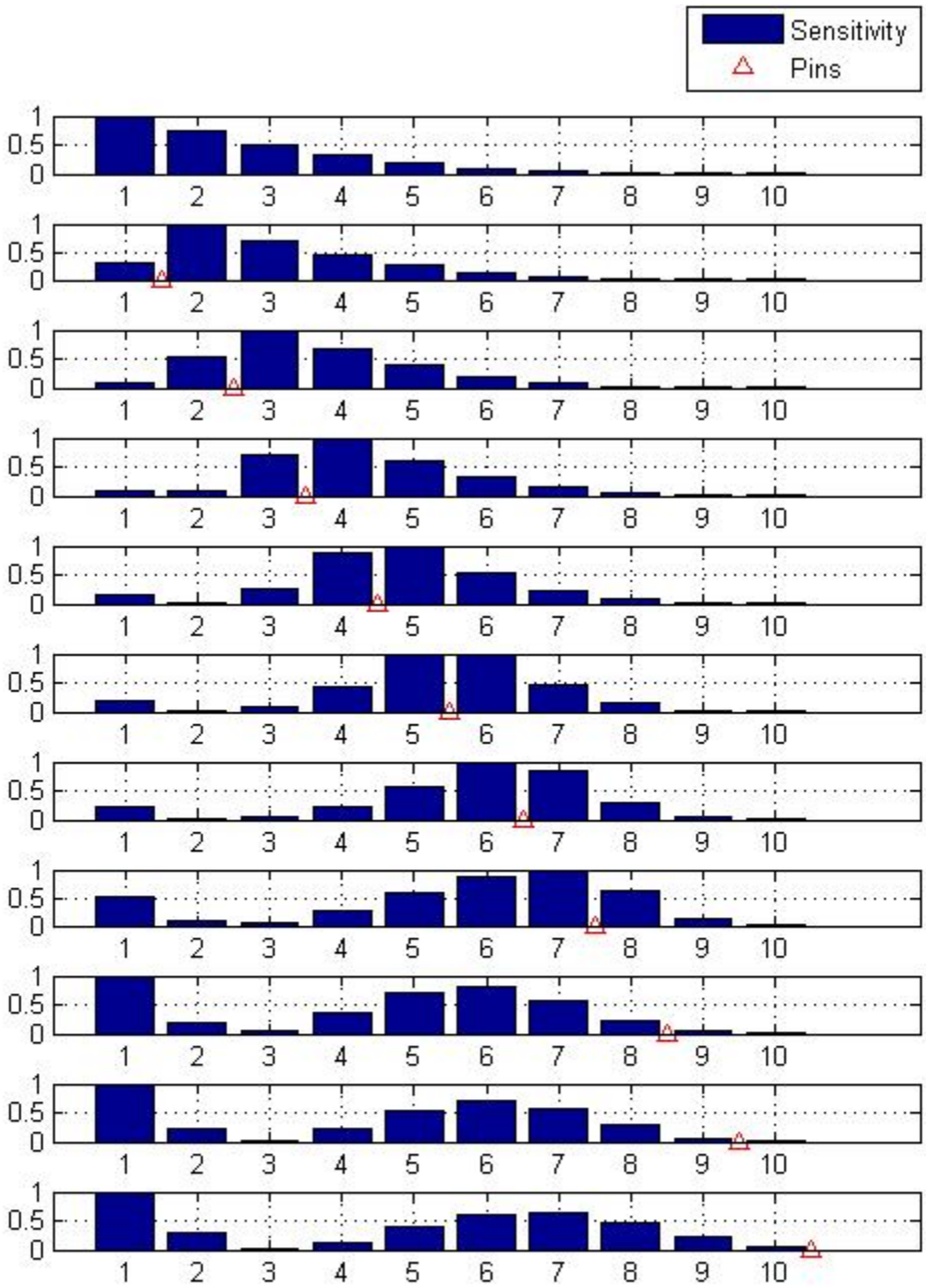

Figure 36. First Mode of Sensitivity Matrix of Baseline (Plot 1) and of Each ABC System (Plots 2-11)

Next, the solution to the fundamental Equation (2.31) is pursued using two approaches. The first one uses all the configurations described in Figure 36, thus

constructing an overdetermined *11x10* sensitivity matrix, while the second uses only the ABC configurations (Plots 2-11 of Figure 36), thus constructing a square matrix. These solutions are demonstrated in Figures 37 and 38, where the prediction of this model for all the elements being in error recursively is provided.

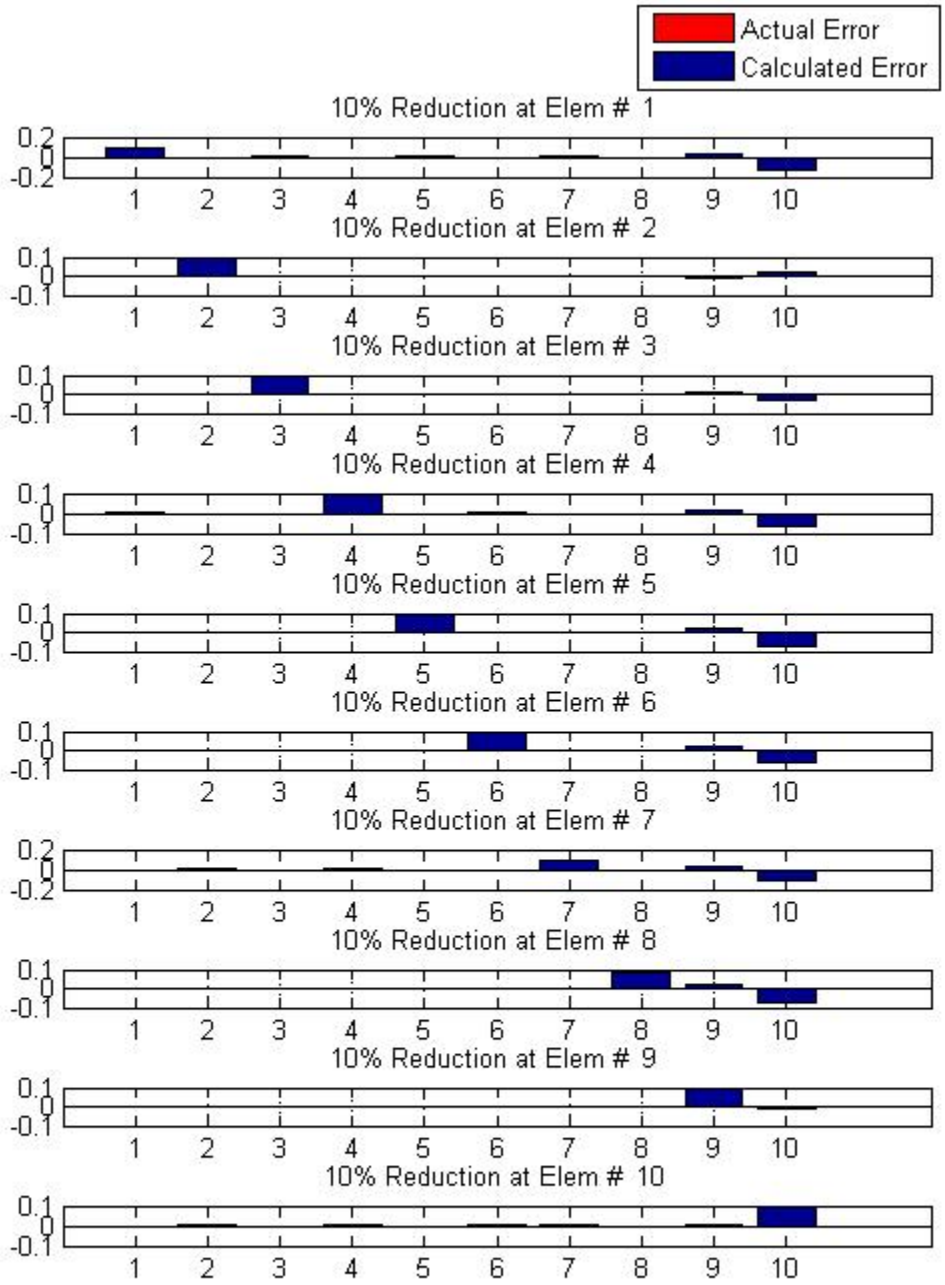

Figure 37. Solution Using Mode 1 of Baseline System and of Each ABC System

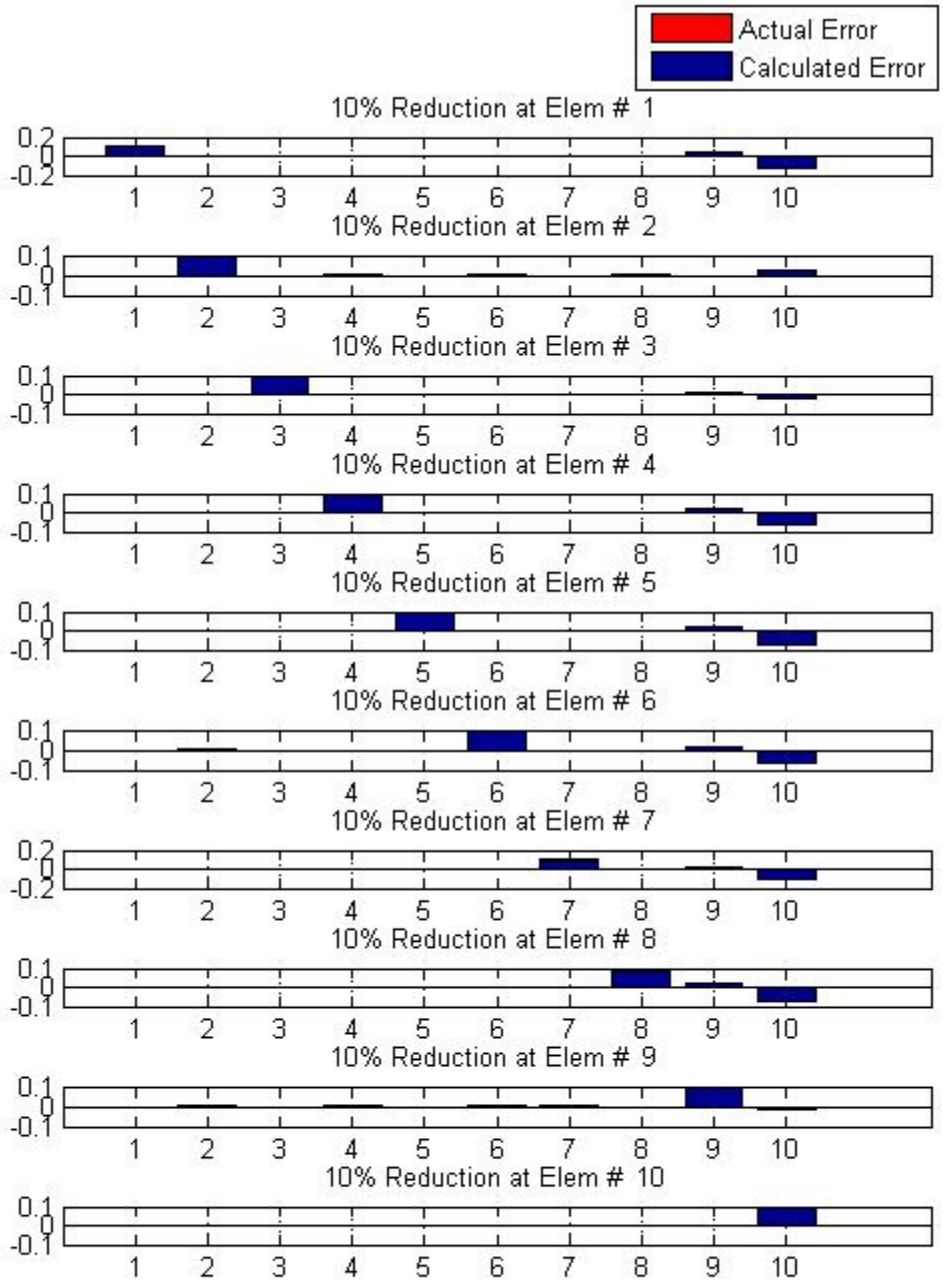

Figure 38. Solution Using Mode 1 of Each ABC System Only

The two solutions provided in the above figures are quite similar since the sensitivity matrices used in each case do not have many differences in terms of sensitivity distribution along the structure, and since the frequencies difference vector used is almost

the same. What is also obvious, is that the use of these ABC configurations is quite encouraging since, at no cost, a relatively good solution is reached with the actual error being predicted in all cases, both in location and in magnitude, the only drawback being the presence of bias considerably comparable to the true error in some of the cases (when actual element in error is 1, 4, 5, 6, 7, 8). Towards the direction of eliminating this bias, other configurations will be pursued later in this thesis.

A very important observation that is made from studying Figure 36 and imagining these plots as the rows of a sensitivity matrix is that, as was described before, the last three rows seem almost identical. This means that they add a degree of linear dependency between them, which does not provide the linear system with any useful additional information, but also constitutes a discrepancy in the whole procedure of the linear system solution as was stated in the introductory chapter. Therefore, only one of these three configurations may essentially be used as a means of adding data to the system while the other two must be replaced by other more useful configurations. It can be seen that even by excluding the configuration that corresponds to a constraint imposed on the eighth translational DOF (plot 9 of Figure 36), which is the one closer to the second mode of the baseline system, and thus using a square sensitivity matrix, the solution of Figure 39 is achieved. This solution is somehow similar to those of Figures 37 and 38, but yet not best since there is still a degree of linear dependency between the last two rows.

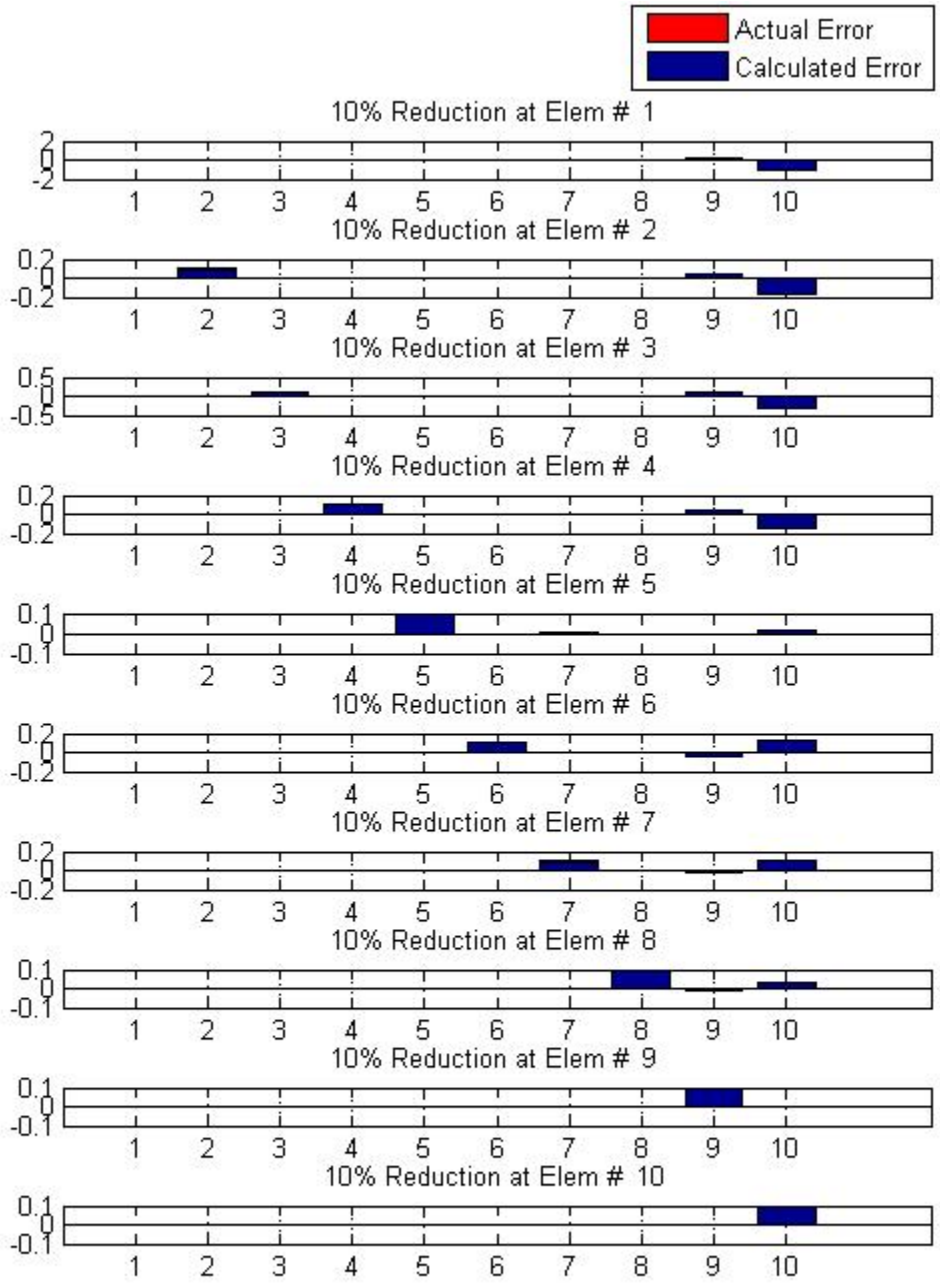

Figure 39. Solution Using Mode 1 of Baseline and of Each ABC System Excluding the One That Constrains the Eigth Translational DOF

Moreover, it can be observed that up to the point that the similar rows described above are excluded, the remaining sensitivity matrix presents a trend that reveals a very

large degree of linear independency and well-conditioning and which is the milestone of the present work. This is the concept of a diagonally dominant or a tridiagonal dominant matrix that is described in the following subchapter and which will be sought through baseline, ABC and grouped element sensitivities configurations. This kind of matrix is a kind of banded matrix in terms of having its larger values on the main diagonal and on the first diagonal below and/or above the main diagonal. In sensitivity terms, it means that there exists a sensitivity concentration around all the different elements of the structure, uniquely identified in each row of the sensitivity matrix. This kind of matrix will be called diagonally dominant banded for the purpose of this thesis since, to the author's knowledge; there is no official mathematical definition that can describe it.

The first attempt at constructing such a sensitivity matrix using modes from the baseline system and from the ABC systems described so far is made using first, fifth and twentieth modes of the baseline system (plots 1, 5 of Figure 11 and plot 10 of Figure 12) and the first mode of each ABC system that imposes a constraint to translational DOF 1 through 7 respectively (plots 2 through 8 of Figure 36). That way, an effort to achieve high sensitivity values to all the elements of the cantilever beam in different sensitivity rows is made, along with keeping out rows that do not provide any useful information for the linear system solution, such as the three last plots of Figure 36. The sensitivity matrix then built is demonstrated in Figure 40 and the solution, with respect to the design variables, is provided in Figure 41. A second attempt uses the same configurations described in the first, replacing the fifth mode of the baseline with the second mode of the ABC system that constrains the eighth translational DOF. The sensitivity matrix constructed and the corresponding solutions are provided in Figures 42 and 43, respectively.

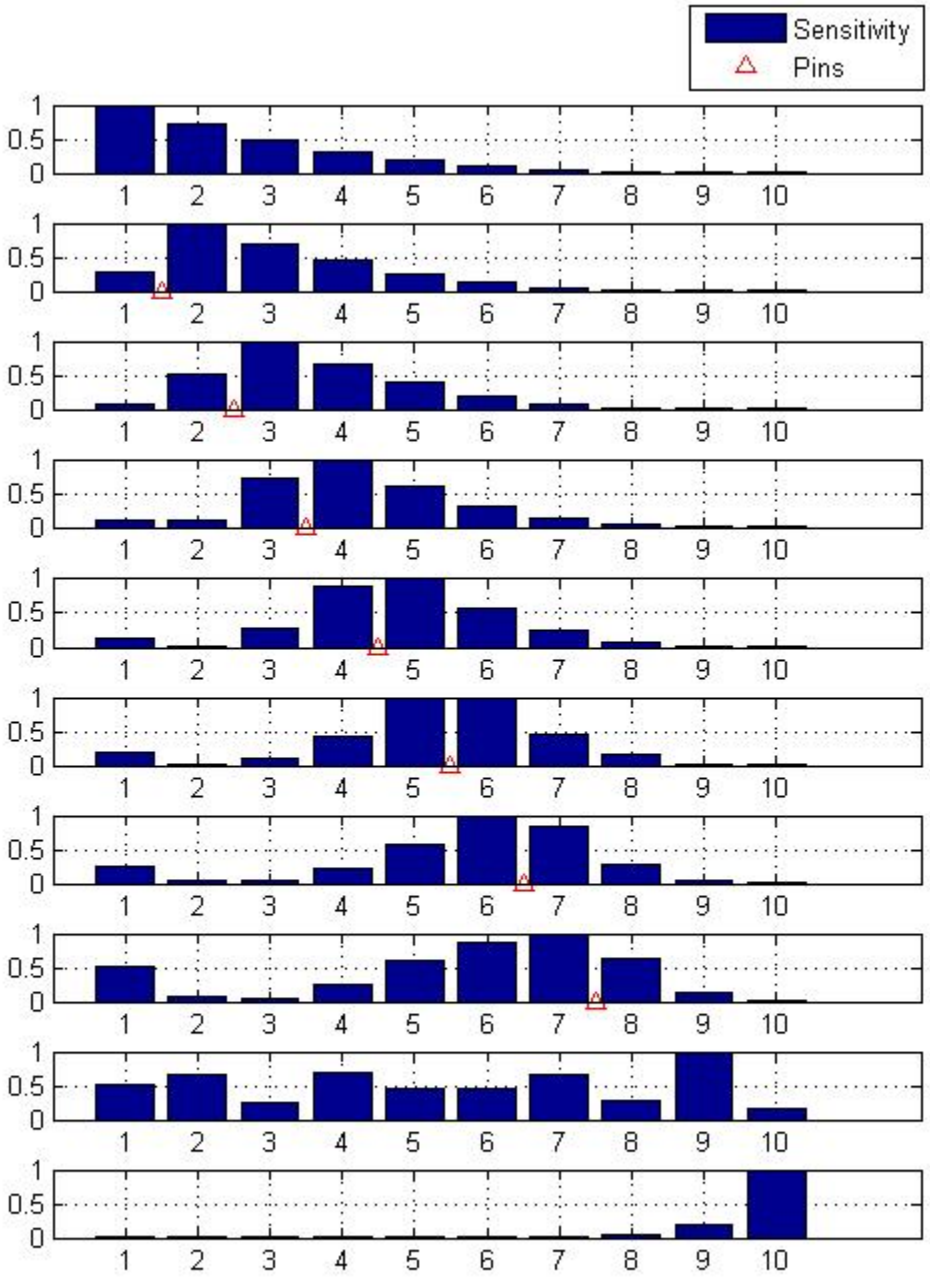

Figure 40. Sensitivity Matrix of Mode 1, 5, 20 of Baseline (Plots 1, 9, 10) and Mode 1 of Each ABC System That Constrains Translational DOF 1 Through 7 (Plots 2–8)

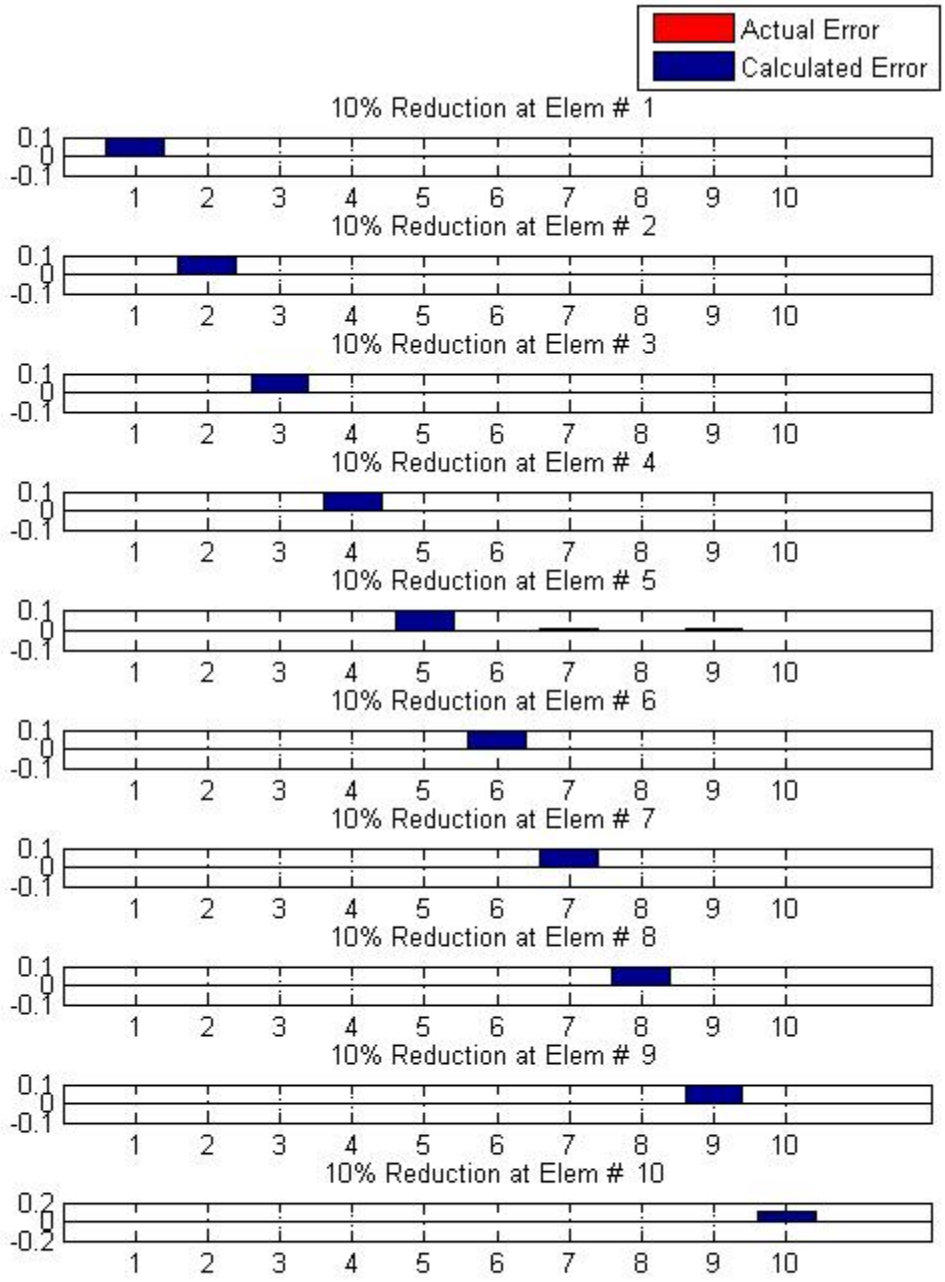

Figure 41. Solution Using Mode 1, 5, 20 of Baseline and Mode 1 of Each ABC System That Constrains Translational DOF 1 Through 7

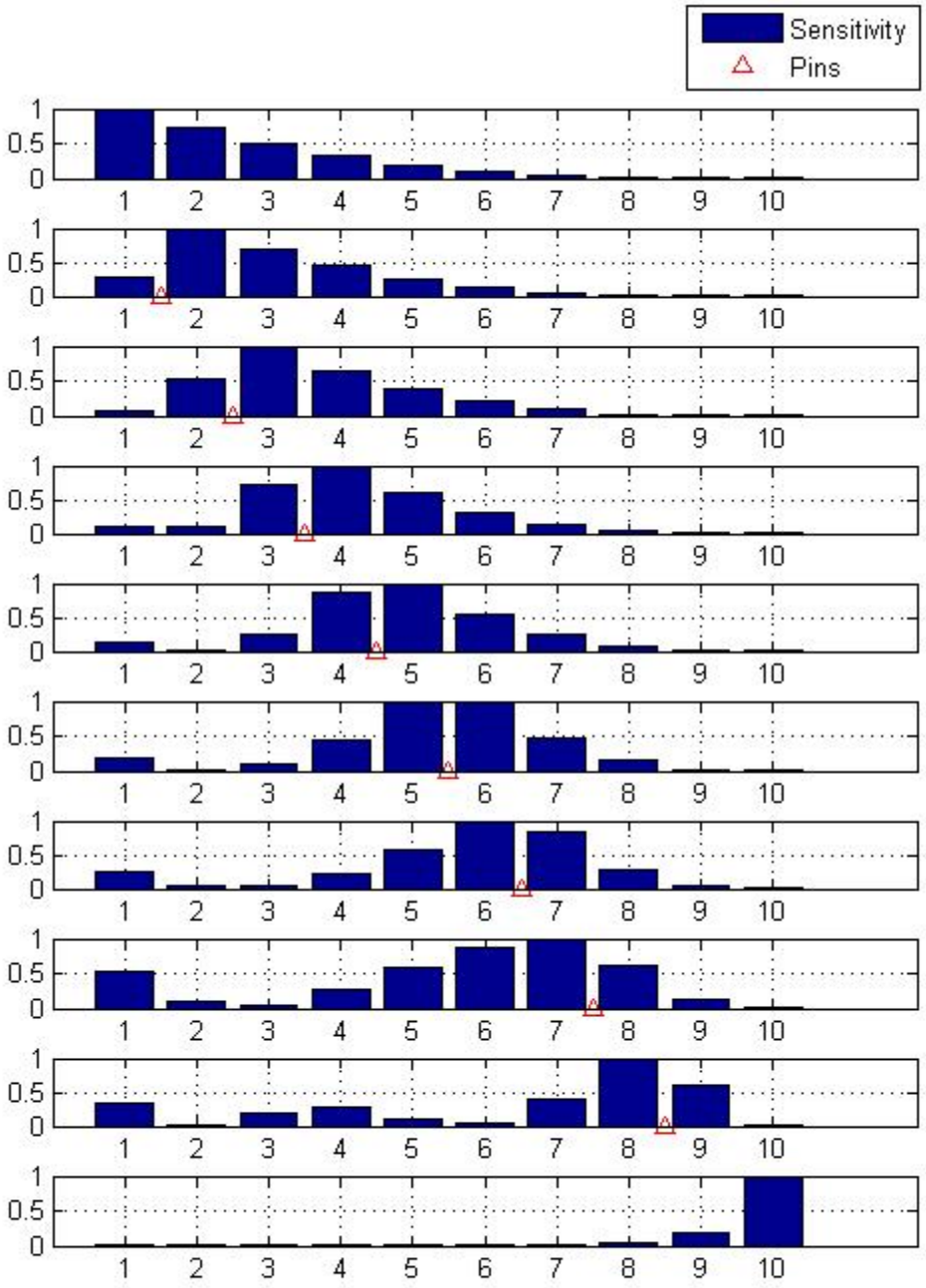

Figure 42. Sensitivity Matrix of Mode 1, 20 of Baseline (Plots 1, 10) And Mode 1 of Each ABC System That Constrains Translational DOF 1 through 7 (Plots 2–8) and Mode2 of ABC System That Constrains Translational DOF 8 (Plot 9)

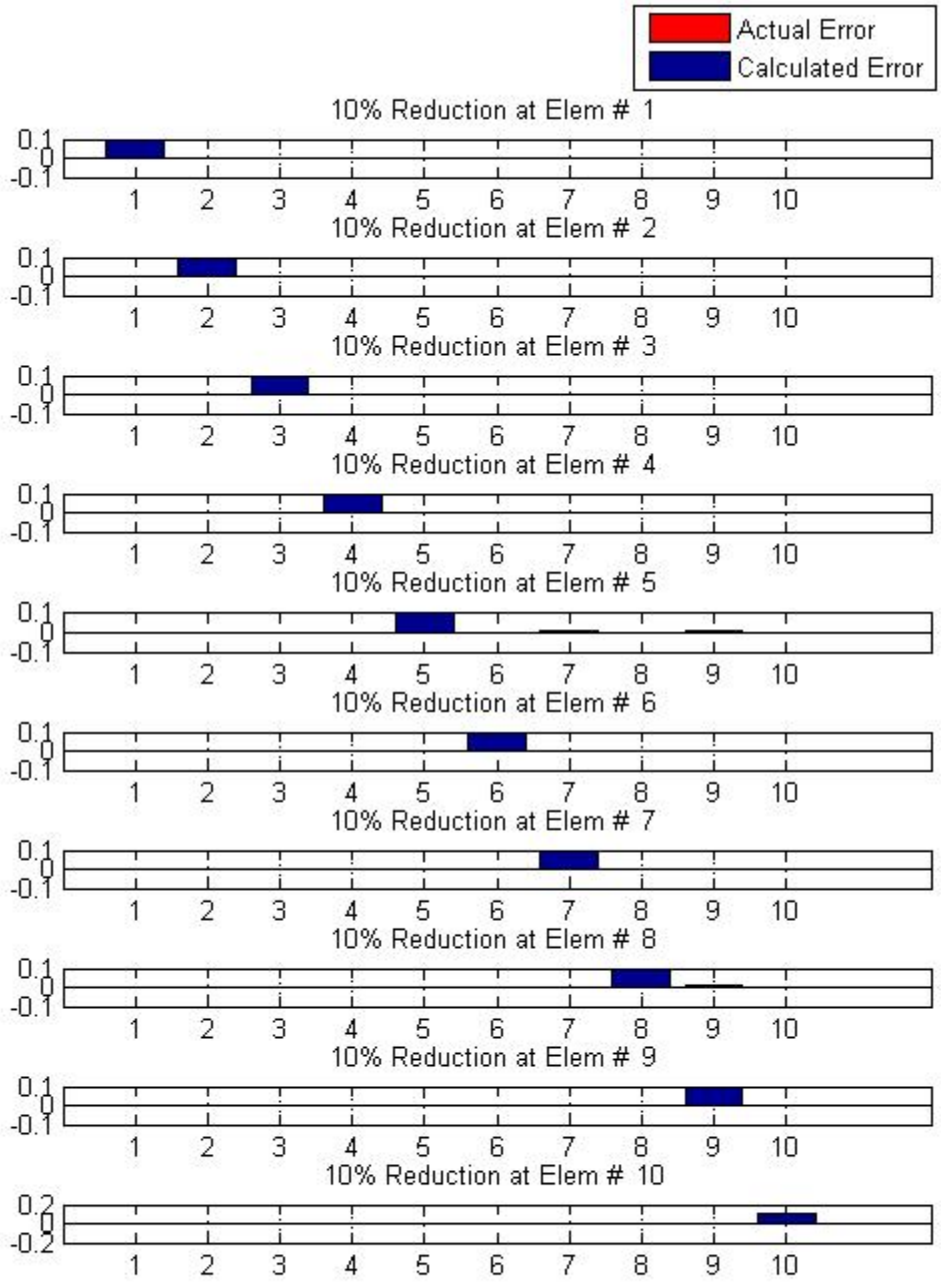

Figure 43. Solution Using Mode 1, 20 of Baseline and Mode 1 of Each ABC System That Constrains Translational DOF 1 Through 7 and Mode2 of ABC System That Constrains Translational DOF 8

As seen in the previous figures, the solutions provided by using these configurations are quite accurate, both in location and in magnitude, as far as the error prediction is concerned. Of course, these examples deal with a very simple structure, for which several ABC configurations with not only one constraint can be used, as long as natural frequencies of those systems are within the frequency spectrum available. Speaking of the available frequency spectrum, it should also be noted that modes higher than those implemented by the nature of each problem, which in general are a few lower modes, cannot be used as it is done with the twentieth mode of the baseline system in the above examples. Knowing this, and that the use of ABC systems may not be unlimited as mentioned, it is shown later in this work how other methods of enhancing the test data, like grouped element sensitivities, can be combined with the use of ABC systems, aiming at the construction of a diagonally dominant banded sensitivity matrix.

3. Diagonally Dominant Matrix

A short description of a diagonally dominant matrix is provided in [26]. According to that reference, a matrix is said to be diagonally dominant if in every row of the matrix, the magnitude of the diagonal entry in that row is larger than or equal to the sum of the magnitudes of all the other (non-diagonal) entries in that row. The concept can be extended to column entries. More precisely, the matrix *A* is diagonally dominant if:

$|a_{ii}| \geq \sum_{j \neq i} |a_{ij}|$ for all i, where a_{ij} denotes the entry in the *ith* row and *jth* column.

It is very important to note here that if a linear system is examined where elementary row operations, such as switching rows, are allowed either through a permutation matrix or just by switching the corresponding entries of the right hand side vector, instead of examining the criterion of diagonal dominance for the diagonal entry, the maximum value of each row can be considered. Then, if the matrix under consideration has a maximum value at different entries for each row covering its whole length, with suitable row switching, it can take the form of a diagonally dominant matrix. Implementing this concept in the global sensitivity matrix used for model updating, if appropriate configurations for a structure can be found and combined together such that

in each row, different elements are subject to the highest sensitivity values while the rest of the values satisfy the criterion described above, this matrix can be said to be a diagonally dominant one. Furthermore, if the strict mathematical definition of diagonal dominance is not satisfied, but there is a significant concentration of high sensitivity values around the diagonal entries, then this matrix can be called a diagonally dominant banded matrix, as stated previously in this chapter.

The main issue regarding this type of matrix is that its properties make it of particular use in several cases. It has been proved that convergence is guaranteed if a diagonally dominant matrix is used in many methods, like Jacobi or Gauss Seidel, for solving linear systems. Also, no partial pivoting is necessary for a strictly column diagonally dominant matrix when performing Gaussian elimination. By the Gershgorin circle theorem, a strictly (or irreducibly) diagonally dominant matrix is non-singular. This result is known as the Levy–Desplanques theorem [26]. These applications are of major importance in FE model updating since they guarantee that there is going to exist a solution to the linear system, which can be solved well-conditioned and with no concern about dependencies that may diverge the solution. The only concern is finding configurations that can sufficiently add data to the underdetermined problem, aiming at creating a diagonally dominant sensitivity matrix.

D. MANIPULATING GROUPED ELEMENT SENSITIVITIES

It has been mentioned above that grouping neighboring elements by simply adding their sensitivities values, with no sacrifice of the total sensitivity as long as they have the same sign, is an effective way of selecting parameters. Figures 32 and 33 show how the grouped element sensitivities are constructed for each mode of the cantilever beam examined, using pairs of two neighboring elements. The next thing to be considered is how these configurations can essentially be used to enlarge the available data and to assist in the effort of constructing a diagonally dominant banded matrix. Doing so can lead to a sensitivity matrix, which combines baseline, ABC and grouped element sensitivities information.

Consequently, it must be shown that grouped element sensitivities data can replace other data in the global sensitivity matrix. At first sight, this seems to be a difficult task, since from what is shown in Figures 32 and 33, if only one miscellaneous mode is examined, its length will be five, corresponding to the five pairs formed from the grouped elements. But the global sensitivity matrix where this grouped element sensitivity mode is to be used has length 10, corresponding to the number of individual elements of the structures which are not grouped. Note here that the desirable use of additional data is towards the enhancement of the determinability of the sensitivity matrix, and not towards the design variables increase, and that can be performed by using grouped element sensitivities as extra rows for the global sensitivity matrix. Therefore, there must be a way found for this five-component row to be permuted to a 10 component row and then added to the global sensitivity matrix, without any loss of its properties.

For that purpose, the twentieth mode will be considered in for the concept used for that permutation to be explained. The highest value of this mode occurs in the last pair of the cantilever beam elements, which are elements 9 and 10. Assume that this value is denoted by $T^{20}_{gr,9and10}$. Then, the rate of change of the sum of the rigidities of elements 9 and 10, with respect to the change of the twentieth natural frequency will be equal to $T^{20}_{gr,9and10}$. In other words:

$$T^{20}_{gr,9and10} = T^{20}_{el,9} + T^{20}_{el,10} = \frac{\Delta DV_{gr,9and10}}{\Delta \omega^2_{20}} = \frac{\Delta DV_{el,9} + \Delta DV_{el,10}}{\Delta \omega^2_{20}} \tag{4.5}$$

From Equation (4.5) it can be seen that this particular sensitivity value can be used to characterize and identify the potential change in the design variable of element 9 or 10 or both, due to the change of the twentieth natural frequency of the system. That leads to the conclusion that $T^{20}_{gr,9and10}$ can be used as the sensitivity value corresponding to one of the elements 9 or 10, while the other will have zero sensitivity value, when both elements are considered in a sensitivity row. This can be equivalently expressed by the

fact that if, for example, one of the two rigidities of elements 9 and 10 is reduced by 10 percent, that is either $\Delta DV_{el,9}$ or $\Delta DV_{el,10}$ is 0.1, then the total decrease to their group will be 10 percent too.

This conclusion allows a wide range of possible manipulations of the grouped element sensitivities data in order to be appropriately used as enhancement measures of the global sensitivity matrix determinability. Figure 44 demonstrates two possible ways of how the twentieth mode of the grouped element sensitivity can be used in the global sensitivity matrix (of length 10) for providing a sensitivity row with highest value at both element 9 and element 10, by simply adding zeros to the elements that are not required to have the sensitivity value desired.

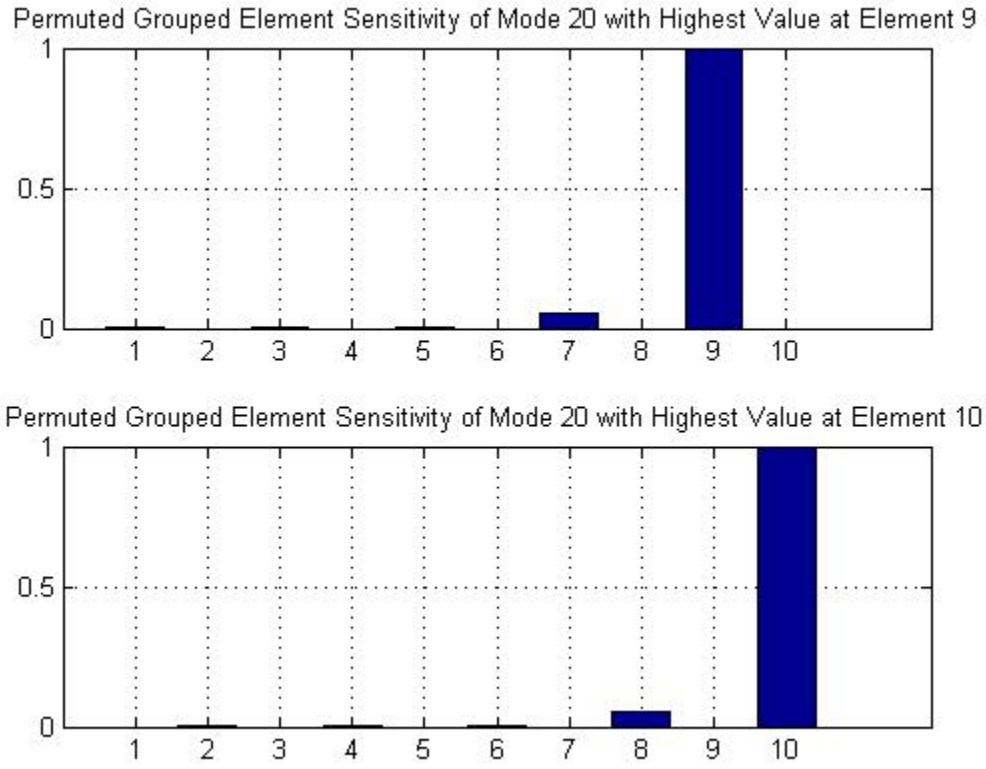

Figure 44. Mode 20 of Grouped Element Sensitivity Permuted to Attribute Highest Value Either to Element 9 (Plot 1) or to Element 10 (Plot2)

E. COMBINING BASELINE, ABC AND GROUPED ELEMENT SENSITIVITIES FOR A DIAGONALLY DOMINANT BANDED MATRIX

The ultimate purpose of this work is to combine baseline, ABC and grouped element configurations in a an essential manner into a global sensitivity matrix, which will be able to predict change to the design variables of a system, given the difference between the natural frequencies of the system to measure (potentially damaged) and those of the original (undamaged) model. Having said that, the configurations of Figure 40 will be used again, that is modes 1,5,20 of the baseline system and mode 1 of each ABC system that constrains the translational DOF 1 through 7, with two different alterations. In the first, mode 5 of baseline system will be replaced by the twentieth mode of grouped element sensitivities permuted to have the highest value at the ninth element (plot 1 of Figure 44), while in the second mode 20 of baseline system will be replaced by the twentieth mode of grouped element sensitivities permuted now to have the highest value at the tenth element (plot 2 of Figure 44). The concept of these replacements is to prove that modes of the baseline system that contribute to the diagonally dominant banded matrix with high sensitivity values at certain elements, can be mutually replaced by modes of grouped element sensitivities that have high values at the same elements, respectively. It is even better, under the principles instituted for the diagonally dominant banded matrix, if the replacing modes, apart from only high value at certain elements, have a significant sensitivity concentration around the element with the highest sensitivity value, but this is something that is achievable depending on the nature of each problem.

Considering the first case mentioned above, the configurations used are presented in terms of sensitivity distribution per row in Figure 45, and the solution reached using these configurations is depicted in Figure 46.

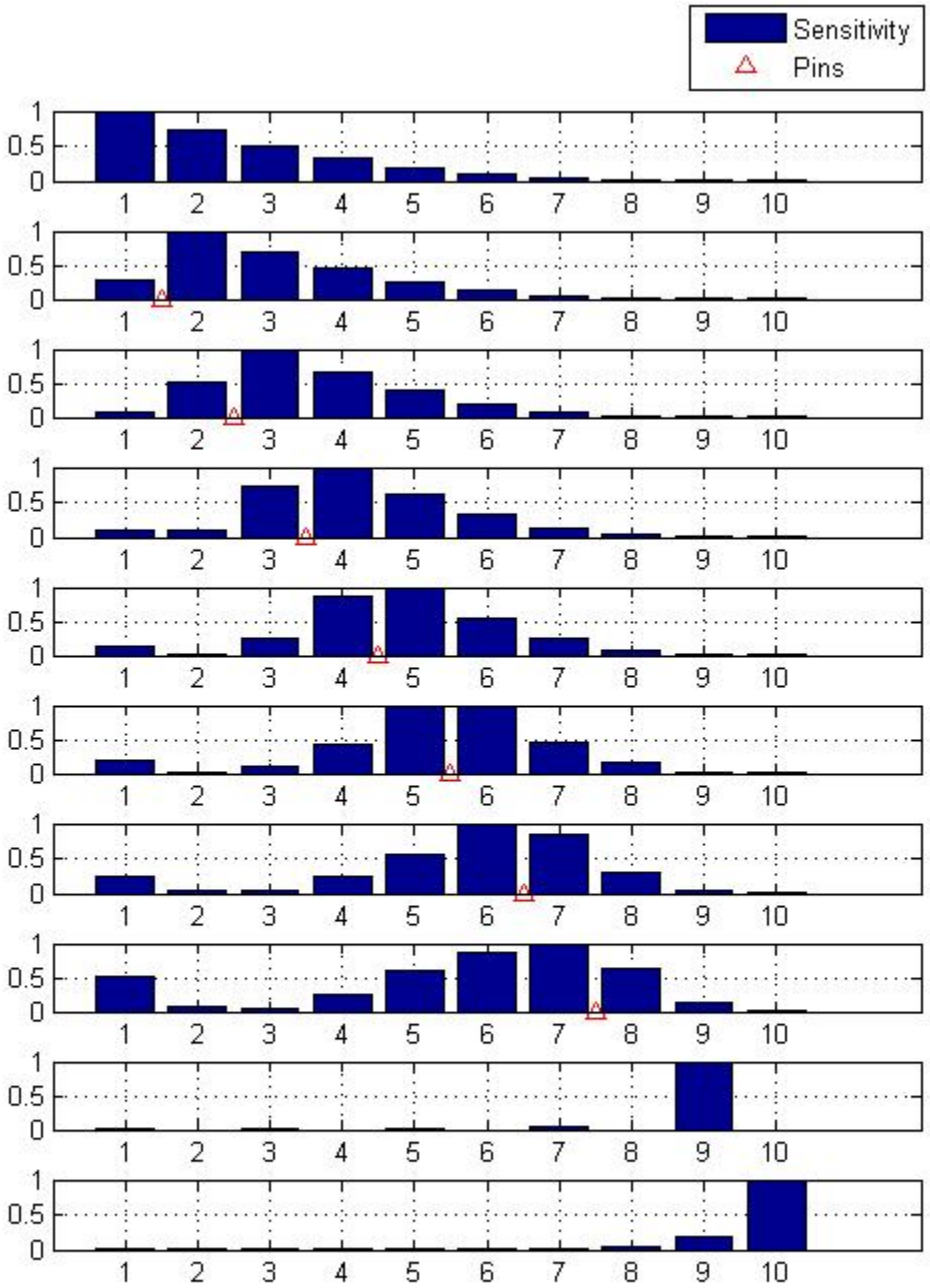

Figure 45. Sensitivity Matrix of Mode 1, 20 of Baseline (Plots 1, 10) and Mode 1 of Each ABC System That Constrains Translational DOF 1 Through 7 (Plots 2–8) and Mode 20 of Grouped Element Sensitivities With Highest Value at Element 9 (Plot 9)

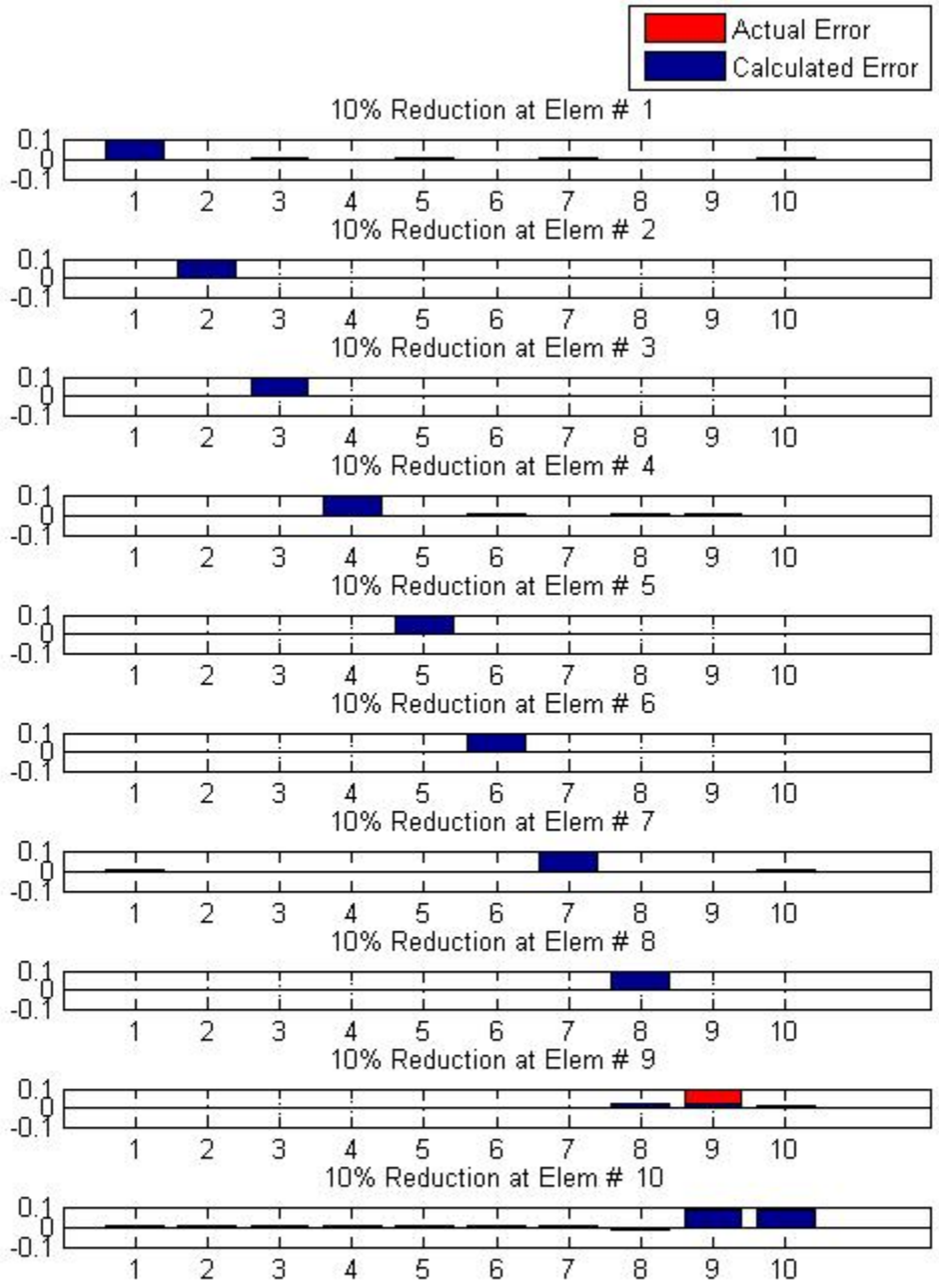

Figure 46. Solution Using Mode 1, 20 of Baseline and Mode 1 of Each ABC System That Constrains Translational DOF 1 Through 7 and Mode 20 of Grouped Element Sensitivities With Highest Value At Element 9

It is obvious from Figure 46 that this combination of configurations works fine for predicting the error when it occurs in elements 1 through 8, but it is not positive for errors near the free end of the cantilever beam. It has to be mentioned here that even if sensitivity matrix is full rank, there is a discrepancy regarding the frequency difference vector $\left\{\Delta\omega^2\right\}$. This discrepancy is related to the use of the same values in its last two entries, since the twentieth natural frequencies of the baseline and the experimental model are the same for both the original and the grouped element model. This is a very important observation because it leads to the conclusion that there is a limitation imposed when grouped element sensitivities configurations are used along with baseline ones. This limitation defines that the same modes of baseline and grouped element sensitivities cannot be used together in a global sensitivity matrix, because the subject of using repeated eigenvalues is raised and this produces discrepancies to the linear system solution. This limitation can be further applied to the use of ABC systems that have natural frequencies very close to those of the baseline system, as was discussed for the first eigenvalue of the ABC system that constrains the eighth translational DOF (plot 9 of Figure 36) in comparison with the second eigenvalue of the baseline system.

Considering, now the second case where the twentieth mode of the baseline system is replaced by the twentieth mode of the grouped element sensitivities permuted to have highest sensitivity value at the tenth element, Figure 47 is generated by the sensitivity distribution along the rows of the sensitivity matrix created by these configurations. No repeated eigenvalues limitation is present and Figure 48 is produced to demonstrate the solution given from the linear system using this matrix.

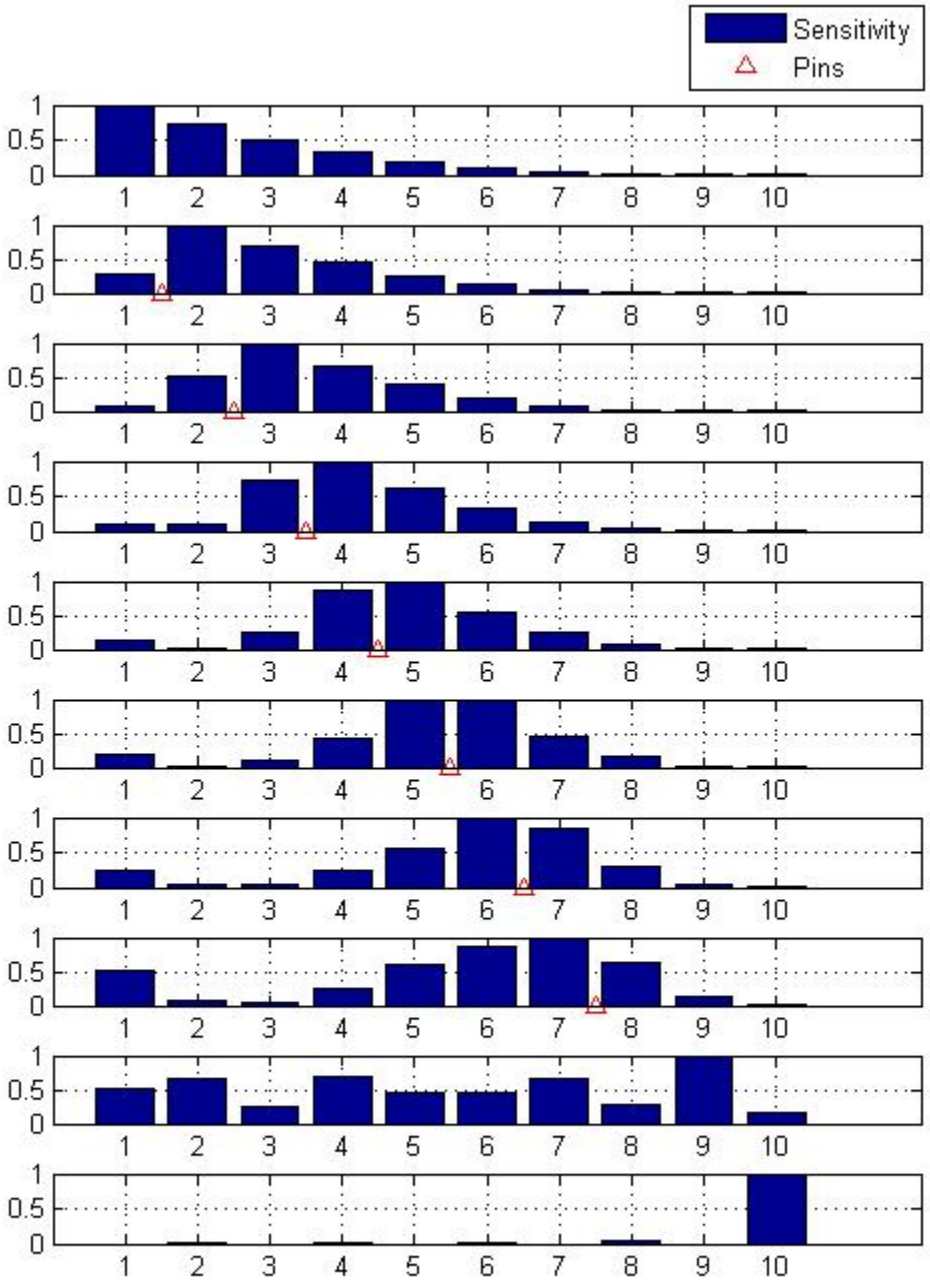

Figure 47. Sensitivity Matrix of Mode 1, 5 of Baseline (Plots 1, 9) and Mode 1 of Each ABC System That Constrains Translational DOF 1 through 7 (Plots 2–8) and Mode 20 of Grouped Element Sensitivities With Highest Value at Element 10 (Plot 10)

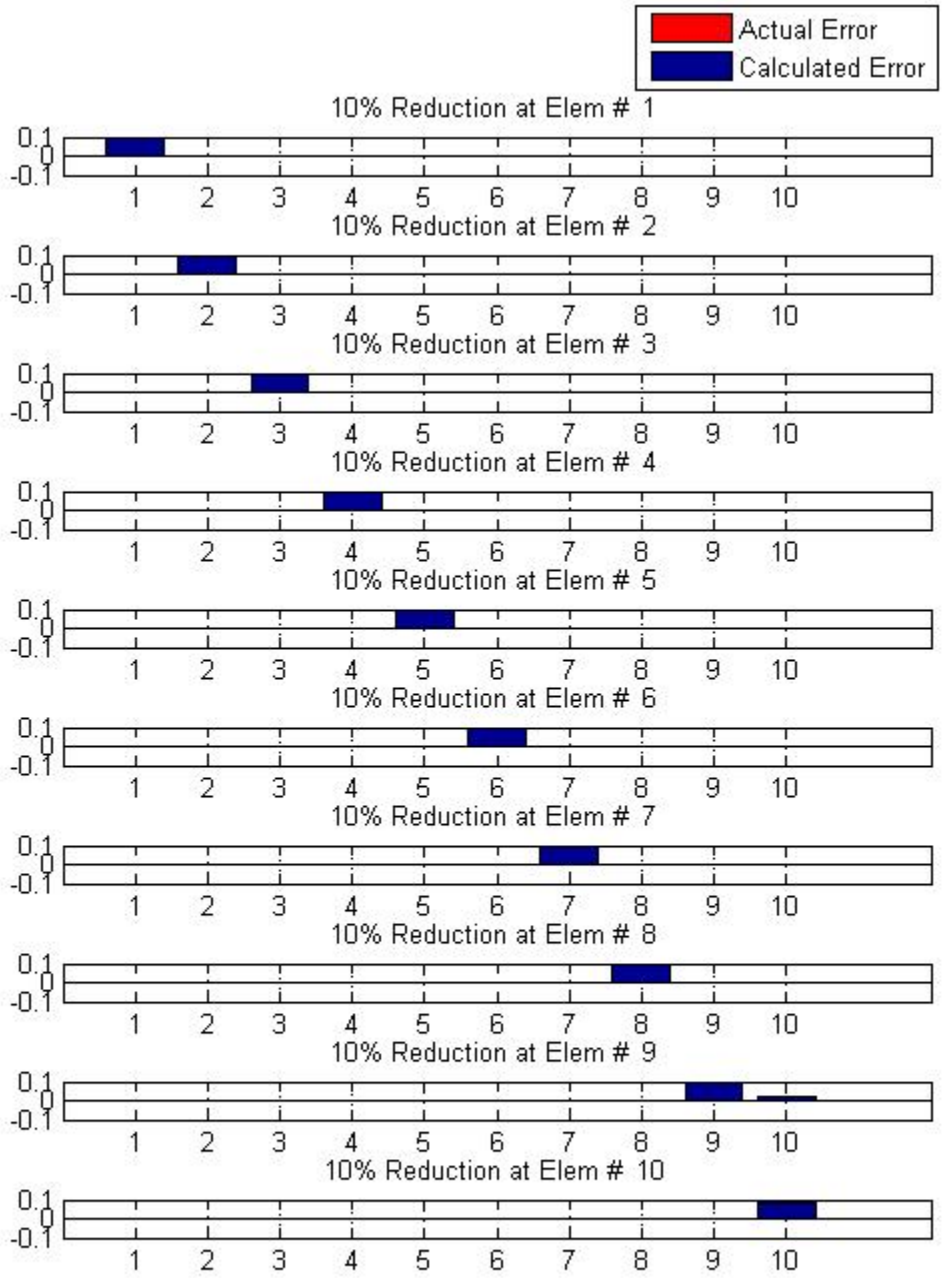

Figure 48. Solution Using Mode 1, 5 of Baseline and Mode 1 of Each ABC System That Constrains Translational DOF 1 Through 7 and Mode 20 of Grouped Element Sensitivities With Highest Value at Element 10

Figure 48 provides a great result as far the location and the magnitude of the error is concerned, wherever in the structure it may occur. It clearly demonstrates that baseline, ABC and grouped element sensitivities configurations can be essentially combined into one global sensitivity matrix for the structure, which has the properties of a diagonally dominant banded matrix as described previously in this work. With proper attention to all the limitations mentioned before, it is possible to reveal any potential damage in a structure or to update an FE model.

In addition to what is concluded above, the same concept can be extended to cases where actual error occurs in more than one element of the structure. For this purpose, Figure 49 is generated and includes the solution using the configurations depicted in Figures 41, 47 and 45, respectively, with actual error occurring simultaneously in elements 1, 3 and 10. Again, it is proved that optimal configurations are those who adopt the concept of a diagonally dominant sensitivity matrix, but also considering issues generated by using similar modes of different systems.

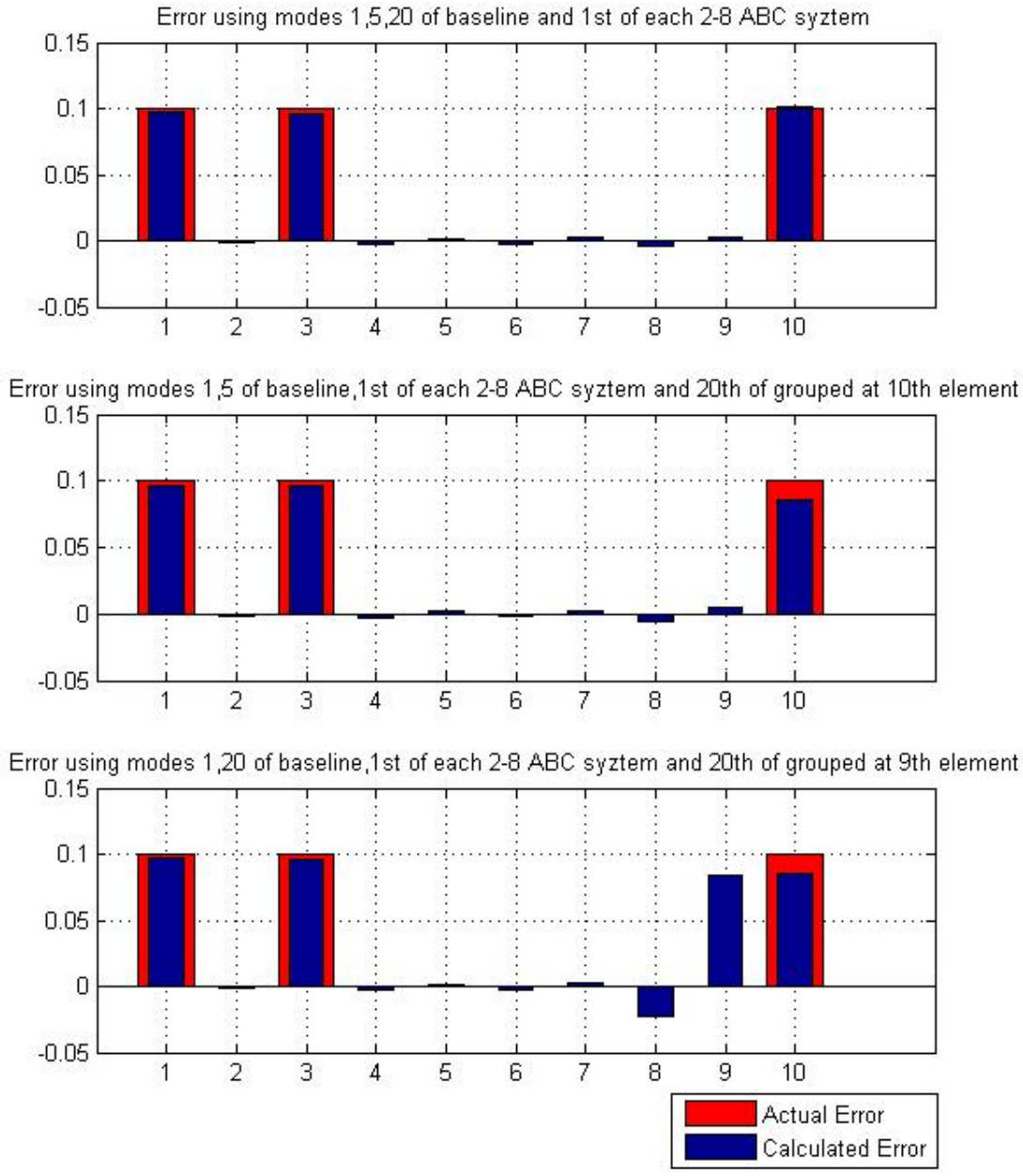

Figure 49. Solution For Actual Error in Elements 1, 3, 10 Using: Plot 1-Configurations of Figure 41, Plot 2-Configurations of Figure 47, Plot 3-Configurations of Figure 45

V. CONCLUSIONS/RECOMMENDATIONS

A. CONCLUSIONS

1. The natural frequencies of the ABC systems can easily be identified from a square experimentally measured FRF matrix. These natural frequencies will interlace the natural frequencies of the baseline system in accordance with the Cauchy interlace theorem. The eigenvalue/eigenvector sensitivities of these ABC systems can be calculated using the same FE model as that used to generate the baseline system sensitivities.

2. There is an exact and direct correlation between the stiffness sensitivity matrix and the flexural properties of the structure. This means that strain energy modes have the same distribution in the structure as their corresponding stiffness sensitivity modes.

3. For overdetermined full rank problems, the use of Matlab operators "\" and "pinv" both return the same least square solution to the linear system created by the fundamental Equation (2.31), which minimizes the Euclidean norm of the residual, once with QR decomposition and once with the SVD method.

4. For underdetermined or rank deficient problems, the solutions obtained from the use of those two operators are not the same. In this case, "pinv" gives a least norm solution, in the sense that the length of the solution vector is minimum, while "\" returns a basic solution with the significance of having a number of non-zero values equal to or less than the rank of the sensitivity matrix.

5. Using only one mode for the identification of the structure, the "\" operator gives a solution that has one non-zero value corresponding to the element with the highest sensitivity value , while using the "pinv" operator returns a solution that is scaled by the sensitivity distribution of the mode used and eventually by the strain energy of the same mode.

6. The use of "\" turns out to be more effective for system identification because it provides a more transparent result in terms of error localization and it makes clear that the use of modes with locally concentrated sensitivity values will reveal errors at the corresponding elements where errors exist.

7. Solving underdetermined systems, that is using fewer modes than the number of elements potentially in error, will identify potential damage in, at most, as many elements as the number of modes used. This means that

an error can be uniquely identified anywhere in a structure only if a square full rank sensitivity matrix is used that is of a size equal to the number of elements potentially in error.

8. Mode shape design sensitivity data may sometimes be used for the augmentation of the modal frequency data used for the sensitivity based FEM updating, as long as the availability and suitability of the measurement locations is appropriate, and the accuracy associated with those measurements is within the requirements tolerance.

9. A useful means of compensating for an insufficient amount of test data is the grouped element sensitivities permuted in such a way as to match the sensitivity matrix length by simply adding zeros in elements that are not required to have a sensitivity value, and the total sensitivity of the group being assigned to the remaining member of that group. Grouped element sensitivities are not useful when the same modes of the baseline system are used, because issues of repeated eigenvalues and perhaps of mode quasi-dependencies are raised.

10. Baseline, ABC and grouped element sensitivities configurations can be used together in one sensitivity matrix with the only limitation being the use of modes from different systems that might be close to each other, hence creating quasi-dependencies and close-to-repeated eigenvalues issues.

11. If baseline, ABC and grouped element sensitivities are used to create a "global" square sensitivity matrix, which clearly concentrates high sensitivity values around every element in the structure in different modes, under the concept of, as described, a "diagonally dominant banded" matrix, then error can be identified anywhere in this structure both quantitatively, in terms of location, and qualitatively, in terms of magnitude.

B. RECOMMENDATIONS

1. Verify that the concept of the "diagonally dominant banded" matrix can be applied to the identification of errors associated with mass/density parameters.

2. Create an algorithm/program that chooses the best combination from a variety of ABC and/or grouped element sensitivities sets, along with baseline sensitivities, into a sensitivity matrix that can identify a parameter error regardless of its location. This should be approached under the constraint of the availability of modes in a certain test bandwidth and the criterion of minimum computational time relative to the size and the complexity of the structure. If the conditions set above make this

procedure prohibitive, find combinations of configurations that create underdetermined sensitivity matrices, capable of damage prediction, each one in different areas/elements of the structure, as some regions of a structure may be more neuralgic than others.

THIS PAGE INTENTIONALLY LEFT BLANK

LIST OF REFERENCES

[1] J. E. Mottershead and M. I. Friswell, "Model updating in structural dynamics: A survey," *Journal of Sound and Vibration*, Vol. 167, 2, pp. 347–375, 1993.

[2] M. I. Friswell, and J. E. Mottershead, *Finite Element Model Updating in Structural Dynamics*, London: Kluwer Academic Publishers, 1995.

[3] G. Lallement, and J. Piranda, "*Localisation Methods for Parameter Updating of Finite Element Models in Elastodynamics*," 8th International Modal Analysis Conference, 1990, Orlando, Florida USA, pp. 579–585.

[4] M. I. Friswell, S. D. Garvey, and J.E. T. Penny, "*The Importance of Vector Subspaces in Modal Analysis,*" 16th International Modal Analysis Conference Santa Barbara, California USA, 1998.

[5] M. I. Friswell, J. E. Mottershead, and H. Ahmadian, "Combining subset selection and parameter constraints in model updating," *Journal of Vibrations and Acoustics*, Vol. 120, pp. 854–859, 1998.

[6] J. E. Mottershead et al., "Selection and updating of parameters for an aluminum space frame mode," *Mechanical Systems and Signal Processing*, Vol. 14, 6, pp. 923–944, 2000.

[7] G.H. Kim and Y.S. Park, "*An Automated Parameter Selection Procedure for Updating FEM*," 22nd International Modal Analysis Conference, Dearborn, Michigan USA, 2004.

[8] H. Shahverdi, C. Mares, and J. E. Mottershead, "*Clustering of Parameter Sensitivities in the Finite Element Model Updating of a Lynx Helicopter,*" 1st International Conference on Innovation and Integration in Aerospace Sciences, Queen's University Belfast, 2005.

[9] H. Shahverdi, et al., "Finite element model updating of large structures by the clustering of parameter sensitivities," *Applied Mechanics and Materials*, Vols. 5–6, pp. 85–92, 2006.

[10] H. Shahverdi, et al., "Clustering of parameter sensitivities: Examples from a helicopter airframe model updating exercise," *Shock and Vibration*, Vol. 16, 1, pp. 75–87, 2009.

[11] J. H. Gordis, "Omitted coordinate systems and artificial constraints in spatially incomplete identification," *Modal Analysis*, Vol. 11, pp. 83–95, 1996.

[12] D. A Rade, G. Lallement, and L.A. Da Silva, *"A Strategy for the Enrichment of Experimental Data as Applied to an Inverse Eigensensitivity-Based FE Model Updating Method,"* 14th International Modal Analysis Conference, Dearborn, Michigan USA, 1996.

[13] J. H. Gordis, "Artificial boundary conditions for model updating and damage detection," *Mechanical System and Signal Processing*, Vol. 13, 3, pp. 437–448, 1999,

[14] Z. Tu and Y. Lu, "FE model updating using artificial boundary conditions with genetic algorithms," *Computers and Structures*, Vol. 86, pp. 714–727, 2008.

[15] Y. L, and Z. Tu, "*Artificial Boundary Condition Approach for Structural Identification: A Laboratory Perspective,"* 26th International Modal Analysis Conference, Orlando, Florida USA, 2008.

[16] D. J. Ewins, *Modal testing: Theory and Practice*, Research Studies Press LTD, 1984.

[17] D. J. Ewins, *Modal Testing 2: Theory, Practice and Application*, Research Studies Press LTD, 2000.

[18] R. A. Lagunes Arteaga, "Finite element based structural damage detection using artificial boundary conditions," M.S. thesis, NPS, Monterey, CA, USA, 2007.

[19] R. L. Fox and M. P. Kapoor, "Rates of change of eigenvalues and eigenvectors," *AIAA*, Vol. 6, 12, December 1968.

[20] R. B. Nelson, "Simplified calculation of eigenvector derivatives," *AIAA*, Vol. 14, 9, September 1976.

[21] J. H. Gordis, "Eigenvector sensitivity analysis: An informal survey of selected contributions to the literature," SDRC Engineering Services.

[22] P. Blelloch, "Calculation of eigenvector derivatives for structural systems," SDRC Engineering Services.

[23] MATLAB® R2010A, The Mathworks, Inc. Natick, MA.

[24] C. C. Flanigan, "*Correlation of Finite Element Models Using Mode Shape Design Sensitivity*," 9th International Modal Analysis Conference, Firenza, Italy, 1991.

[25] B. N. Parlett, *The Symmetric Eigenvalue Problem*, Prentice Hall, 1980.

[26] “Diagonally Dominant Matrix,” *Wikipedia, The Free Encyclopedia* [Online: July 20, 2010], [Cited: July 31, 2010], http://en.wikipedia.org/wiki/Diagonally_dominant_matrix

THIS PAGE INTENTIONALLY LEFT BLANK

INITIAL DISTRIBUTION LIST

1. Defense Technical Information Center
   Ft. Belvoir, Virginia

2. Dudley Knox Library
   Naval Postgraduate School
   Monterey, California

3. Joshua H. Gordis
   Naval Postgraduate School
   Monterey, California

4. Knox T. Millsaps
   Naval Postgraduate School
   Monterey, California

5. Jonathon J. VanSlyke
   Naval Postgraduate School
   Monterey, California